An Innovative Model-based Velocity Integration Procedure with an Application in Eastern Saudi Arabia

BY

Abdulaziz Mohammed Saleh Al-Moqbel

A Thesis Presented to the

DEANSHIP OF GRADUATE STUDIES

KING FAHD UNIVERSITY OF PETROLEUM & MINERALS

DHAHRAN, SAUDI ARABIA

In Partial Fulfillment of the
Requirements for the Degree of

MASTER OF SCIENCE

In

GEOPHYSICS

June 2010

KING FAHD UNIVERSITY OF PETROLEUM AND MINERALS

DHAHRAN 31261, SAUDI ARABIA

DEANSHIP OF GRADUATE STUDIES

This thesis, written by **Abdulaziz Mohammed Al-Moqbel** under the direction of his Thesis Adviser and approved by his Thesis Committee, has been presented to and accepted by the Dean of Graduate Studies, in partial fulfillment of the requirements for the degree of **MASTER OF SCIENCE IN GEOPHYSICS.**

Thesis Committee

Dr. Abdullatif Al-Shuhail
Chairman

Dr. Mohammed Makkawi
Member

Dr. Ming-Ren Hong
Member

Dr. Abdulaziz Al-Shaibani
Department Chairman

Dr. Salam A. Zummo
Dean of Graduate Studies

22/6/15
Date

DEDICATION

This thesis is dedicated to my parents, my wife, my children, my brothers and my sisters.

ACKNOWLEDGMENTS

Acknowledgment is due to King Fahad University of Petroleum and Minerals for supporting this research, and Saudi Aramco for the opportunity to work on this thesis.

I am deeply grateful to my thesis advisor, Dr. Abdullatif Al-Shuhail for his relentless guidance, support and prompt review of my work.. I am also thankful to Dr. Mohammed Makkawi for his valuable suggestions and comments. I am deeply appreciative to Dr. Mig-Ren Hong for his support and encouragements.

I would like to thank the Earth Sciences Department Chairman Dr. Abdulaziz Al-Shaibani and other faculty members for their support.

Finally, my great appreciations go to all my family for their support, encouragement to continue my study.

TABLE OF CONTENTS

LIST OF TABLES

LIST OF FIGURES

Page

THESIS ABSTRACT

Name: Abdulaziz Mohammed Saleh Al-Moqbel
Title: An Innovative Model-based Velocity Integration Procedure with an Application in Eastern Saudi Arabia
Major Field: Geophysics
Date: June 2010

During the workflow of seismic data processing, approximately one third of the processing time is allocated to estimate initial stacking velocity functions. The precision of the current available methods of estimating stacking velocity is limited in vertical and horizontal velocity resolution, especially in cases involving multiples and limited-offset data sets. A new procedure is proposed in this study to effectively build initial stacking velocity functions for processing new seismic lines with improved productivity, increased accuracy and interpretation consistency. The procedure builds a 3-D velocity model from previous surface and borehole seismic surveys as well as interpretation data for seven key horizons. A common-model platform has been used to allow for integration of otherwise independent data types. Results show that using the estimated integrated velocity model has allowed velocity picking in seismic data sets with poor signal-to-noise ratio due to excessive ambient noise or karsting. The model also helped in discriminating stacking velocities in areas with stretched or poor semblance peaks.

Master of Science Degree

King Fahd University of Petroleum and Minerals

Dhahran, Saudi Arabia

June 2010

ملخص الرسالة

الإسم : عبدالعزيز محمد صالح المقبل

عنوان الرسالة : طريقة مبتكرة لدمج معلومات السرعة في قاعدة نموذجية و تطبيقها في المنطقة الشرقية للمملكة العربية السعودية

التخصص : جيوفيزياء

تاريخ التخرج : يونية 2010

خلال سير عمل معالجة المعلومات السيزمية يتم تخصيص ثلث الوقت المخصص لمعالجة المعلومات لتحديد السرعة المبدئية للمعلومات السيزميه . دقة الأساليب المتاحة حاليا لتحديد السرعة المبدئية للمعلومات السيزمية محدود بالوضوح الرأسي و الأفقي خصوصاً في الحالات المتضمنة الإرتدادات و المعلومات ذات الازاحات المحدودة .من خلال هذه الدراسة يمكن وضع طريقة مبتكرة لتحديد السرعة المبدئية للمعلومات السيزمية مع تحسين الإنتاجية و زيادة الدقه و مواكبتها للمعلومات التحليلية. هذه الطريقة تعتمد على إعداد نموذج ثلاثي الأبعاد لمعلومات السرعة من المعلومات السيزمية السابقة و المعلومات السيزمية من الأبار و المعلومات التحليلية لسبع طبقات رئيسية . بالإضافة إلى ذلك فأن النموذج يعتمد على قاعدة توفر القدرة على دمج أي معلومات مستقلة عن ما هو متوفر. اثبتت النتائج أن إستخدام النموذج المدمج لمعلومات السرعة أتاح ممارسة عملية إختيار السرعة المناسبة في المعلومات السيزمية التي تفتقر لوضوح نسبة الإشارة إلى الضوضاء بسبب الضوضاء المحيطة أو بسبب الإنهيارات الطبقية . كما أتاح إستخدام النموذج في التمييز عن السرعة المناسبة عندما تكون قمم الأطياف ممددة أو ضعيفة .

درجة الماجستير في العلوم

جامعة الملك فهد للبترول و المعادن

الظهران، المملكة العربية السعودية

يونية 2010

CHAPTER 1

INTRODUCTION

1.1 INTRODUCTION

In seismic data processing, it is essential to reduce the turnaround time and human decision during every process. Iterative and repetitive processes such as velocity analysis often influence the accuracy of the required precision. The amount of repetition is highly dependent on the accuracy and consistency of the first pass of velocity analysis, usually called the "initial velocities". Improving the initial velocities will highly affect the accuracy and turnaround time of other processes that are dependent on velocities such as residual statics, normal moveout (NMO) correction, and migration.

Seismic velocities are estimated from surface seismic data using one or more of the following methods.

The* $\mathbf{T^2}$-$\mathbf{X^2}$ *Method

The two-way traveltime (T) from the ground surface to a subsurface horizontal interface is related to the offset (X) of the receiver by the following approximate equation:

$$T^2 = T_0^2 + \frac{X^2}{V^2}, \qquad (1)$$

where T_0=2Z/V is the zero-offset traveltime, Z is the depth to the interface, and V is the stacking (or NMO) velocity from the surface to the interface. The square root of equation (1) represents a hyperbola that is symmetric about the X=0 axis. However, when

equation (1) is plotted in the T^2-X^2 plane it corresponds to a line whose intercept is T_0^2 and slope is $1/V^2$. Practically, the line that best fits the traveltime-offset picks can give only an estimation of zero-offset time and stacking velocity of the true traveltime curve (Figure 1.1).

Constant velocity gathers

In this method, a selected CMP gather is plotted repeatedly using a range of constant NMO velocities. The whole CMP gather is NMO-corrected using one single NMO velocity value and the process is repeated until all trial NMO velocities are exhausted. The NMO velocity that best flattens a certain reflector is picked as the NMO velocity of that reflector (Figure 1.2).

Constant velocity stacks

This method relies on looking at a portion of the seismic line. A small group of adjacent CMP gathers are NMO-corrected and stacked using one single NMO velocity and the process is repeated until all trial NMO velocities are exhausted. The NMO velocity at which a reflector shows the best coherency (continuity) is picked as the NMO velocity of that reflector (Figure 1.3).

Velocity spectra

In this method, a CMP gather is selected and hyperbolic curves similar to equation (1) with different stacking velocities are fitted at every time sample along the time axis. The best-fit hyperbola gives to the best-fit stacking velocity at that time at the CMP location.

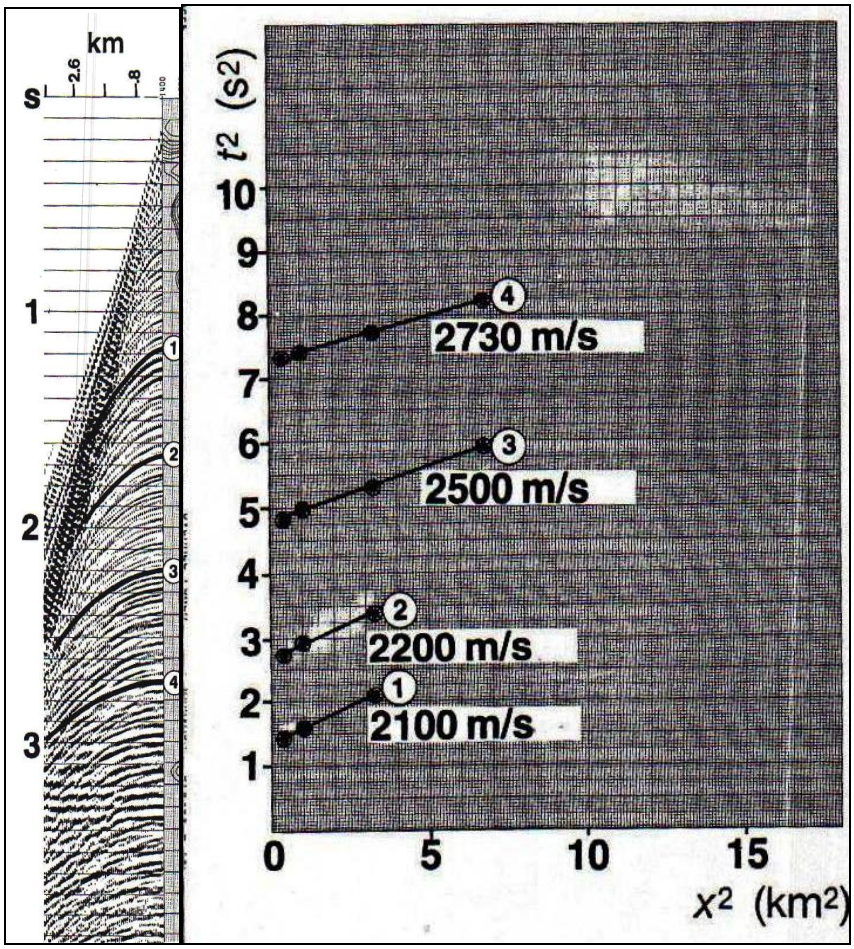

(a) **(b)**

Figure 1.1: **(a)** Common midpoint (CMP) gather showing four distinct reflectors. **(b)** T^2-X^2 plot showing best-fit lines to picked times and offsets along the four hyperbolic curves and their related velocities (adapted from Yilmaz, 1987).

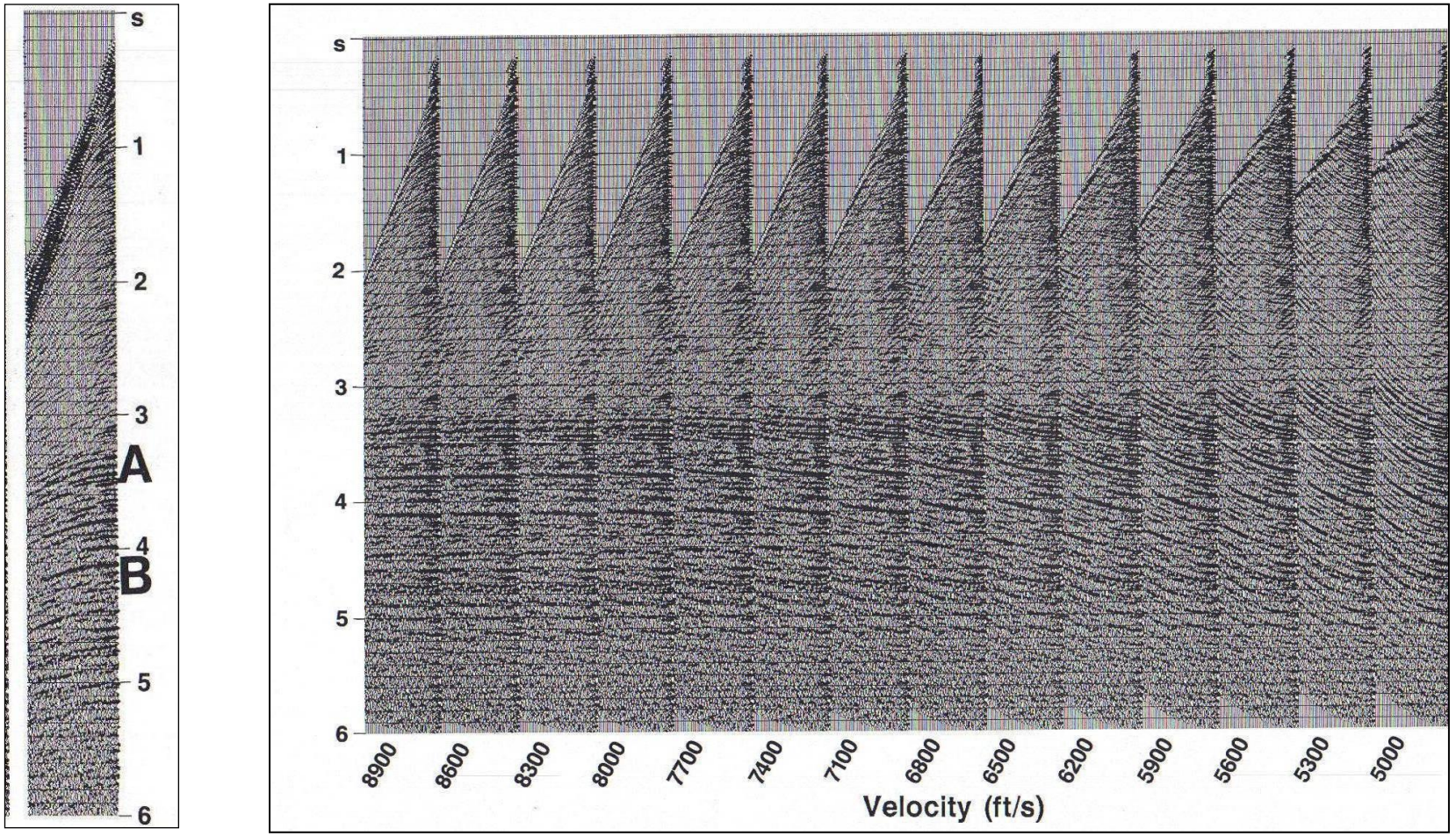

(a) **(b)**

Figure 1.2: **(a)** Input CMP gather. **(b)** Constant velocity gathers of the CMP gather in (a) (adapted from Yilmaz, 1987).

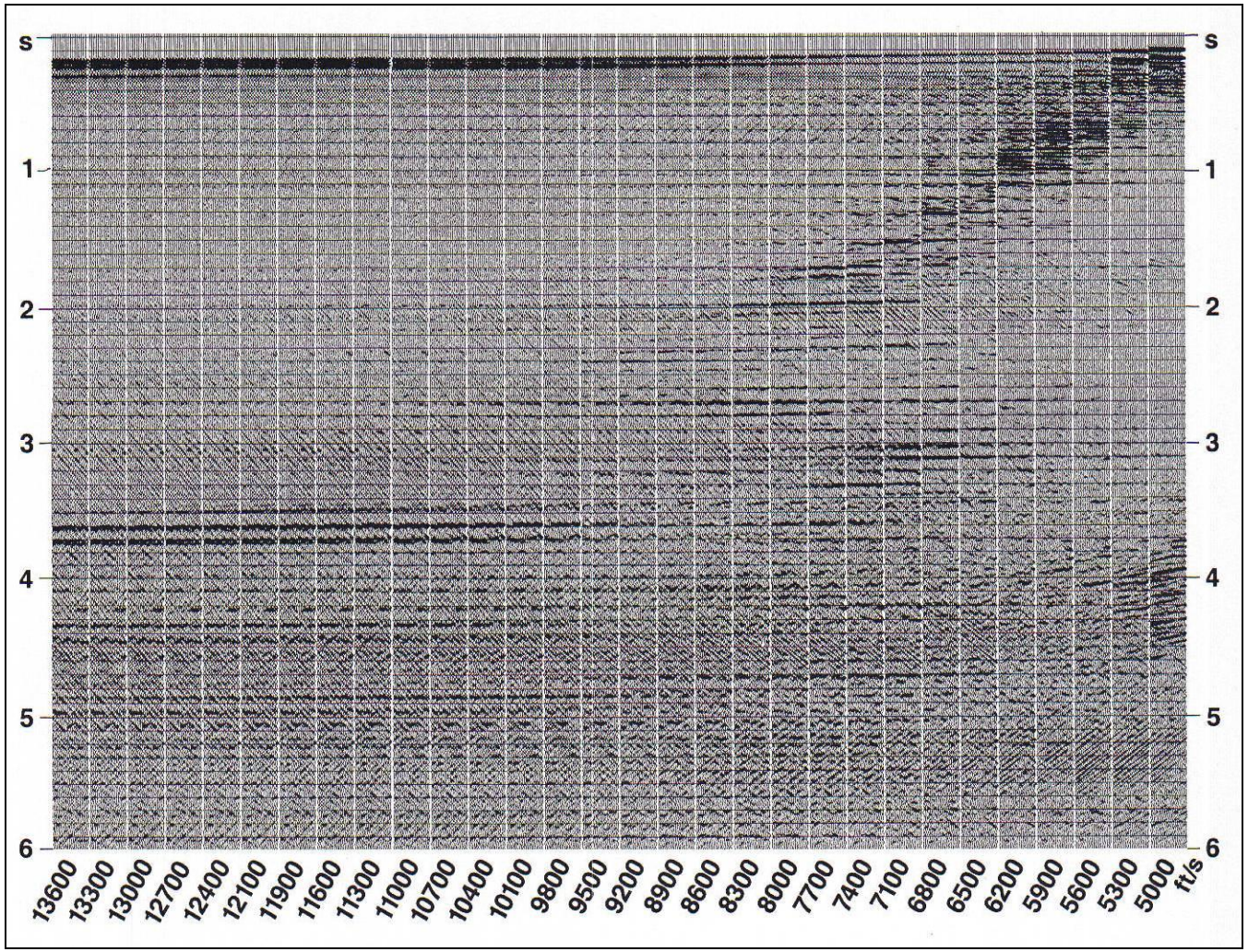

Figure 1.3: Constant velocity stacks of a group of adjacent CMP gathers (Yilmaz, 1987).

The goodness of fit is judged using various coherency measures such as the semblance, cross-correlation and others (Figure 1.4).

1.2 LITERATURE REVIEW

The available tools that are currently used to estimate the initial stacking velocities are either based on visual assessment of the continuity of the reflection or the coherency of the crosscorrelations sum of traces. There have been efforts to enhance the process to provide precise estimate of stacking velocity. One of the methods relies on iterating the velocity values after NMO and time picks to achieve convergence (Tieman, 1993). Diffraction patterns were studied to give an optimum constant stacking velocity (Matsushima et al. 2001). Other methods used the increased resolution of the least squares parabolic radon transform to pick events in the high resolution transform domain (Kabir et al, 1994). Neural networks have been used to automatically detect and pick maximum coherency stacking velocities (Schmidt, 1994). Interval velocities were also conditioned and constrained to estimate stacking velocities (Weizhong, et al. 1988). The Common Reflection Stack (CRS) method, which provides stacking velocities as calculated attributes of the stacks has been used by Bergler et al. (2002). Traveltimes of reflections were also estimated independent of stacks to give a physical meaning of the stacking velocities (Chira, et al. 2003). Stacking operators such as beam stacks or slant stacks were also employed to estimate stacking velocities (Biondi, 1992). These studies were mostly based on data from the reflection but not the reflector. They also rely on

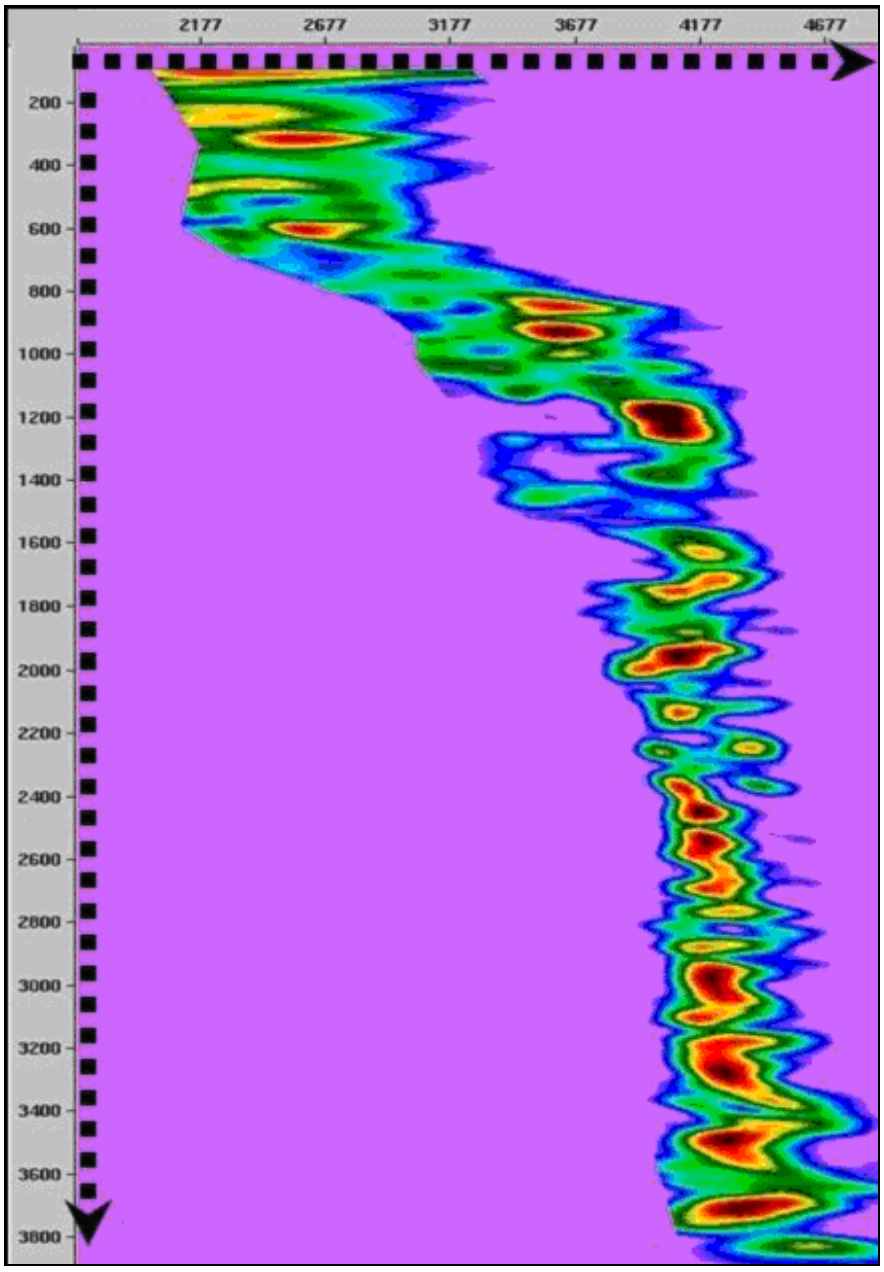

Figure 1.4: Velocity spectrum of a CMP gather. Horizontal axis shows stacking velocity in m/s while vertical axis shows time in ms. Contour colors indicate magnitude of coherency measure (semblance in this case). Hot colors indicate higher while cold colors indicate lower semblance values.

extractions of the data from the stacks. All of these methods either estimate maximum coherency points or maximum continuity of the reflection in the CMP-gather domain or other domains.

1.3 MOTIVATION

The current methods of stacking velocity analysis of seismic reflection data are based on the approximation of the traveltime curves in CMP gathers with hyperbolic trajectories. The analysis is performed in the offset-time framework and generates a time-velocity histogram. Even though it is plotted on axis of time and velocity, the estimated velocity is never precise. Semblance picking is the most popular method amongst the various methods because it gives a velocity spectrum at every reflection. The accuracy of the coherency estimates depends on the adequacy of the model used, CMP in most cases, and the quality of reflections. Coherency can vary from one reflection to another and from one end of the hyperbola to another. A common problem is that at deeper times, the coherency is so wide that picking any point of the spectrum will generate a similar hyperbolic curve for the range of available offsets. The problem is even worse when events are of similar coherency values aligning vertically along the time axis and increasing the chance of picking a multiple reflection instead of a primary reflection. Figures 1.5 and 1.6 show some of these common problems.

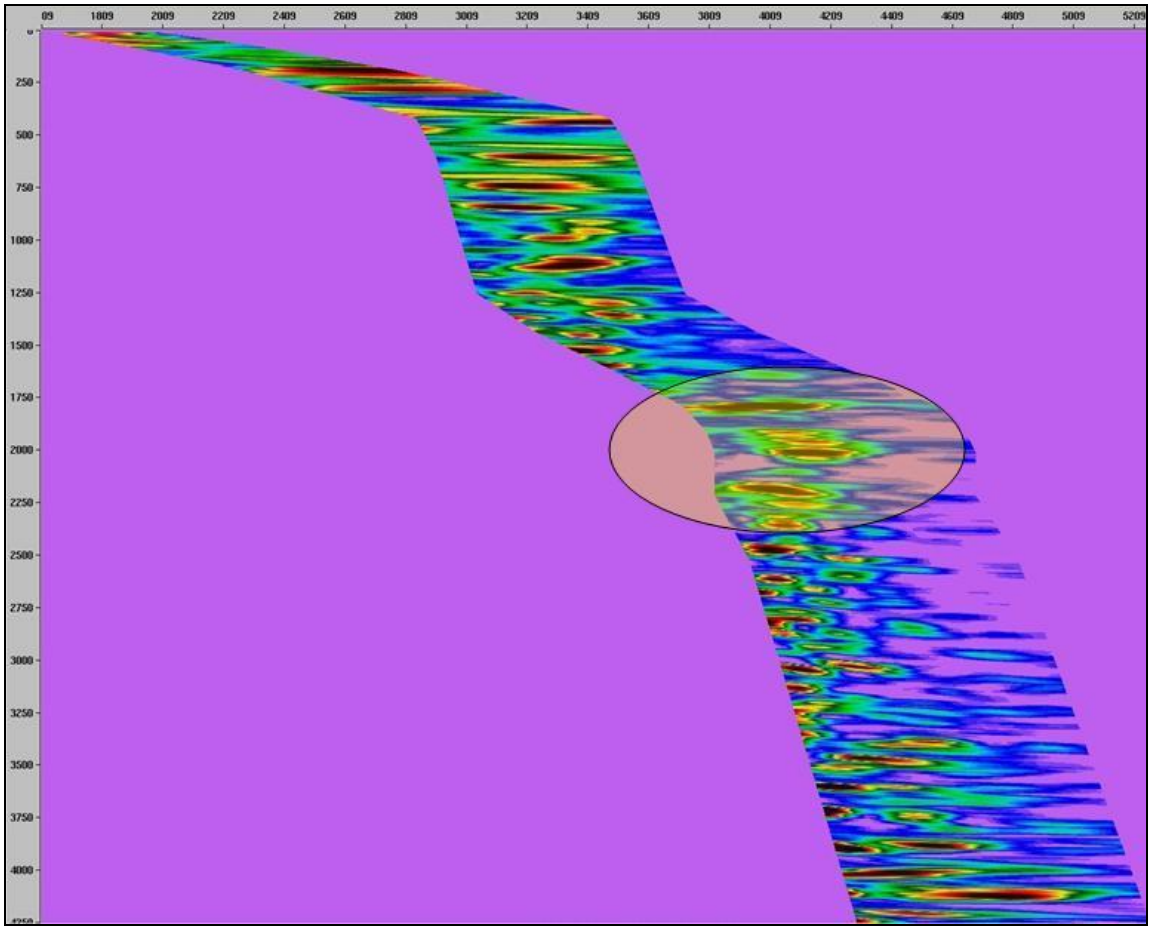

Figure 1.5: An illustration of a semblance plot showing an equivalent value of coherency along a wide range of velocities (at T≈1750 ms) causing a large inaccuracy in the picked velocity.

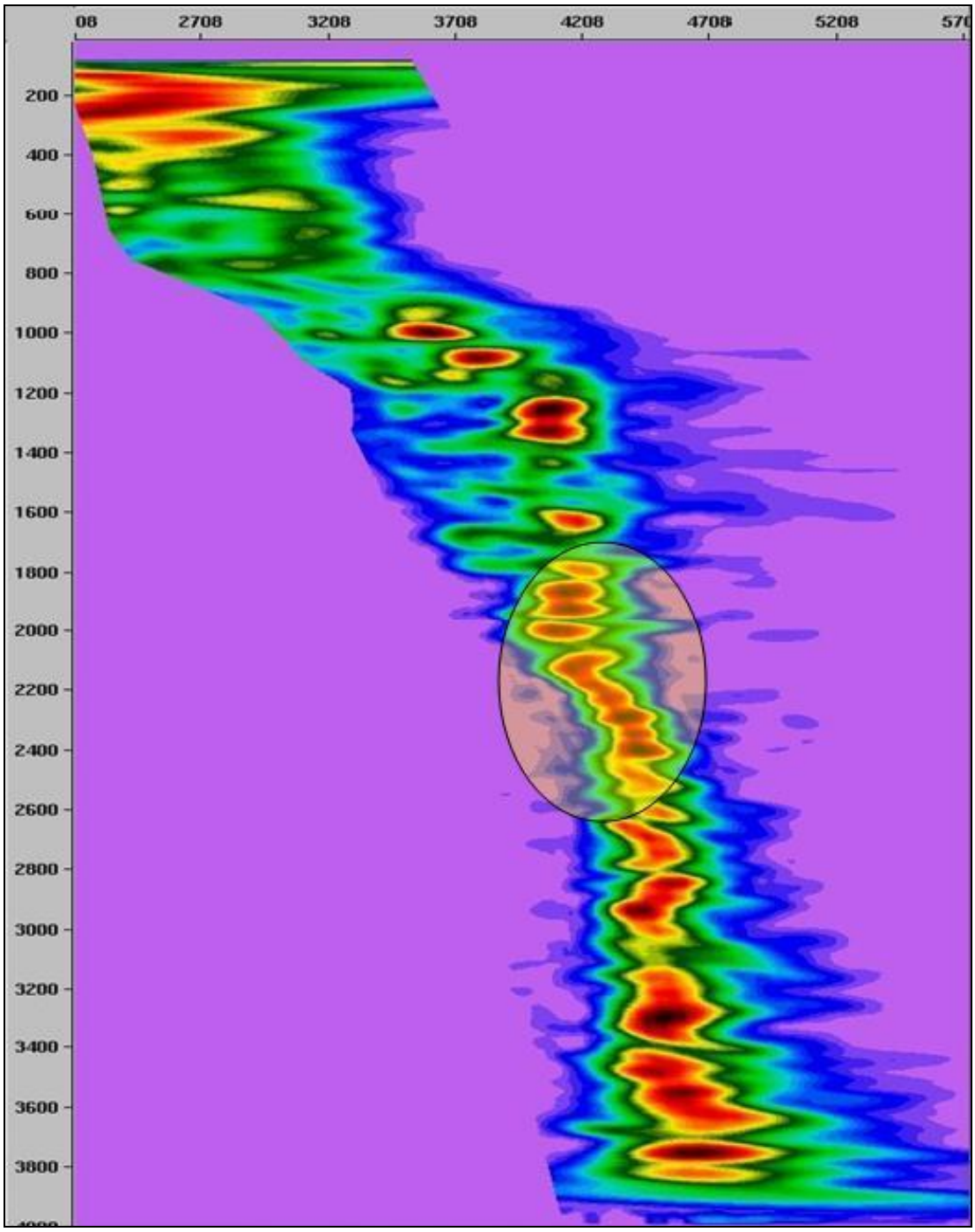

Figure 1.6: An illustration of a semblance plot showing an equivalent value of coherency for a group of reflections (T≈1800-2000 ms) within a CMP increasing the chance of picking a multiple instead of a primary.

1.4 PROBLEM STATEMENT

The available methods of determining the stacking velocity have some severe shortcomings. They are based on measures of either reflection continuity or coherency, which may lead to inaccurate stacking velocity estimation.

1.5 OBJECTIVE

The objective is to provide a mean of giving the stacking velocity picking process a sense of precision and accuracy. It is also important to obtain a consistent pick of the reflector throughout the various locations of seismic surveys. It is also desirable to obtain a tool that has a background of geological reflectors that can lead to a more confident process for stacking velocity picking.

1.6 METHODOLOGY

The velocity analyses collected from previous surveys provide a rich source of velocity functions. Each single survey is processed independently and thus the velocity analysis is independent of any other survey that is adjacent or overlapping. The aim is to collect these surveys and extract the velocity functions assigned to the CMPs within these surveys. These functions provide a good control over larger areas when collected and compiled appropriately. The main obstacle is actually modeling the velocity functions

such that it covers all available surveys consistently. In addition, it is rather important to specify areas where velocity analysis should anticipate any velocity anomalies or difficulties in velocity picking. Thus seismic interpretation data was used to assist in comeing up with the consistency required and verify the existence of velocity anomalies. To accumulate and model such data, a platform was selected. This platform is capable of taking all various data types to generate a unified output suitable for use by processors and interpreters.

To preserve the overall integrity of the seismic velocities, this study rely only on data derived from seismic data at the initial stage. The velocity function used were velocity functions derived from two-dimensional seismic lines as well as velocity functions derived from three-dimensional seismic blocks. It is important to mention that all these velocities are collected from the same stage of processing. In this study, the seismic velocities collected were all collected at a stage called Current State of the Art (CSA) stacking velocities. This means that the stack at the CSA stage have been processed after at least two passes of residuals and three passes of velocities. The already interpreted seismic data was used to assist in establishing interpretation consistency throughout the desired data set. Interpretation means the actual time picks of every available seismic horizon throughout the area of the model. Times picks that are made by the interpreters implicitly carry a great value of verification. This verification includes Vertical Seismic Profile (VSP) calibration, lithology logs, sonic logs, density logs and other interpretation tools to make an accurate time pick. Compiling the velocity functions should provide a

better control of the velocity values while compiling the interpretation time picks will provide a precise location of the time picks for each desired horizon.

A combined input of 2D and 3D stacking velocity functions from previously archived seismic lines is to be imported into a common-model platform as point sets in space and time. These input velocity functions are to be compiled in the platform to access various interpolation and modeling capabilities. These velocity functions will be providing the geographical coordinates as well as the velocity value and time of the pick.

The geological understanding of these velocity functions is provided by collecting time picks of seven key horizons that fall within the area where the velocity functions have been compiled. This should enhance the consistency between interpretation and processing for target-oriented final products in terms of actual time picks and assigned velocity value. By integrating the velocity model with the time picks of seismic horizons, a more precise and consistent solution is delivered for various applications of stacking velocity.

More specifically, the time picks given in space by their geographical coordinates and time will be interpolated into a surface. The interpolated surfaces of various horizons will be then embedded into the cloud of velocity picks throughout the region. The physical property of each horizon, velocity in this case, will be projected on the surface. This projection process will be within a time window defined by the period of the horizon's reflection (Figure 1.7).

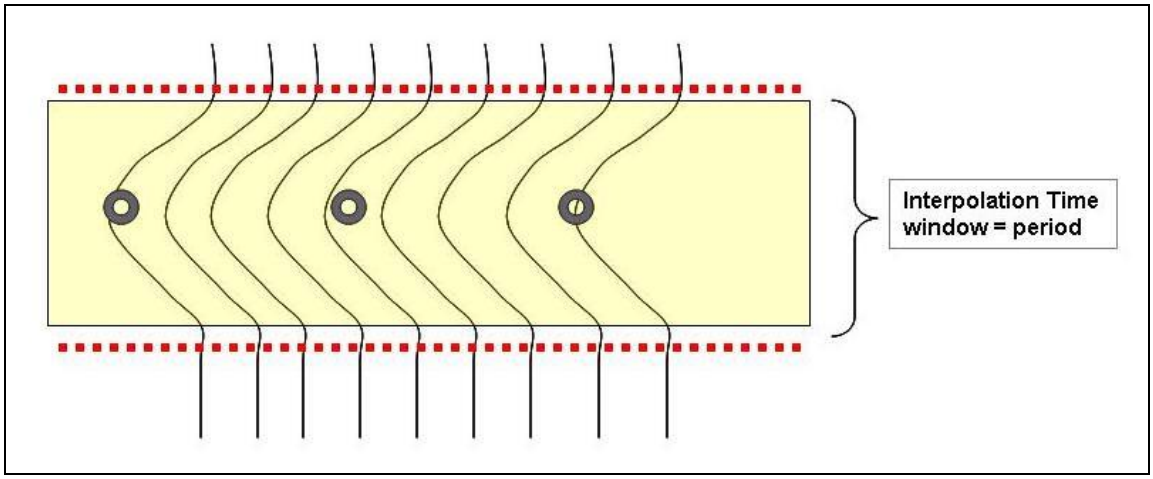

Figure 1.7: calculation of the time window width to be used in projecting velocity onto the interpolated surface of the picked horizon.

After the velocities are projected onto the surface, the velocities will be interpolated throughout the surface, a grid will be generated for the velocity, and another grid is generated for the time (Figure 1.8). This whole process will be processed in the common-model platform mentioned above. The interpolation method will be the Discrete Smoothing Interpolator (DSI). This method presents a discrete approach specially designed for modeling the geometry and properties of natural objects such as those encountered in seismic velocities. Contrary to classical computer-aided design methods based on continuous (polynomial) functions, the proposed approach is based on a discretization of the objects; a method close to the finite element techniques used for solving partial differential equations. Each object is modeled as a set of interconnected nodes having both the geometry and physical properties of the objects, and the DSI method is used for fitting the geometry and properties of complex data (Mallet, 2002).

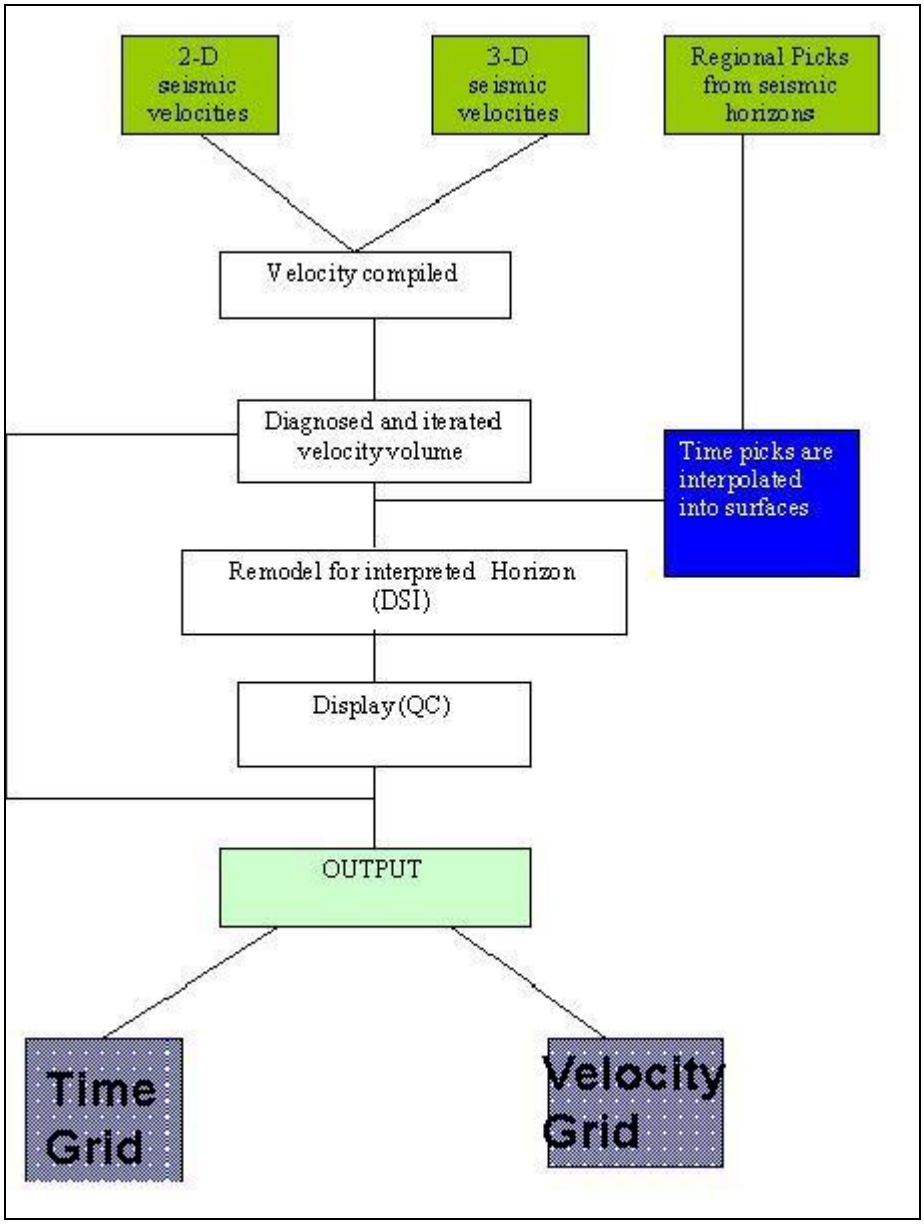

Figure 1.8: Flowchart indicating the steps of the proposed procedure.

Since velocity sampling is random, the interpolator considers the available samples as control nodes, interpolates to generate local roughness, and finds the solution that would

produce the minimum roughness possible over a surface (Mallet, 2002). Finally, a volume is generated by the DSI as smooth as possible. With this created volume, velocity models of any line segment or a sub-volume within the confines of the 3D velocity volume can be generated either for processing purpose as the initial stacking velocity profiles or in some cases for modeling purposes with a conversion of stacking velocities into interval velocities to perform time-to-depth conversion

CHAPTER 2

DATA COMPILATION

2.1 CHOICE OF PLATFORM

There needs to be an emphasis that this kind of study is aimed to involve large amounts of data that should require a platform capable of handling such size. This platform is not expected to be able to only compile data but also to be able to computationally perform sophisticated calculations without malfunctioning or breaking down the platform or the software. Computations such as large interpolations or surface triangulations are quite computer intensive and not all platforms are able to perform when the size of data is such as that used in this study.

The visualization tools play a critical role in investigating possible errors in the data or the computed results. It tells us more about the method and where improvements can be made. These visualization tools will also be used to make critical observations in the data sets or the results of the method applied.

Geological models are represented in geometrical representations so they are either points, curves, surfaces, grids, or any shaped three dimensional model. The geometrical representations are the essential components of modeling geological features both physically and mathematically.

For every natural object, the platform can handle topology, geometry, physical properties and various physical shapes of geological objects.

The compilation process has been a very challenging aspect of this study. A big challenge was the fact that data was available on databases over many areas but there had to be specific of choices to be made as various choices can influence what data was to be generated or studied. A decision had to be made on the data type, data elements, the scale of data, the extent of data -in both space and time- and the size of data. In addition, the age of data had to be selected to limit the amount of data.

2.2 DATA TYPES

All data that were used in this process were either extracted from seismic lines or were collected from the interpretation of seismic lines but only seismic based data types were used to maintain the integrity of the process within the seismic constrains.

2.3 DATA EXTENT

A region was designated for this study. This region is chosen because it has a variety of seismic coverage, some areas were densely covered and other areas were less covered with seismic 2-D line or 3-D seismic surveys. It is also large enough to be a part of a regional study. This region is very active and thus it is more viable to have more than one repetition of seismic surveys to be conducted within it's vicinities.

This designated region is a rectangular area bound by four corner points. Those points have the following Lambert coordinates as the projection coordinates.

Right Top corner

X=22°92'94" Y= 21°02'05"

Left Top corner

X=-10°21'35" Y= 21°02'05"

Right Bottom corner

X=22°92'94" Y= -33°89'40"

Left Bottom corner

X=-10°21'35" Y= -33°89'40"

Below is an areal sketch of this region indicated in Figure 2.1

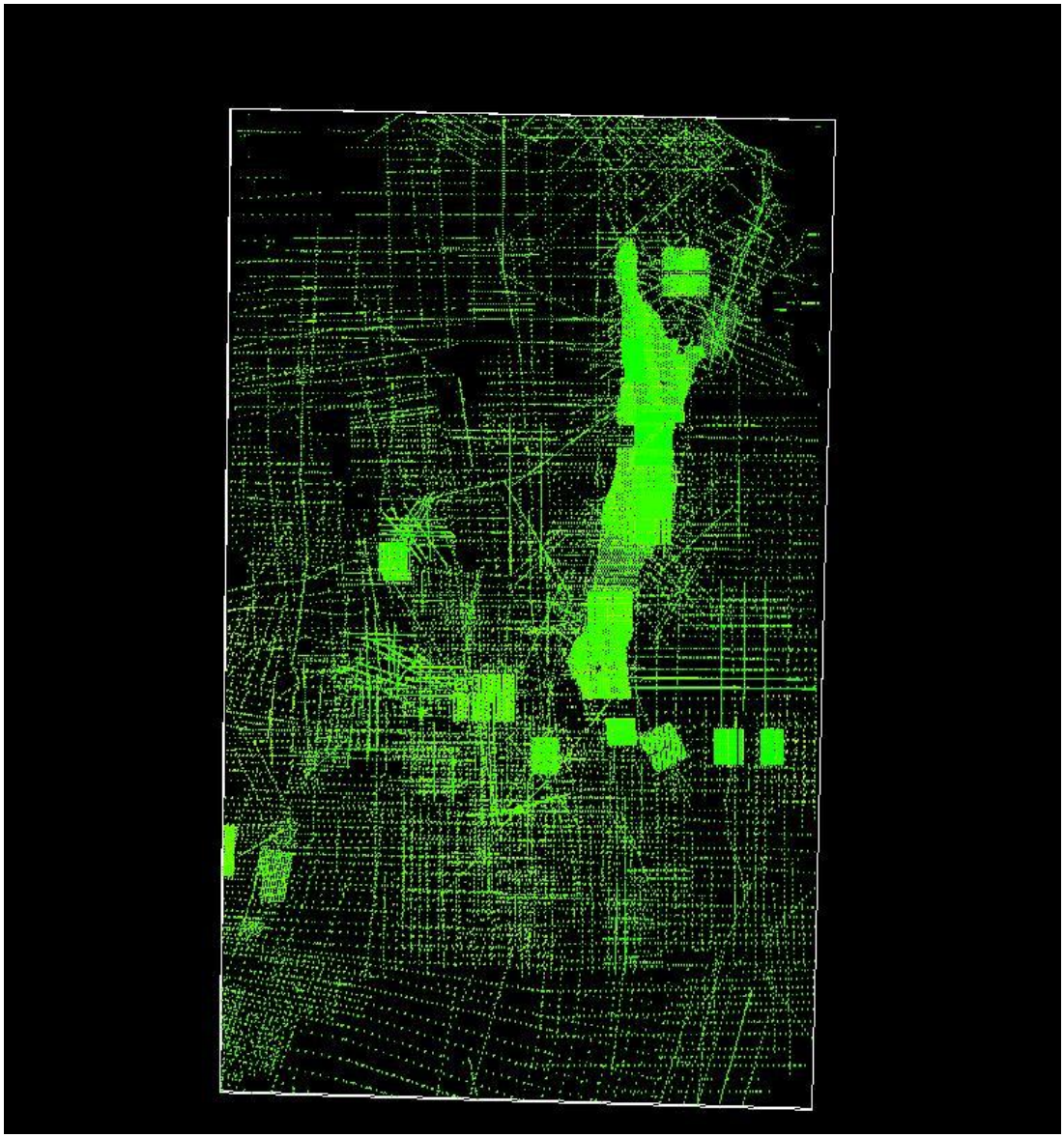

Figure 2.1 The areal extent of the study

This region covers approximately 182,000 squared kilometers of area, 552 KM in length from north to south, and 330 KM in width from east to west. The selection of this area was made on a plane map first by drawing an estimated region and then the coordinate points were taken from this map into the digital interface where it gave a rectangle similar to that rectangle that was on the original map.

2.4 DATA AGE

The oldest data that was used in this study was data that went back as far as January 1980 and a cut off date of January 2000 was applied during the compilation process. The purpose of choosing data within a time period is to limit the amount of data collected and include only data that was produced using fairly recent seismic acquisition technologies.

2.5 DATA ELEMENTS

This region is to be populated by the following data elements:

1-Velocity picks from CDP locations (picked from surface)

2-Seismic time picks of key regional horizons (picked from the datum)

3- The datum model in time.

2.5.1 Velocity picks from CDP locations

2.5.1.1 DIAGNOSING THE VELOCITY VOLUME

Seismic velocities were compiled from many 2-D seismic and 3-D seismic surveys regardless of acquisition parameters. Since special processing such as migration or dip move out (DMO) can change the value of the measured velocity, a decision was made to choose data of similar processing stage throughout this study. All data is at the CSA stage (Current State of the Art) stage.

2.5.1.2 OBSERVATIONS MADE ON THE VELOCITY VOLUME

From the archival database a large number of CDPs were involved in the study. Each CDP had variable number of velocity picks in it. Each velocity pick was represented by the X coordinate, the Y coordinate, the time in millisecond and the velocity value. Each velocity pick was represented by a point in time with the corresponding coordinate and velocity value as a property. The result of this collection is shown in Figures 2.2 and 2.3.

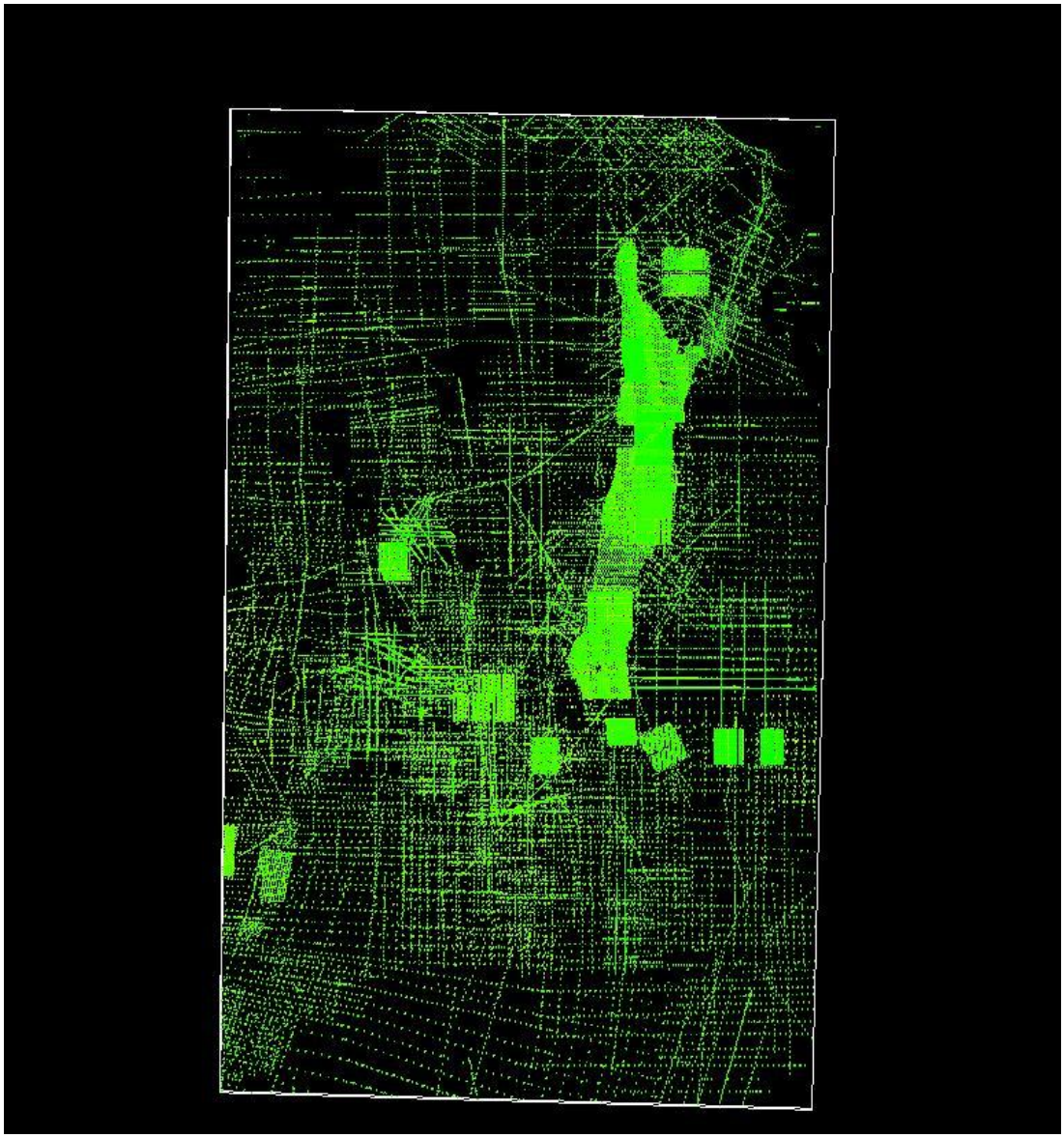

Figure 2.2 The compiled velocity points data represented in 2-D

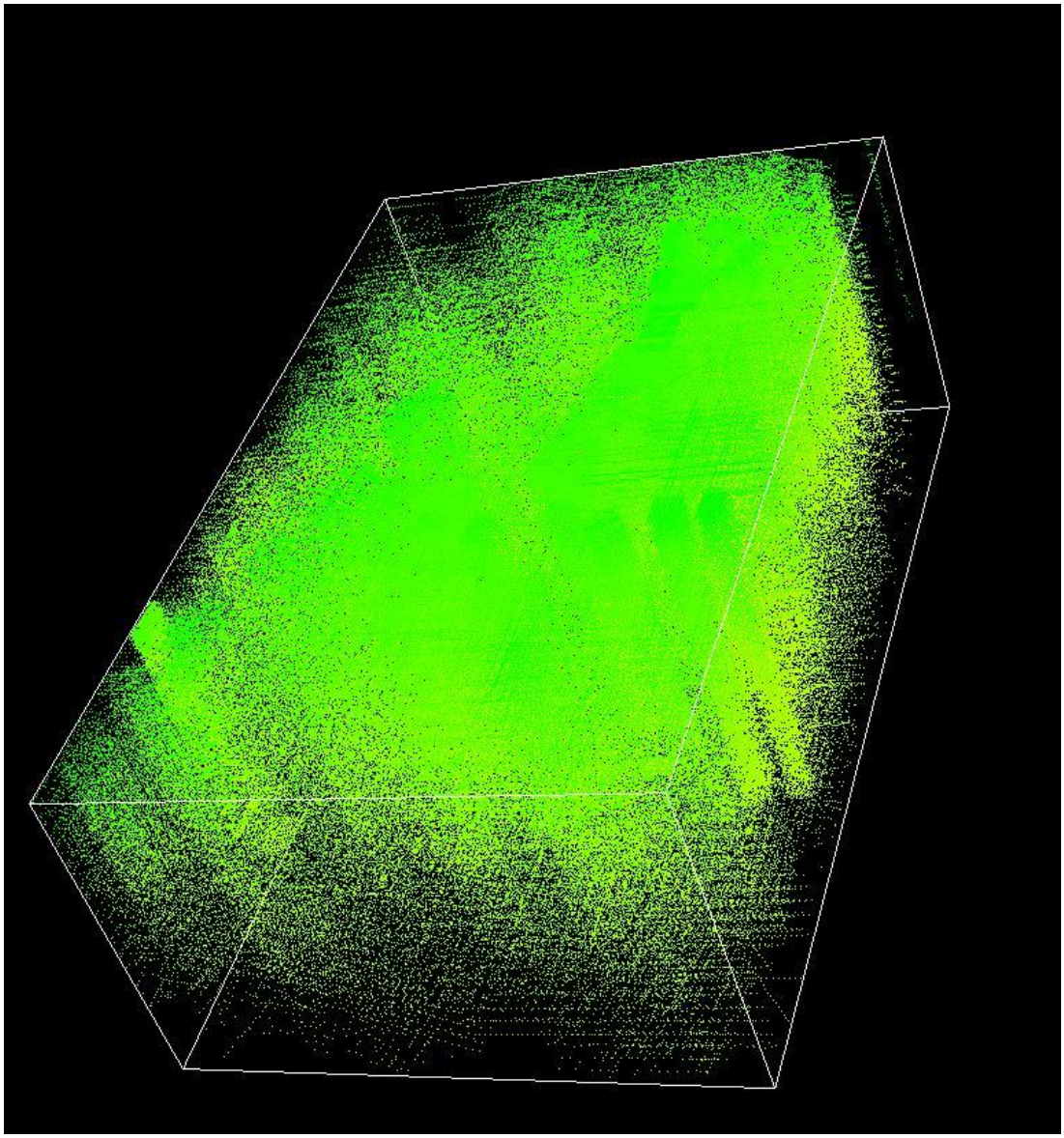

Figure 2.3 The compiled velocity points data represented in 3-D

Within this region, a total number of 1,410,430 points were collected. Each point is represented by location and velocity. Each point has an X coordinate, a Y coordinate, the corresponding time and the measured velocity at that time (Figure 2.3). When color coding the velocity picks based on the value of the velocity where each value is represented by a color, a different looking representation of the cube was obtained (Figure 2.4). The main purpose of color coding the velocity as a property is to use it as a

visual tool of checking the quality of the data and possibly make observations of the velocity patterns in the cube (Figure 2.5). All of these velocity picks are picked between the value of zero to 4000 milliseconds.

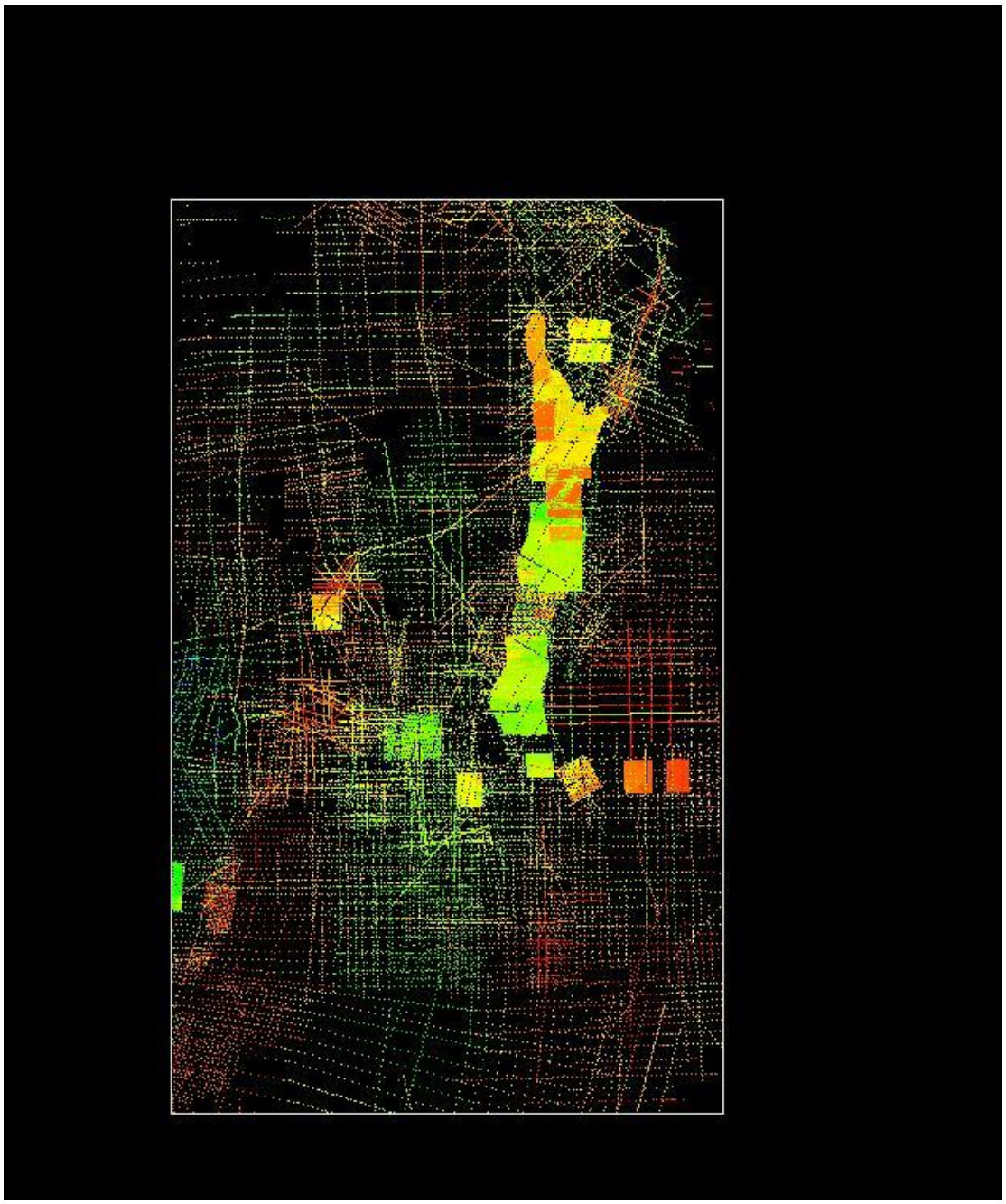

Figure 2.4 The velocity data points color coded and represented in 2-D

A few observations can be made from those pictures. When exaggerating the time axis, a more meaningful explanation is obtained instead of a simple map view image.

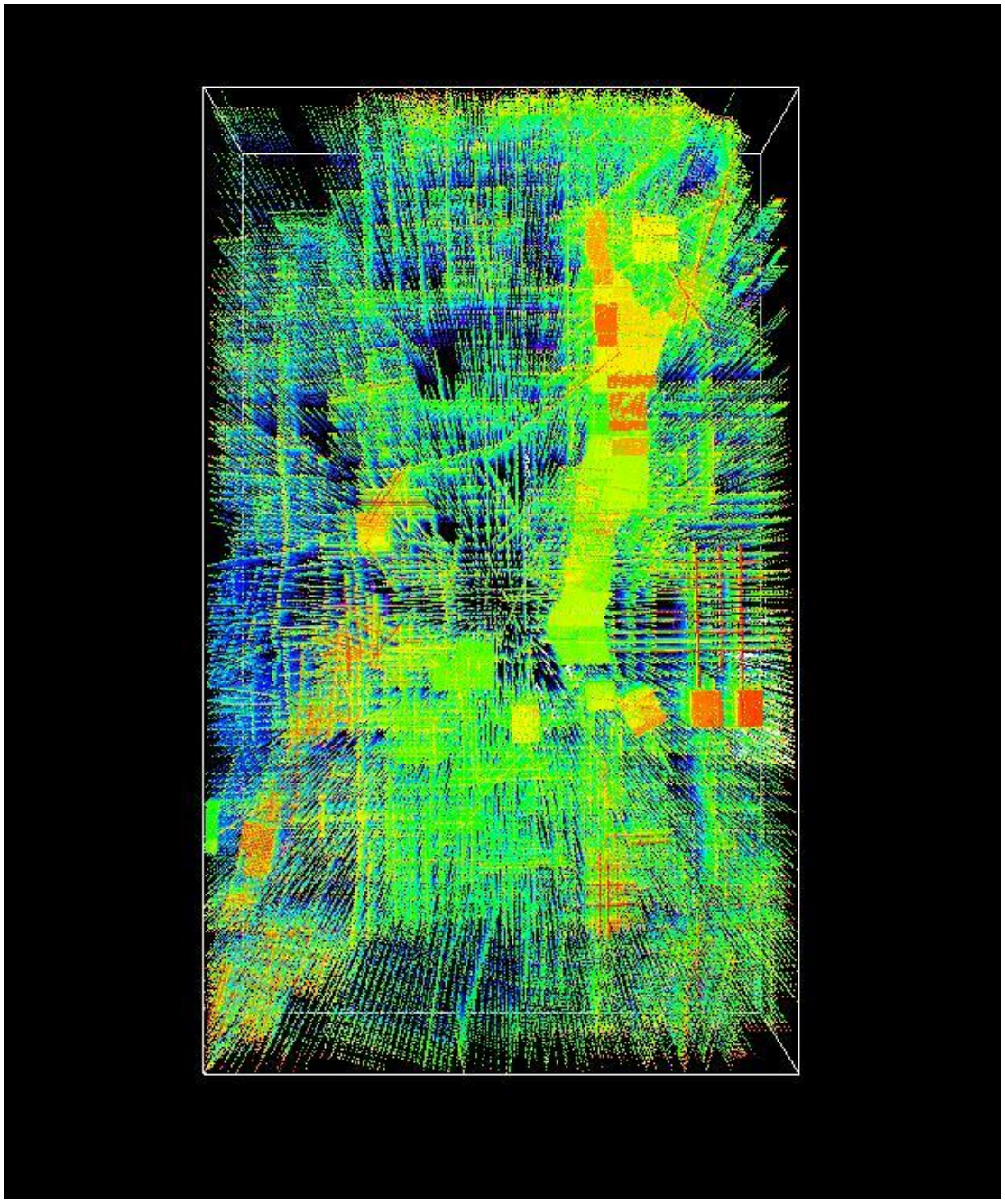

Figure 2.5 The 3-D cube of the velocity points color coded to assist in checking the quality of the velocity picks

The color scale can give very meaningful interpretations when added to the picture (Figure 2.6).

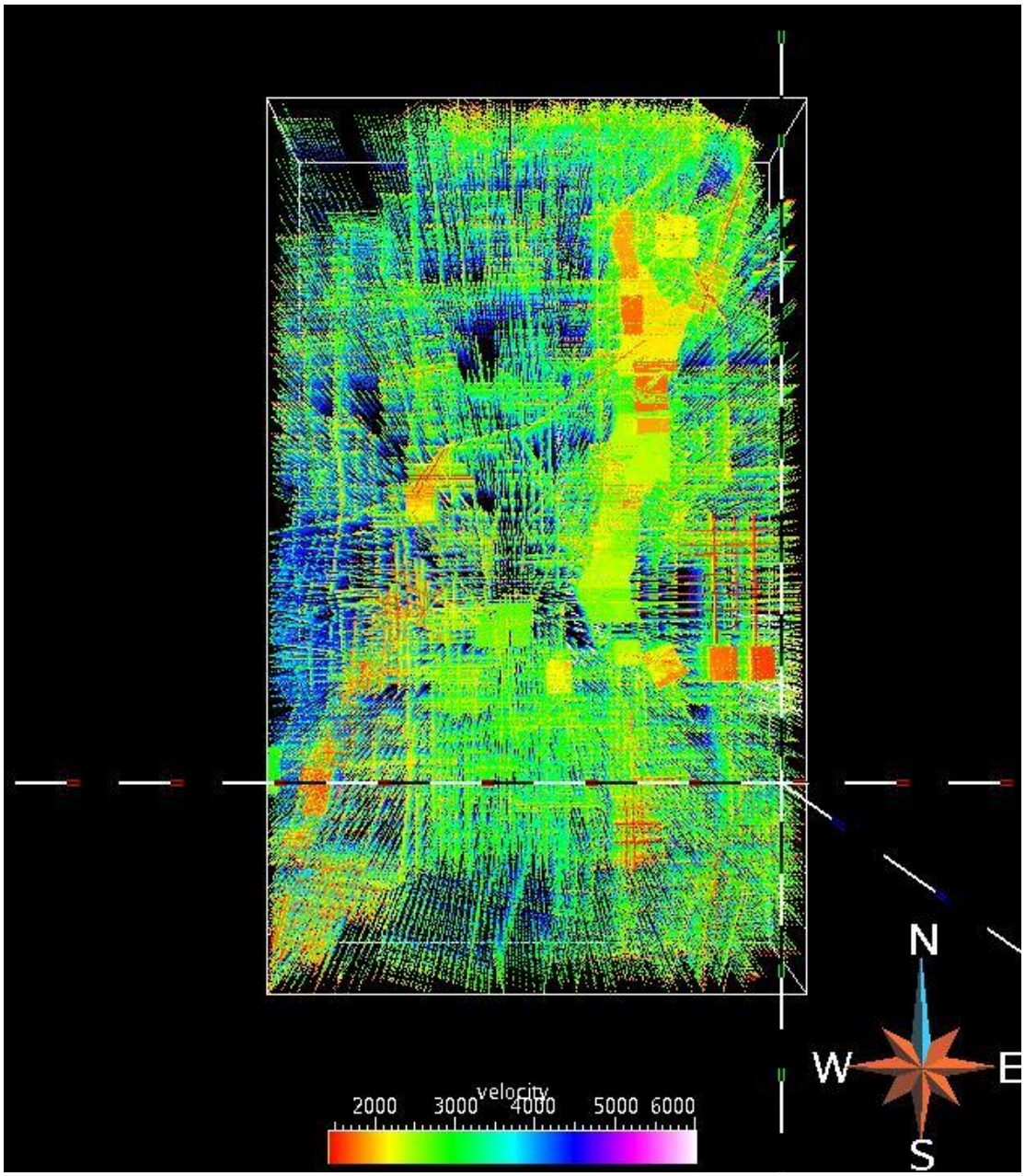

Figure 2.6 The velocity data points in a 3-D cube with the velocity scale color code as well as the direction of the cube and the 3-D dimension bars

First, when a map view is imposed, it becomes obvious that the velocity starts at different values. Also, not all lines start their picks at a time value of zero. Some lines have started

the first time pick at a velocity value of 1400 m/s and some others started at 2000 m/s. Other lines have also shown different values.

An obvious observation is that the velocity coverage over the region is varying from one area to another. Some areas are densely covered with seismic velocity picks and some other areas are less dense. The areas that are covered with 3-D seismic surveys stand out very obviously in the display due to the fact that 3-D seismic surveys are associated with more detailed and well covered seismic velocity picks (Figure 2.7).

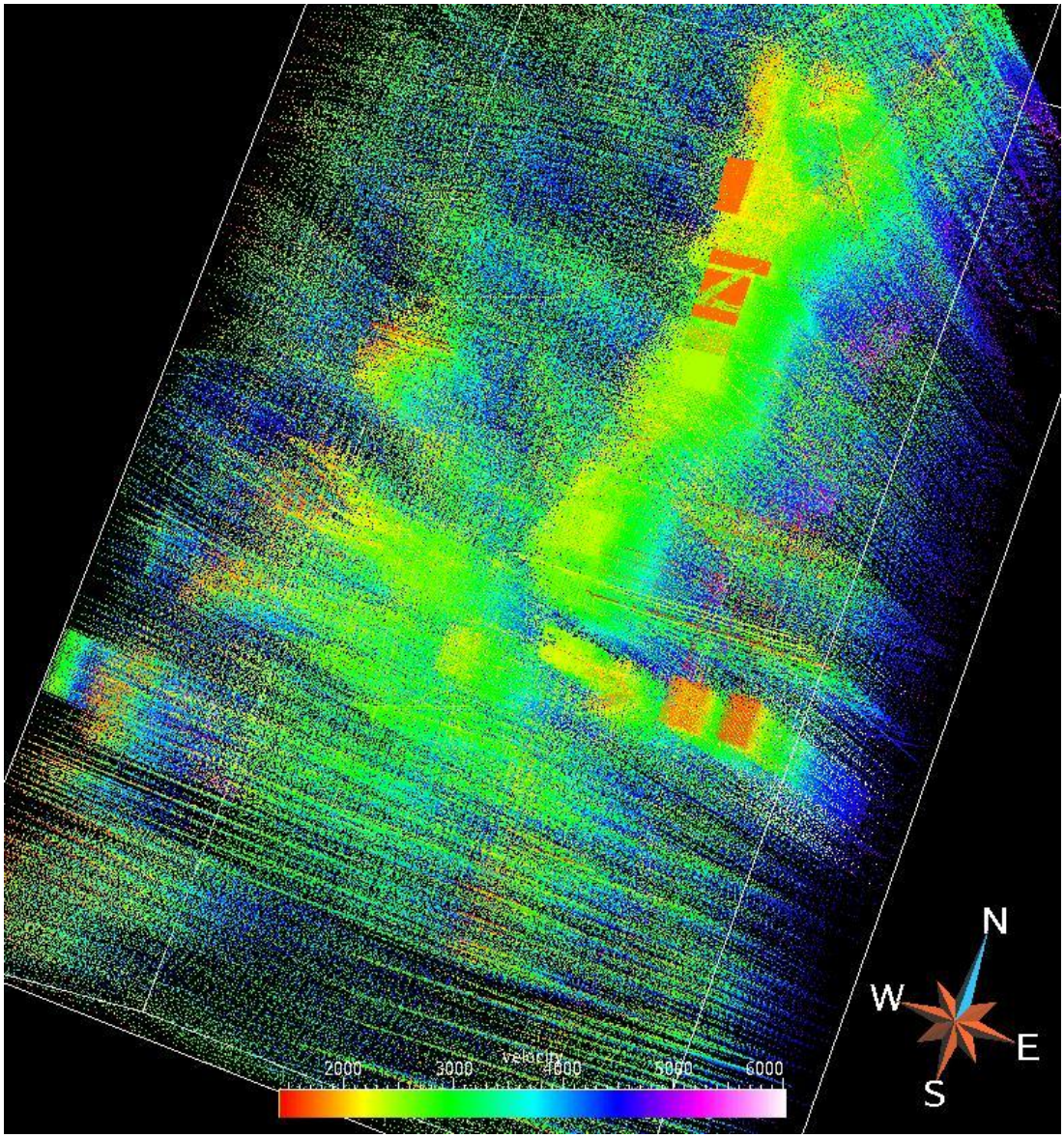

Figure 2.7 The 3-D cube indicating variable data density from one area to another

Processing preferences using exact picks or using interpolated picks at consistent time windows or what is called the (Auto picker) show very clearly in the surveys where the Auto picker has been used (Figure 2.8).

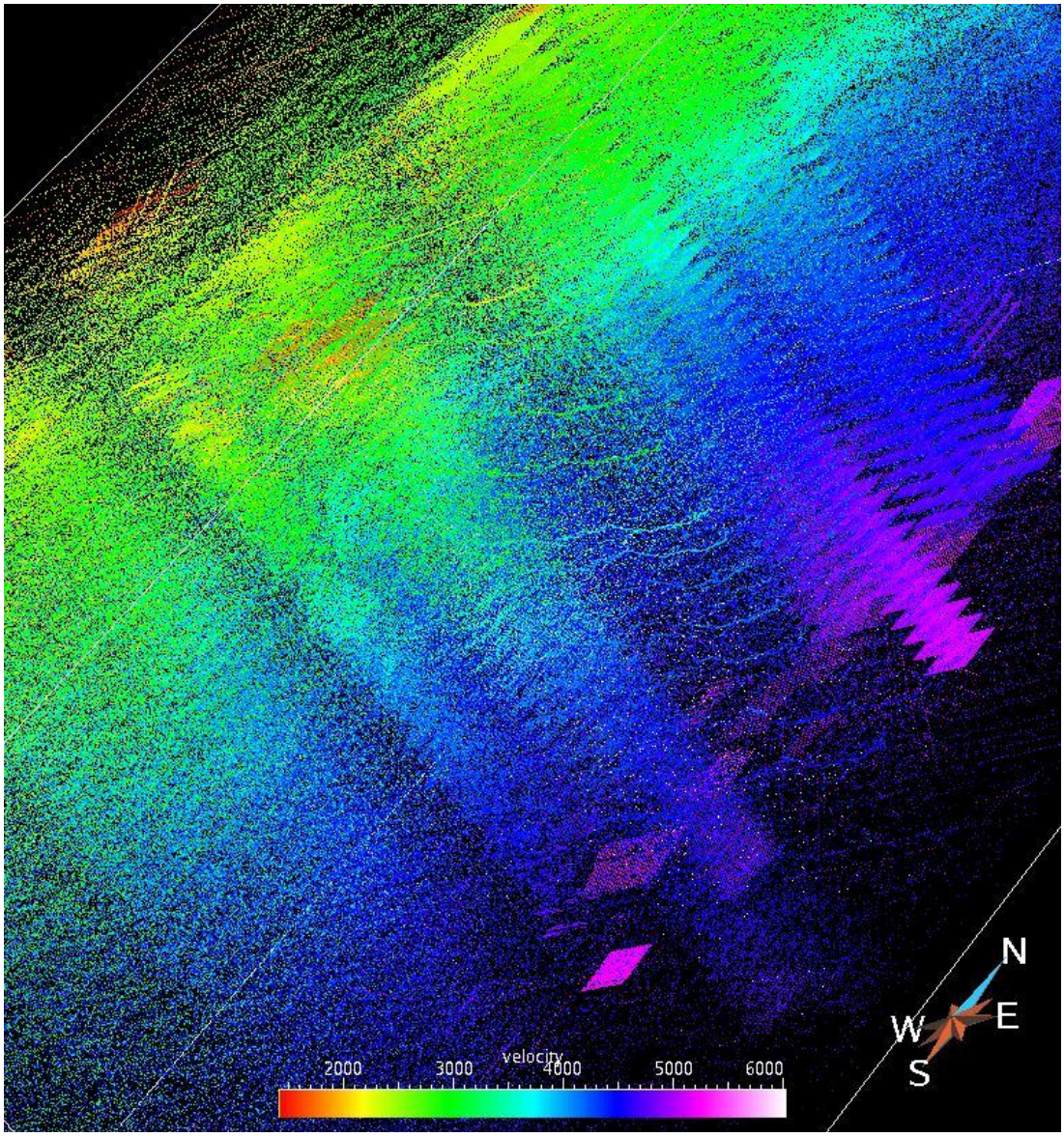

Figure 2.8 A prominent effect of the auto-picker appears in some of the 3-D seismic surveys

This observation can lead the study into resolving an ongoing controversy whether or not the auto picker can be erroneous. Some Auto pickers have been set at a time window of 150 milliseconds and some others at 200 milliseconds, it is just a matter of the processor's preference.

another observation is that the majority of picks don't have such high values up to 5000 m/s unless it is a velocity pick towards the very bottom of seismic surveys (Figure 2.9).

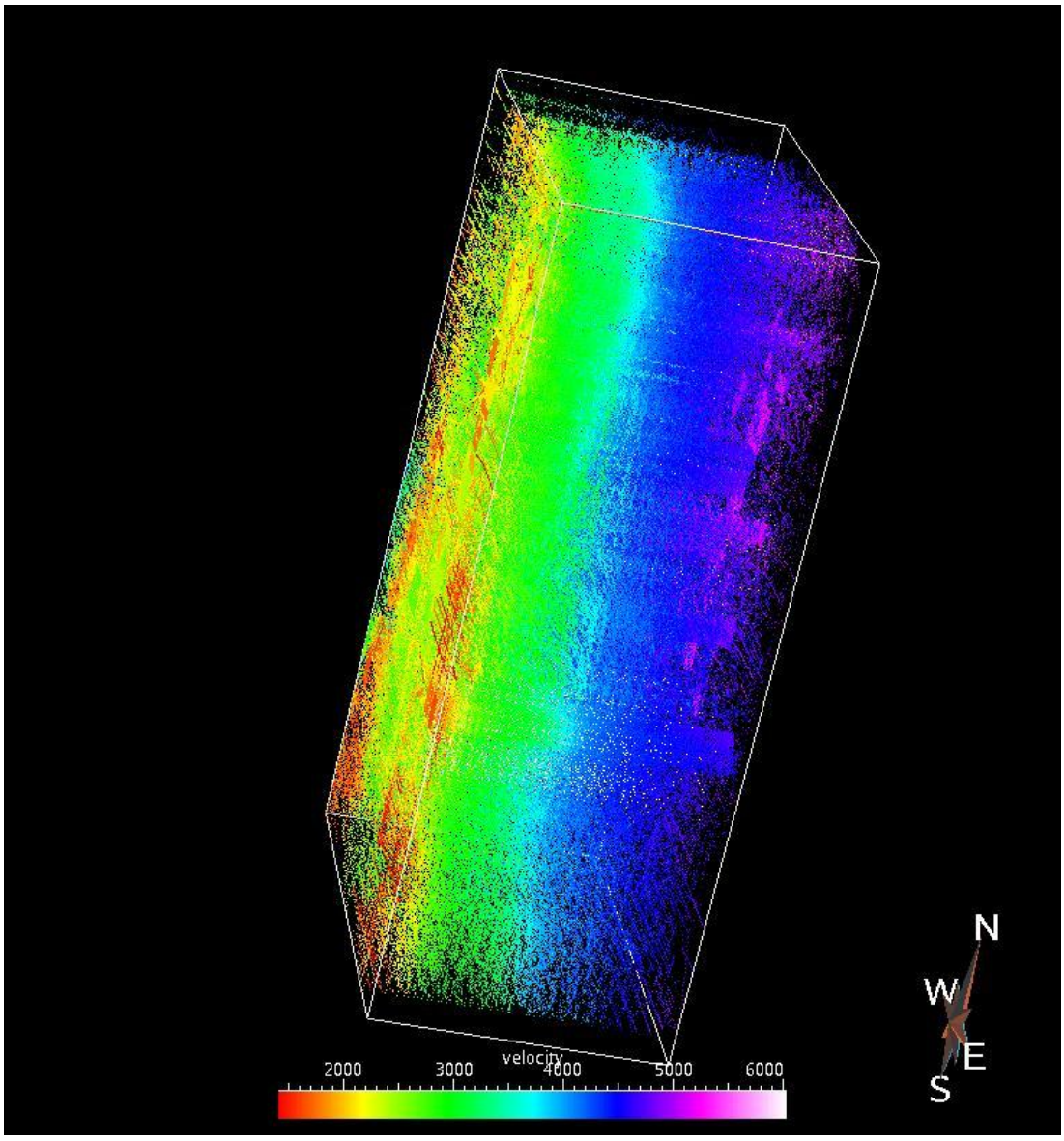

Figure 2.9 A side view of the 3-D velocity data points cube indicating the velocity variation in time. A view from the east.

When investigating how the velocity color codes behave over the regional scale, it would be easy to tell that the velocities tend to follow the geological trends of the region outcropping west and following the structural and geomorphologic phenomena. (Figures 2.10 and 2.11).

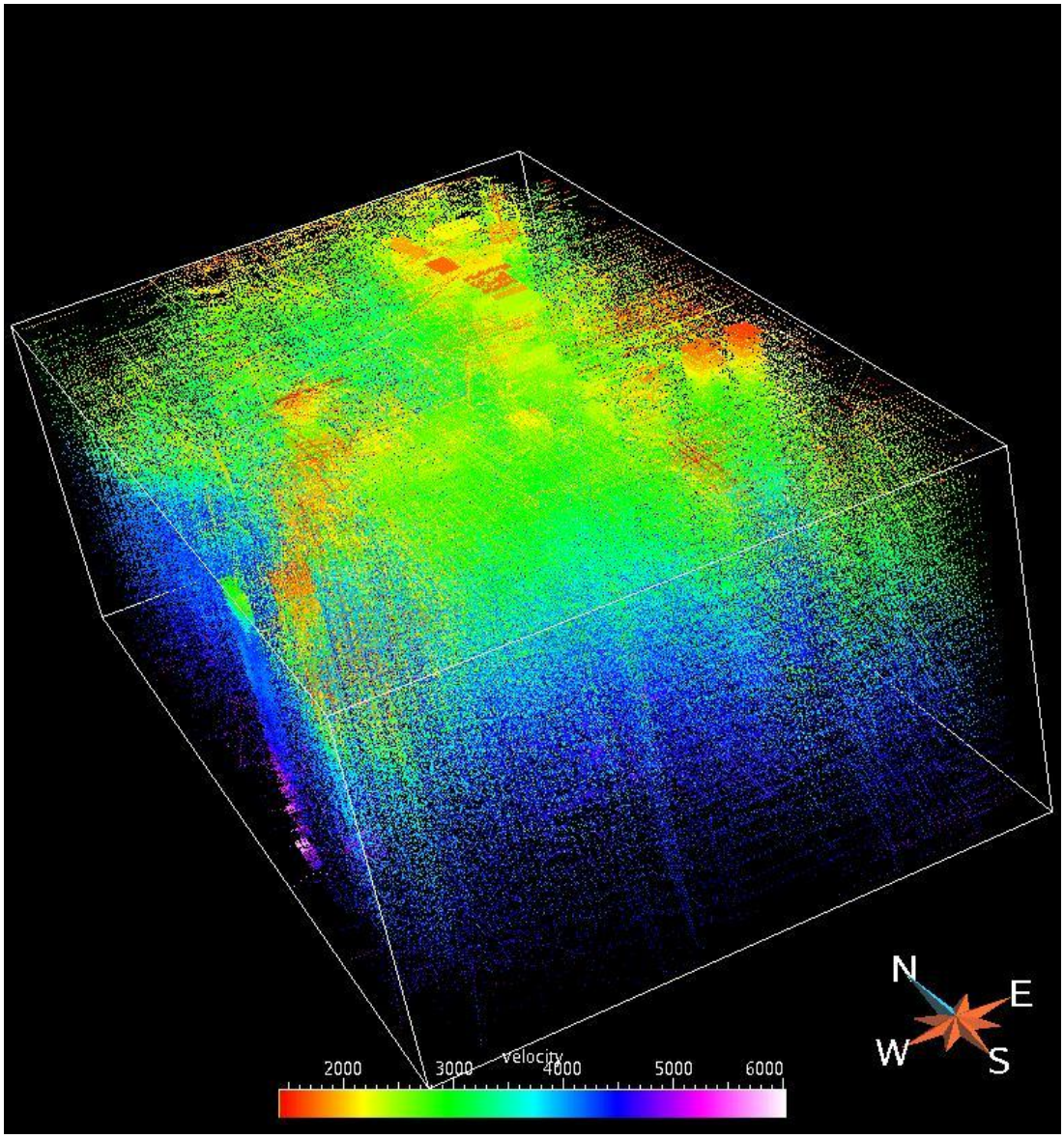

Figure 2.10 A side view of the 3-D velocity data points cube indicating the velocity variation in time. A view from the South West

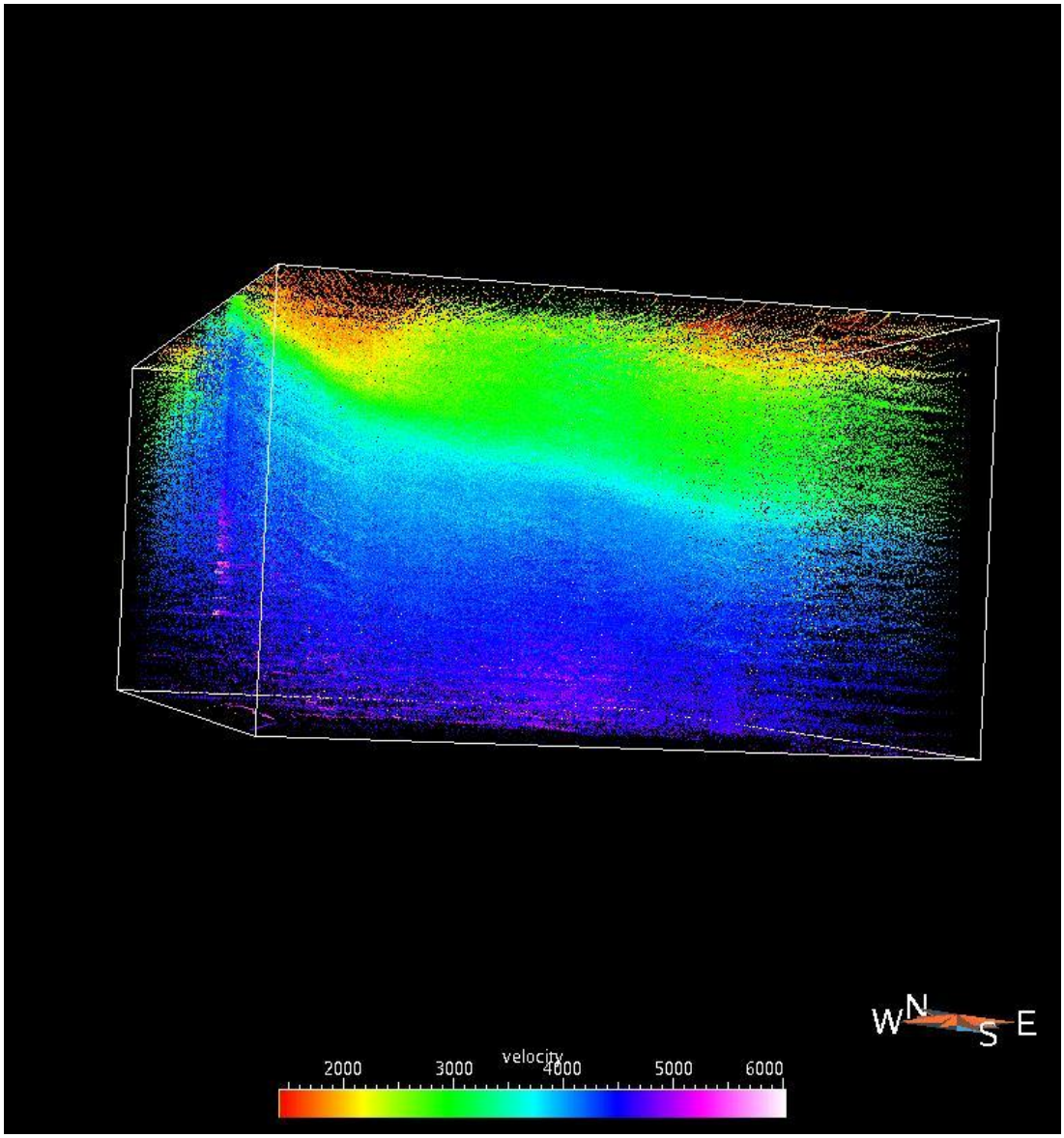

Figure 2.11 A side view of the 3-D velocity data points cube indicating the velocity variation in time. A view from the South. The east west regional dip is obvious through the velocity variation

2.5.2 Seismic time picks of key regional horizons

2.5.2.1 DIAGNOSING THE TIME PICKS

Seismic data interpretations were collected throughout the selected region (Figure 2.12). Those interpretations are given in time picks from seismic stacked sections for a number of key horizons that are quite prominent in the region. A total of seven key horizons were selected for the study. Those time picks were loaded in their corresponding X and Y coordinates as well as their representing time picks. Each pick was represented by a single point.

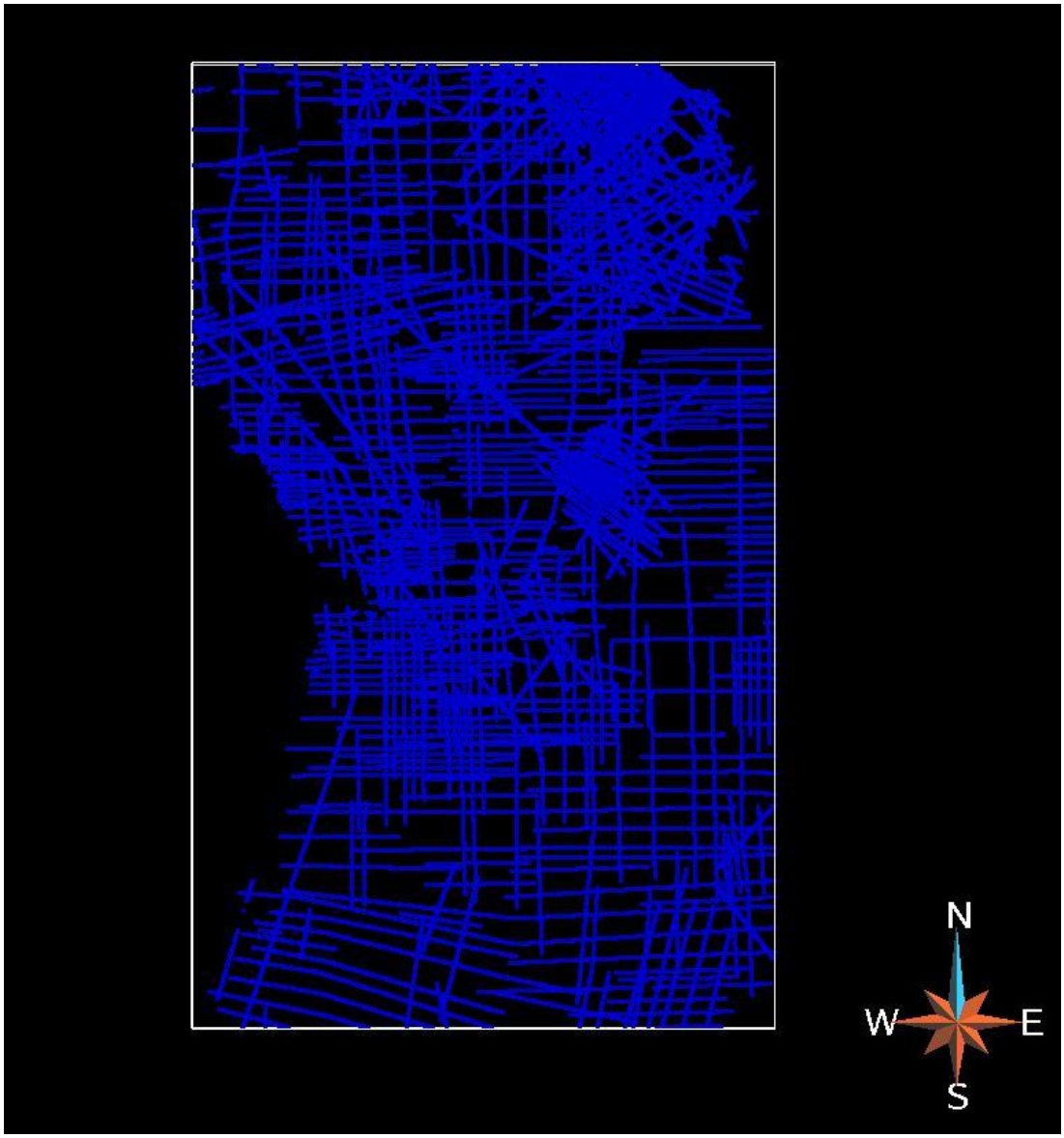

Figure 2.12. A collection of all the regional time picks in time.

Even though these points might appear like they are lines, taking a zoomed view at those points will show the actual point representation of those time picks (Figure 2.13). They will appear more as points when zoomed further (Figures 2.14-2.16).

Figure 2.13. A zoomed collection of all the regional time picks in time.

Figure 2.14. A further zoomed collection of all the regional time picks in time.

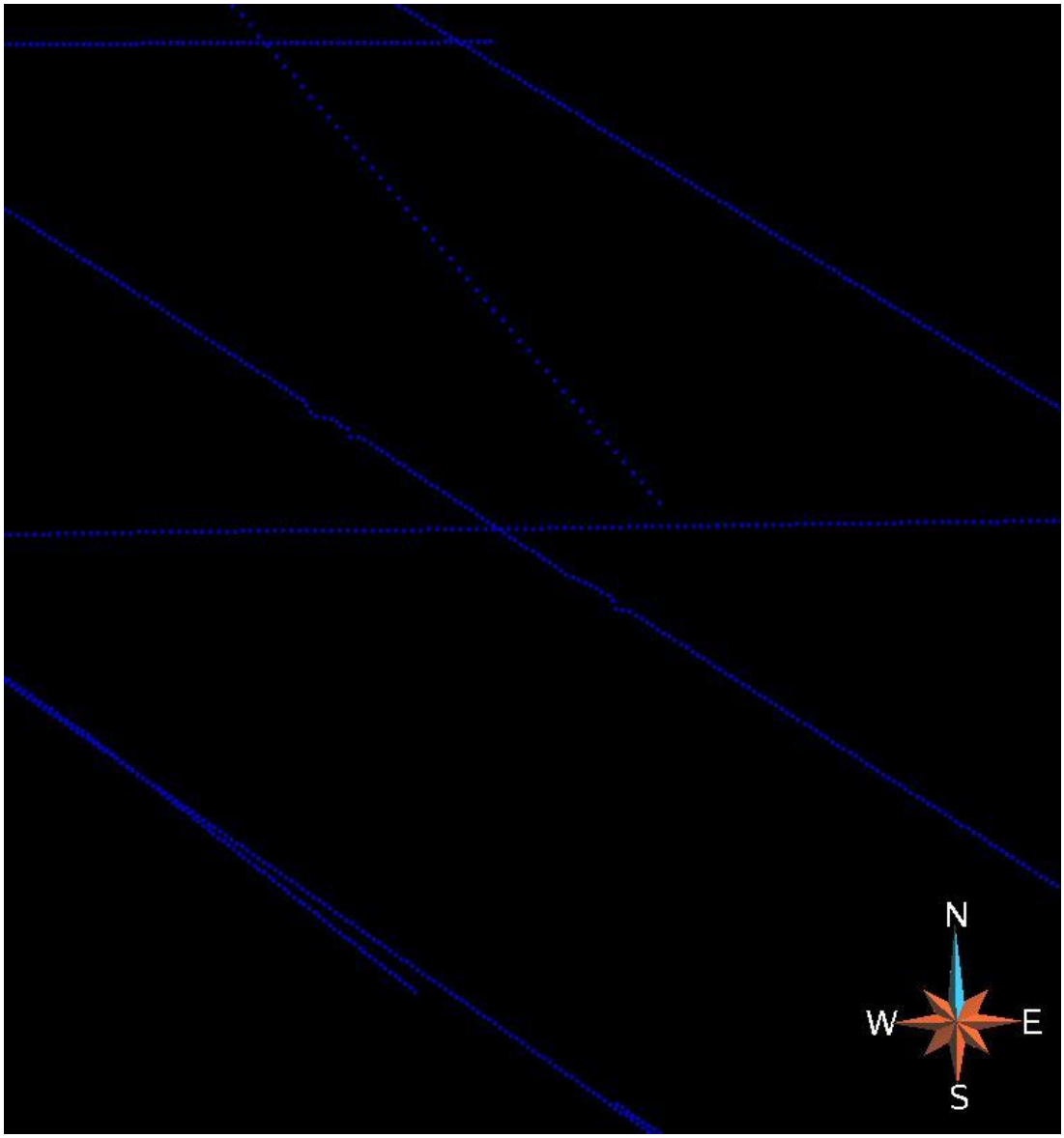

Figure 2.15 A detailed zoomed collection of all the regional time picks in time.

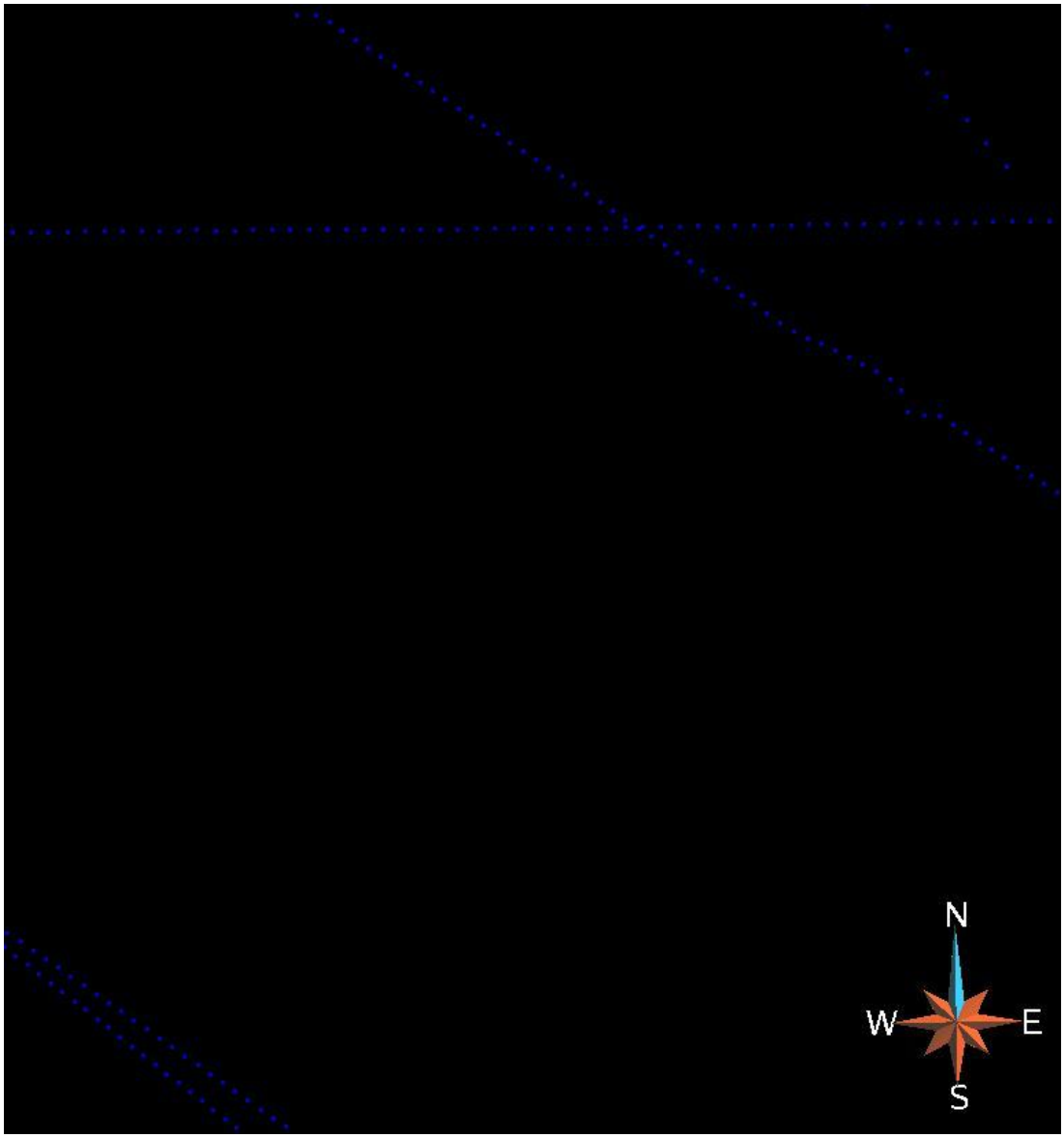

Figure 2.16. A detailed zoomed collection of all the regional time picks in time that show the time picks as points.

2.5.2.2 OBSERVATIONS MADE ON THE TIME PICKS

Time picks points are somewhat evenly spaced due to the Auto picker used to make these picks throughout a seismic section. Most of these points were collected from 2-D seismic lines that were done for regional studies or 2-D lines that were long enough to give such large scale interpretations. 3-D seismic surveys are usually localized and do not extend to cover regional studies of seismic horizons and thus they are rarely used for regional studies.

Horizon 1

A total of 727,511 time picks corresponding to Horizon 1 were collected throughout the region. Those picks are well distributed throughout the assigned region of study (Figure 2.17).

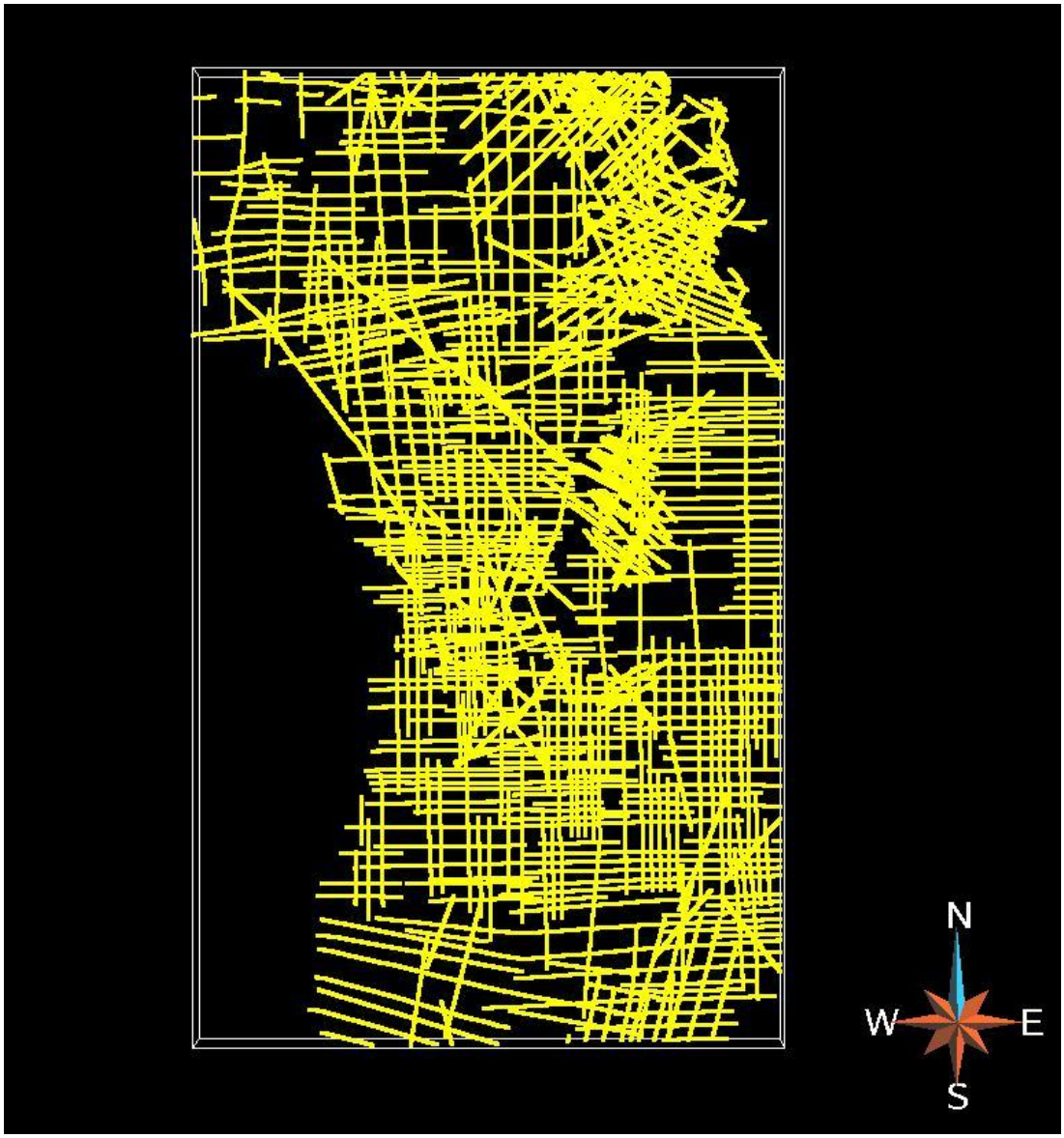

Figure 2.17. The collected time picks for Horizon 1

When color coding the Z axis to show the time picks distribution it becomes obvious that these picks dip east following a regional trend (Figure 2.18).

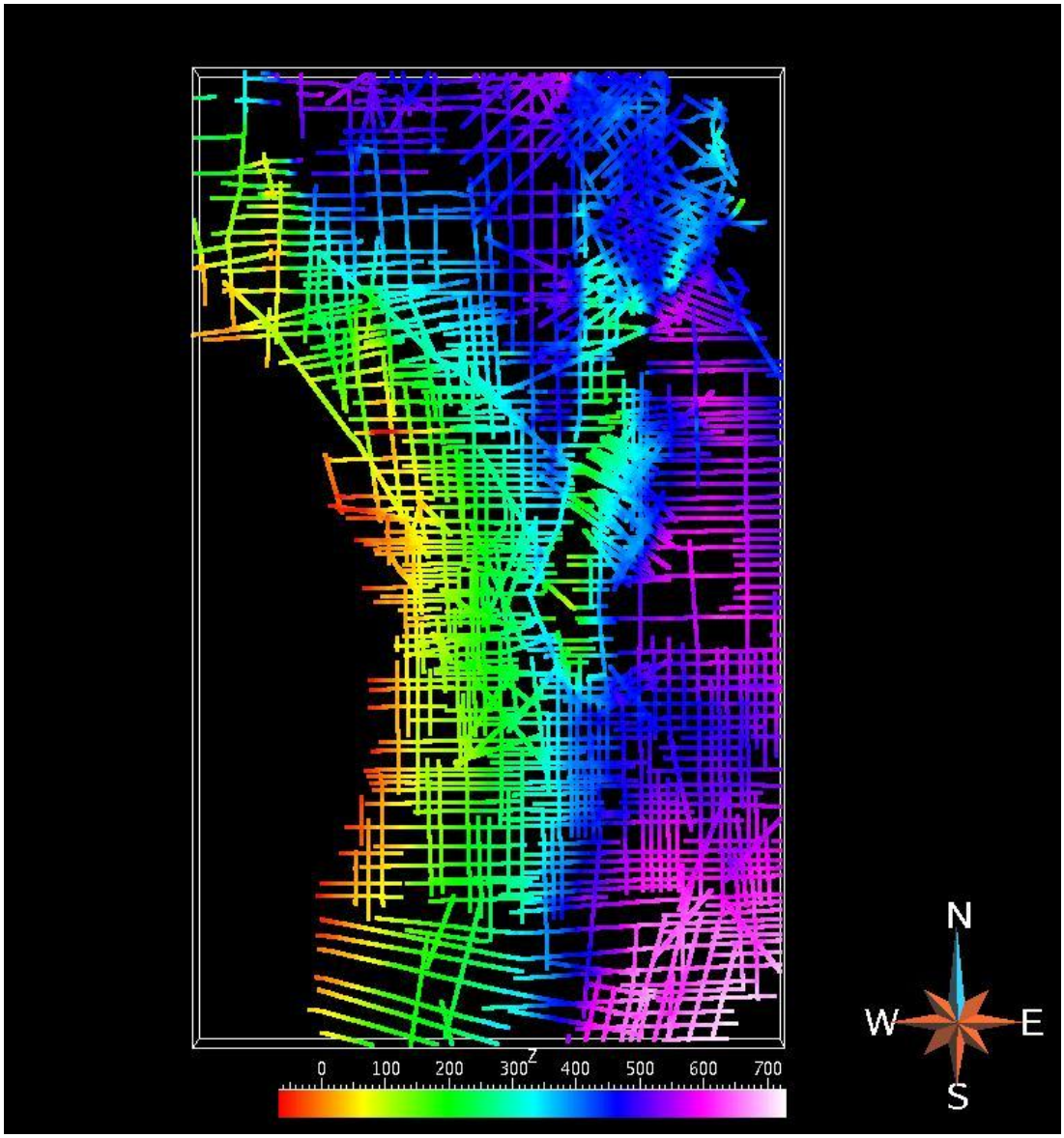

Figure 2.18. The collected time picks for Horizon 1 with the Z axis (time in ms) color coded

Horizon 2

Atotal of 844,359 time picks corresponding to Horizon 2 were collected. Those picks are well distributed throughout the assigned region of study (Figure 2.19).

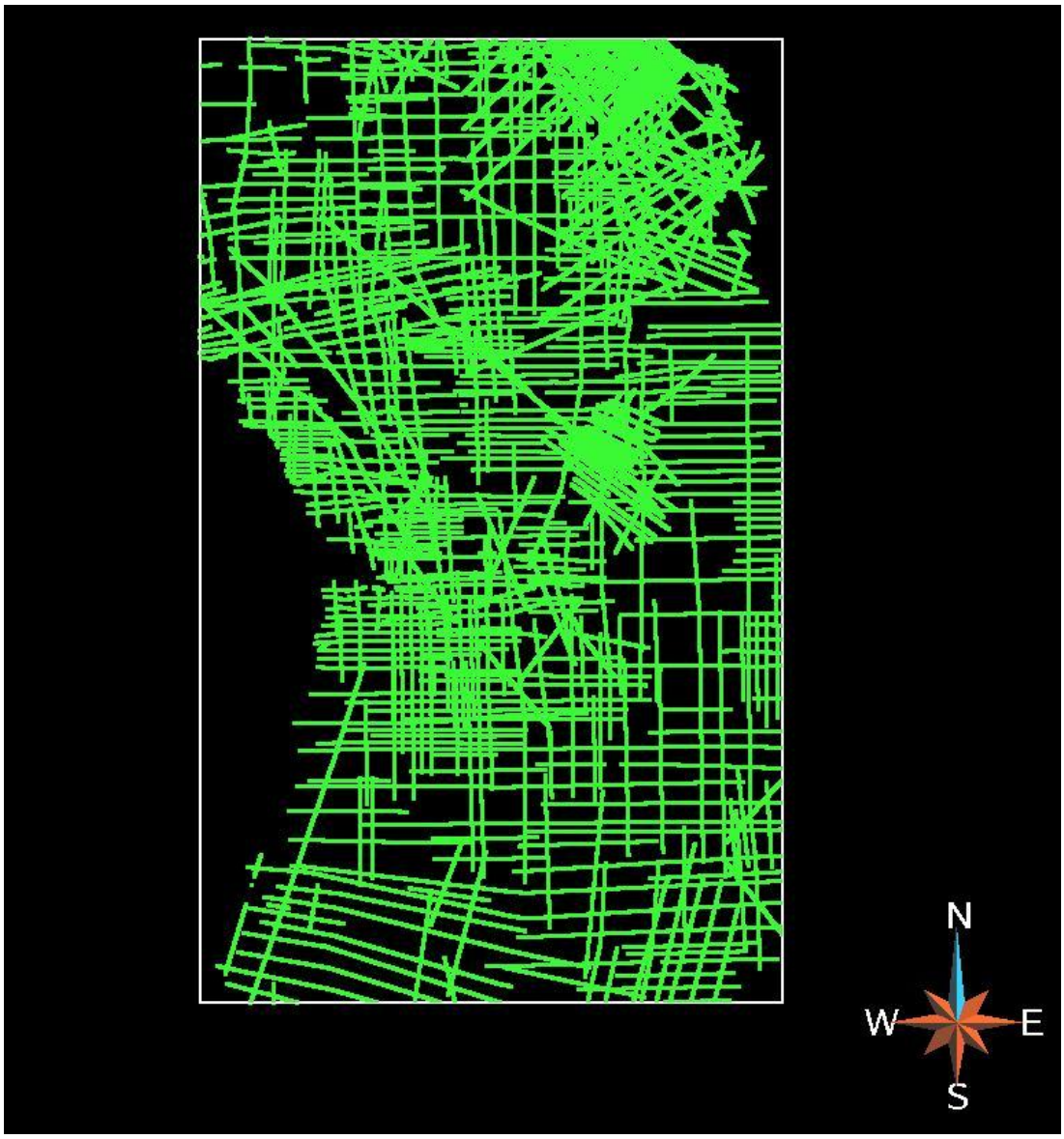

Figure 2.19. The collected time picks for Horizon 2

When color coding the Z axis to show the time picks distribution it becomes obvious that these picks dip east following a regional trend (Figure 2.20).

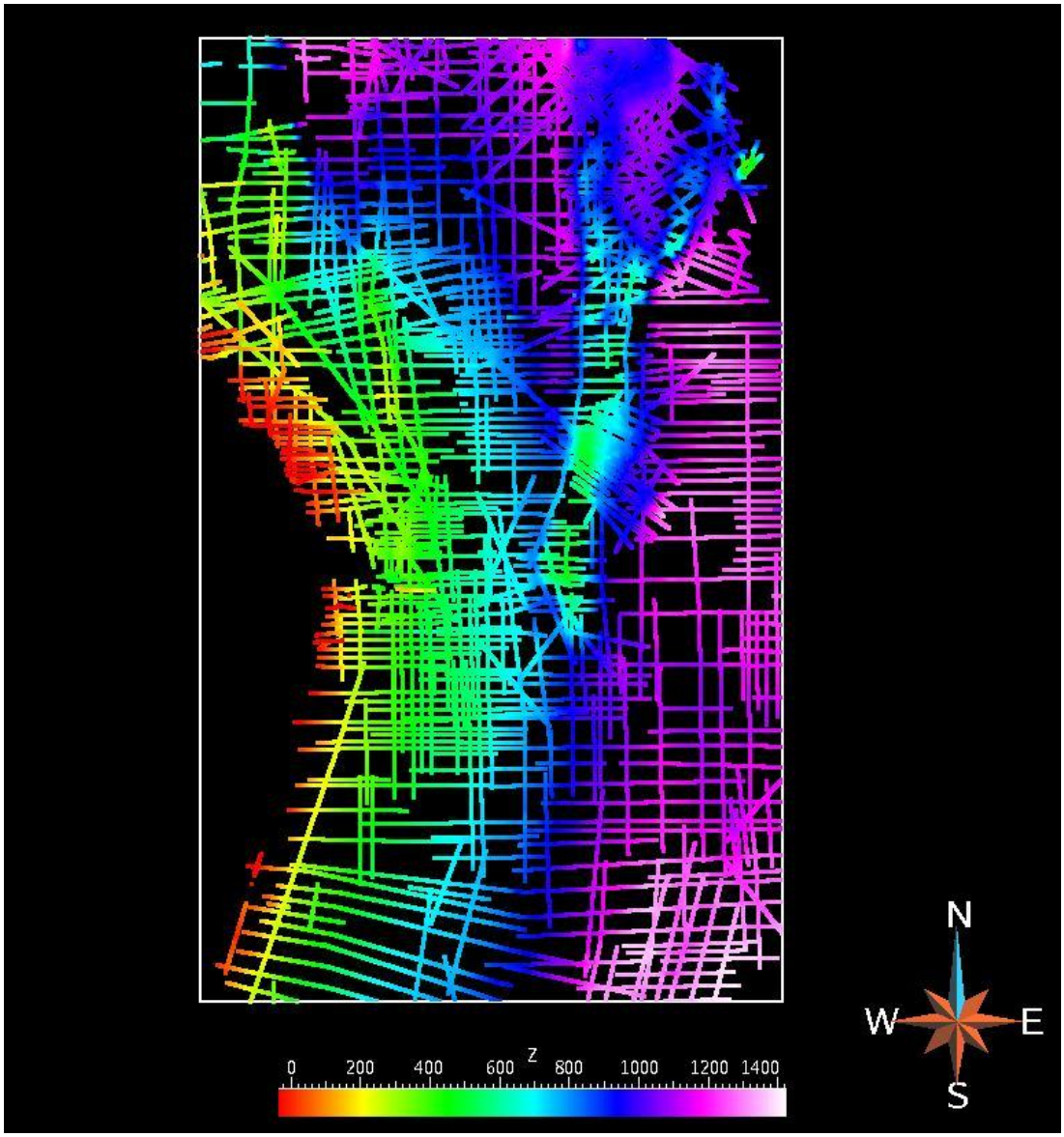

Figure 2.20. The collected time picks for Horizon 2 with the Z axis (time im ms) color coded

Horizon 3

A total of 909,565 time picks corresponding to Horizon 3 were collected. Those picks are well distributed throughout the assigned region of study (Figure 2.21).

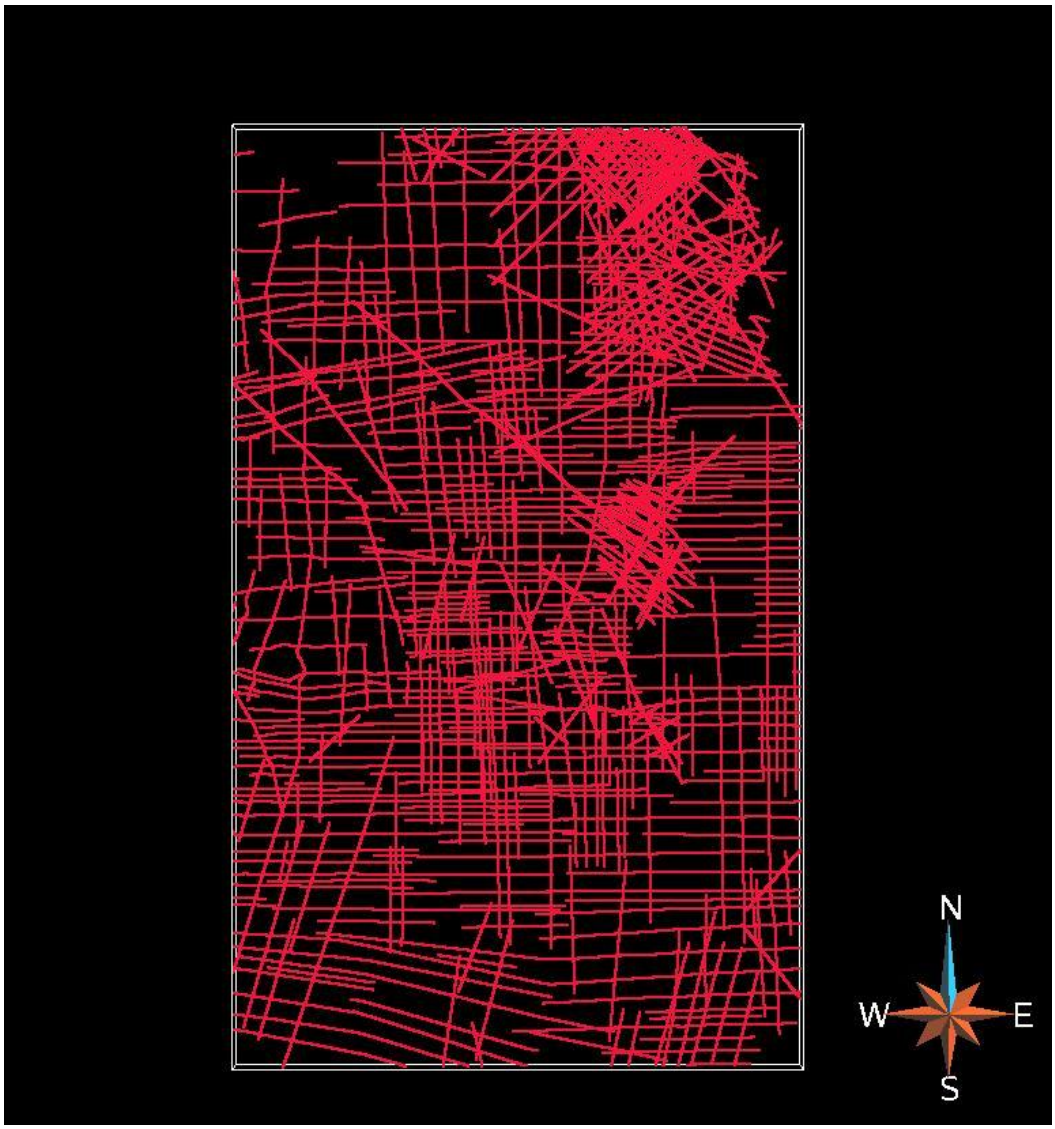

Figure 2.21. The collected time picks for Horizon 3

When color coding the Z axis to show the time picks distribution it becomes obvious that these picks dip east following a regional trend (Figure2.22).

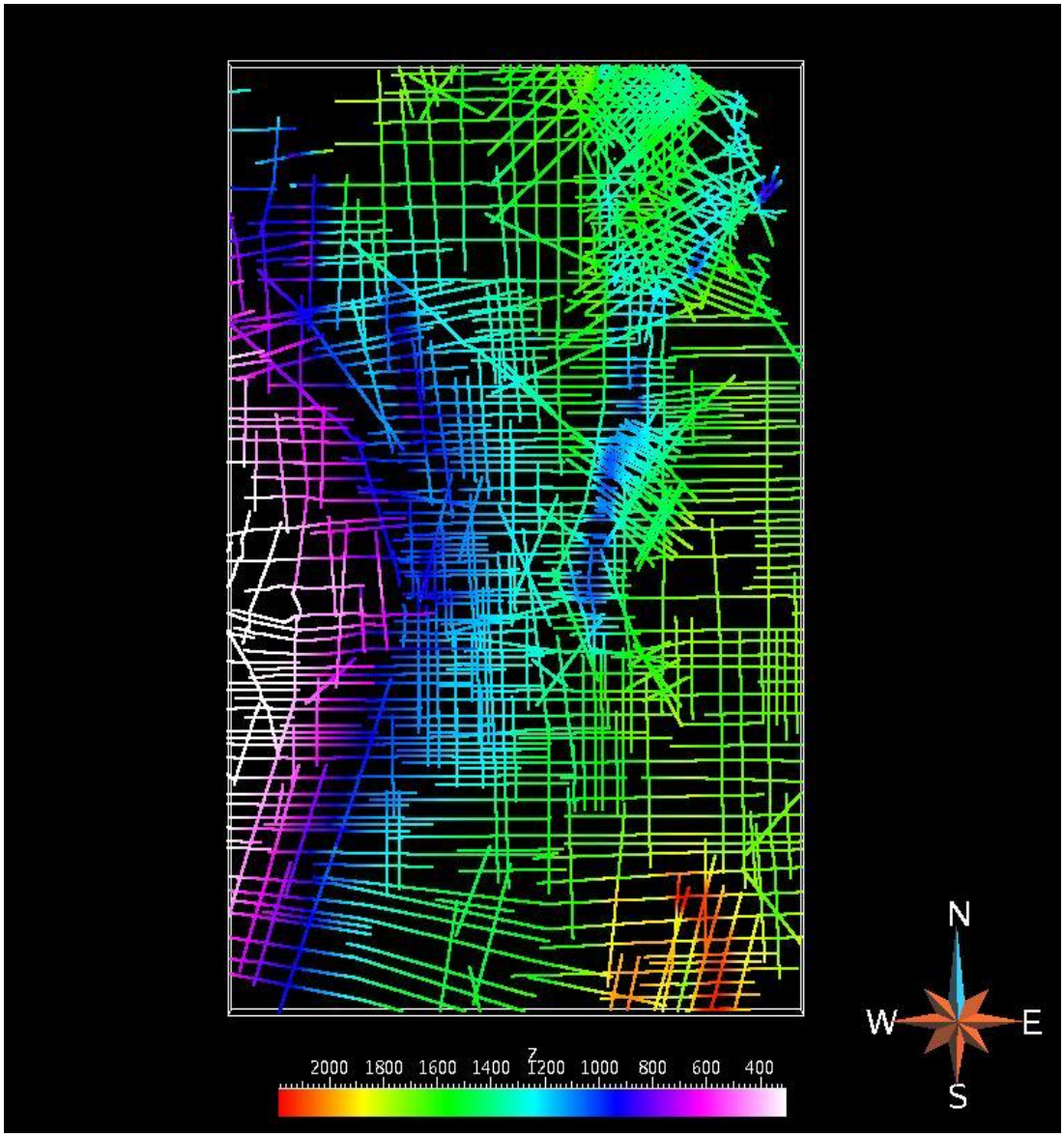

Figure 2.22. The collected time picks for Horizon 3 with the Z axis (time in ms) color coded

Horizon 4

A total number of 754,917 time picks corresponding to Horizon 4 were collected. Those picks are well distributed throughout the assigned region of study (Figure 2.23).

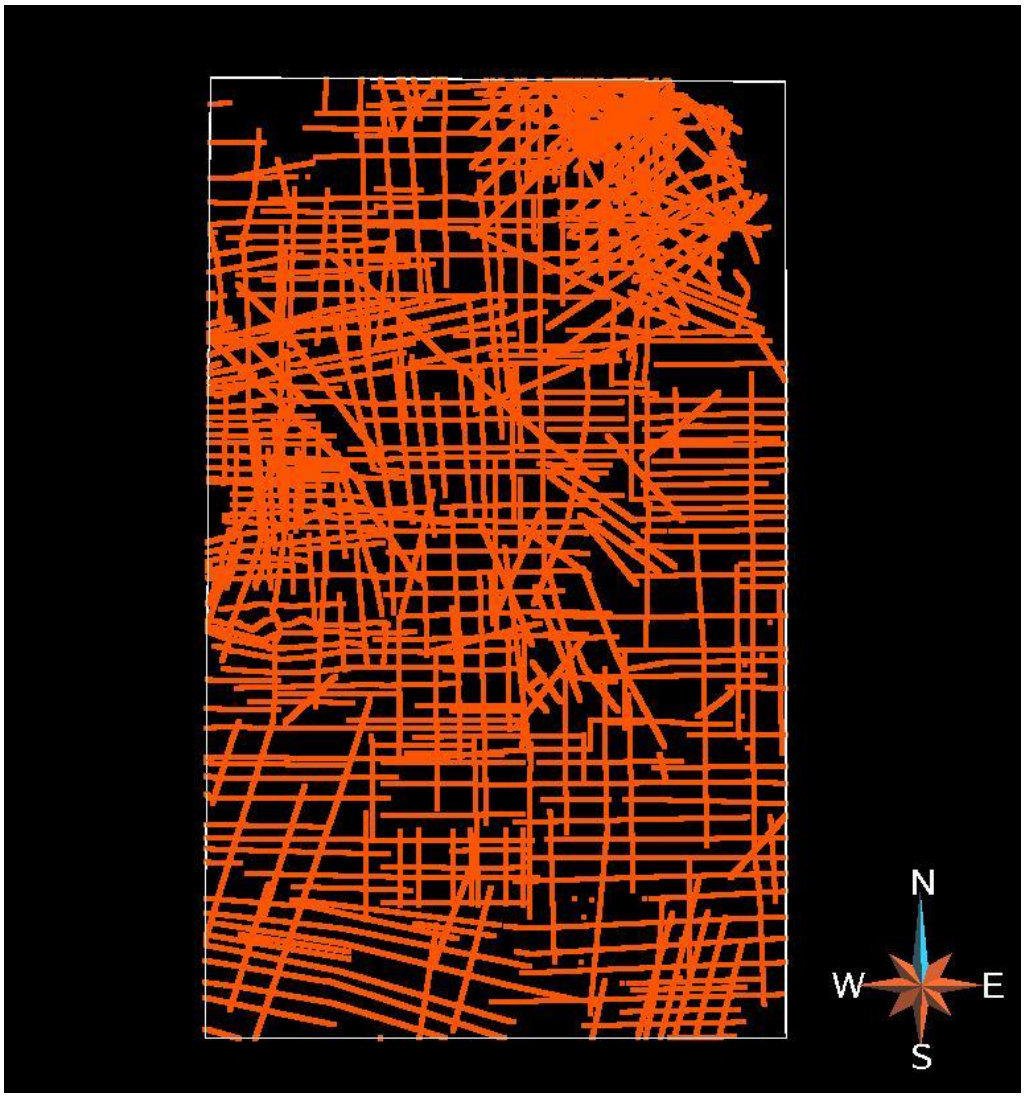

Figure 2.23. The collected time picks for Horizon 4

When color coding the Z axis to show the time picks distribution it becomes obvious that these picks dip east following a regional trend (Figure 2.24).

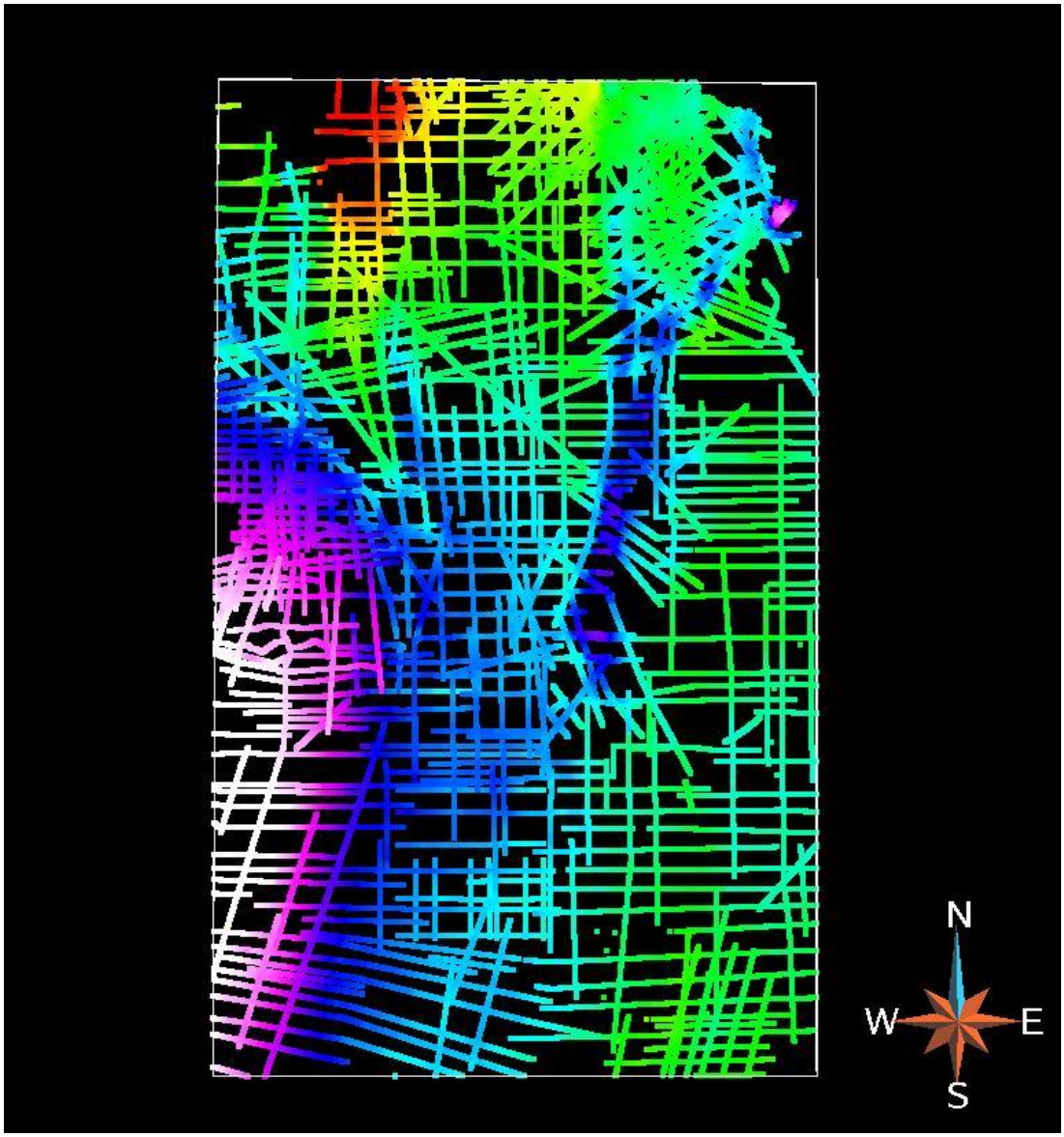

Figure 2.24. The collected time picks for Horizon 4 with the Z axis (time in ms) color coded

Horizon 5

A total number of 888,435 time picks corresponding to Horizon 5 were collected. Those picks are well distributed throughout the assigned region of study (Figure 2.25).

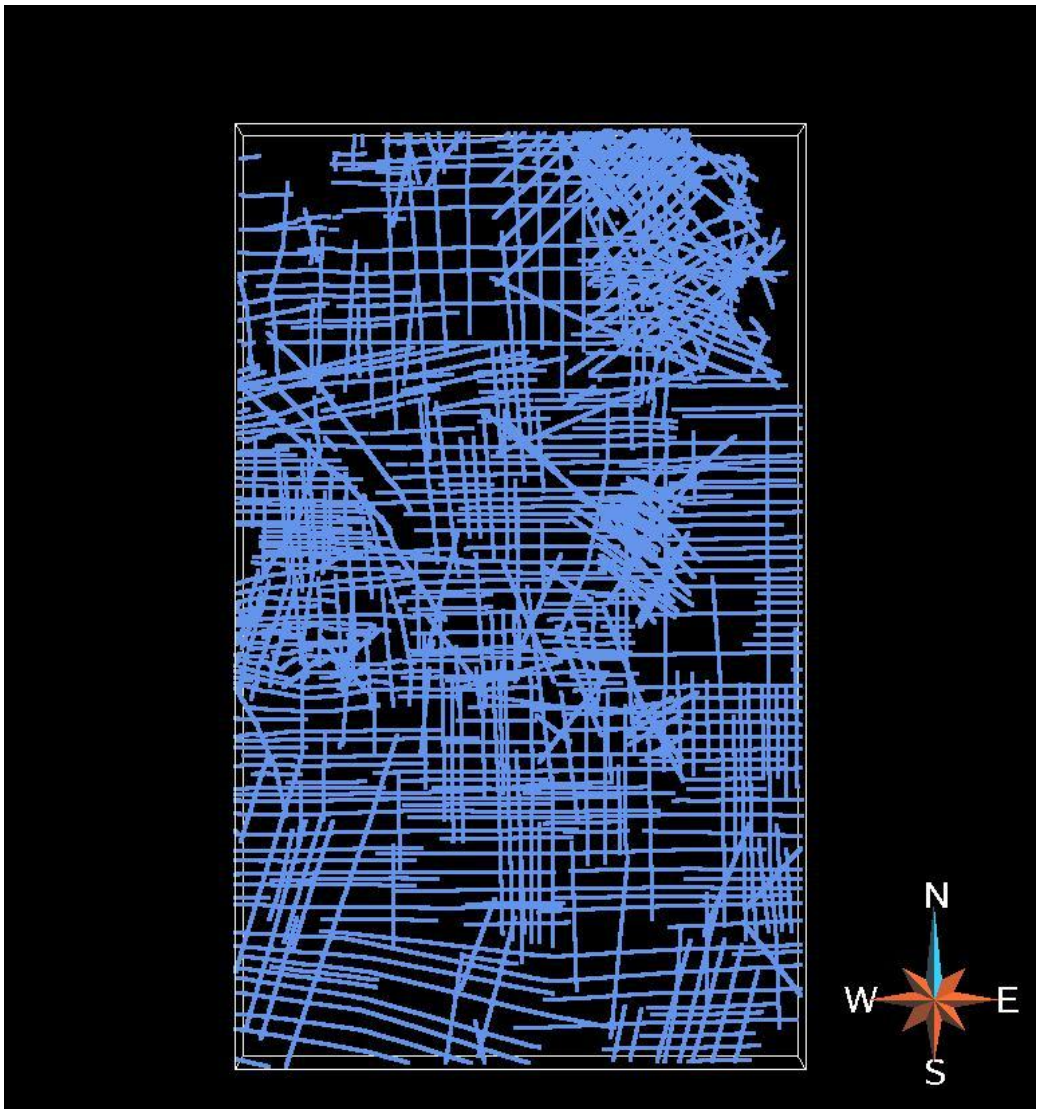

Figure 2.25. The collected time picks for Horizon 5

When color coding the Z axis to show the time picks distribution it becomes obvious that these picks dip east following a regional trend (Figure 2.26).

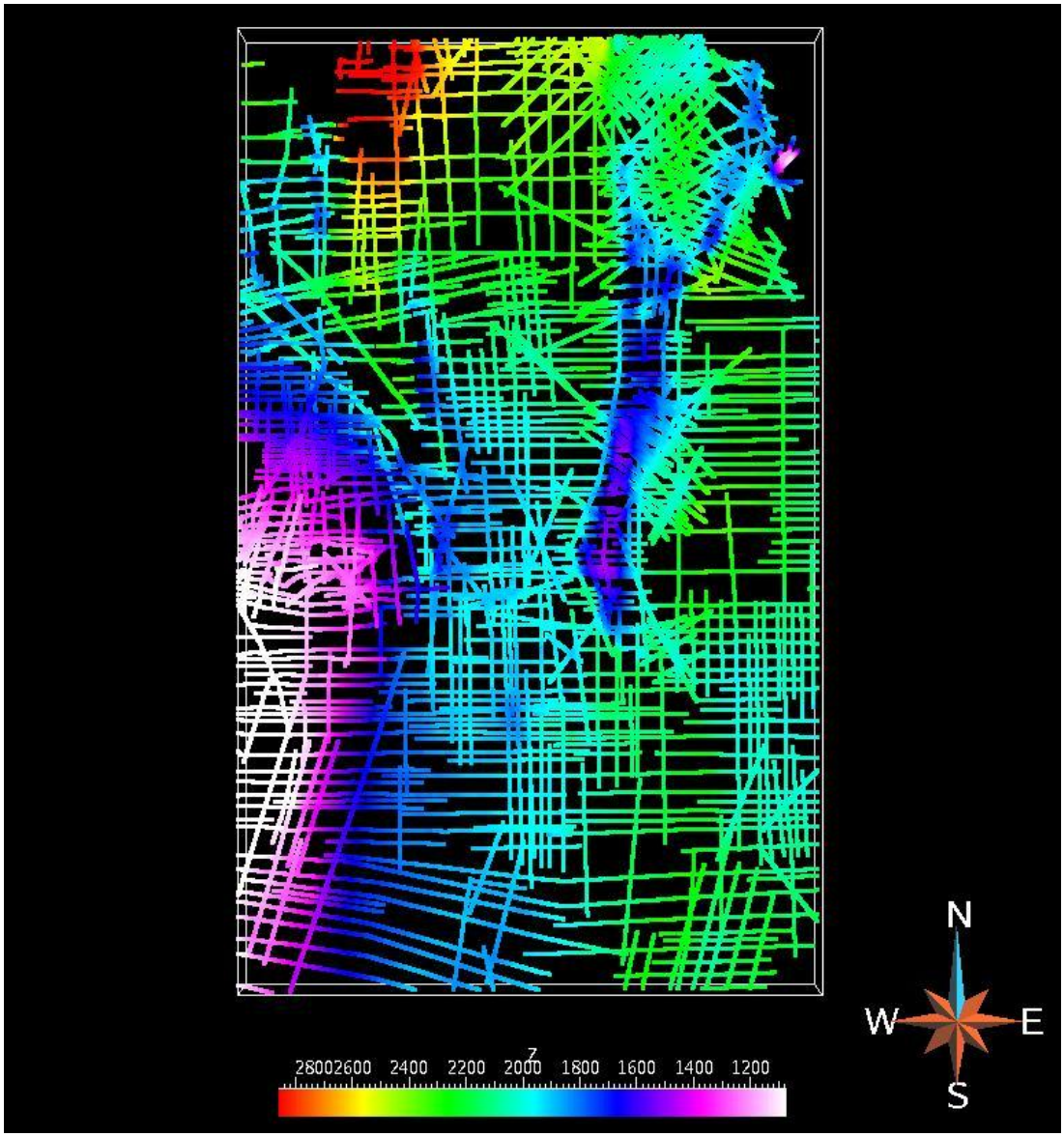

Figure 2.26. The collected time picks for Horizon 5 with the Z axis (time in ms) color coded

Horizon 6

A total number of 689,931 time picks corresponding to Horizon 6 were collected. Those picks are well distributed throughout the assigned region of study (Figure 2.27).

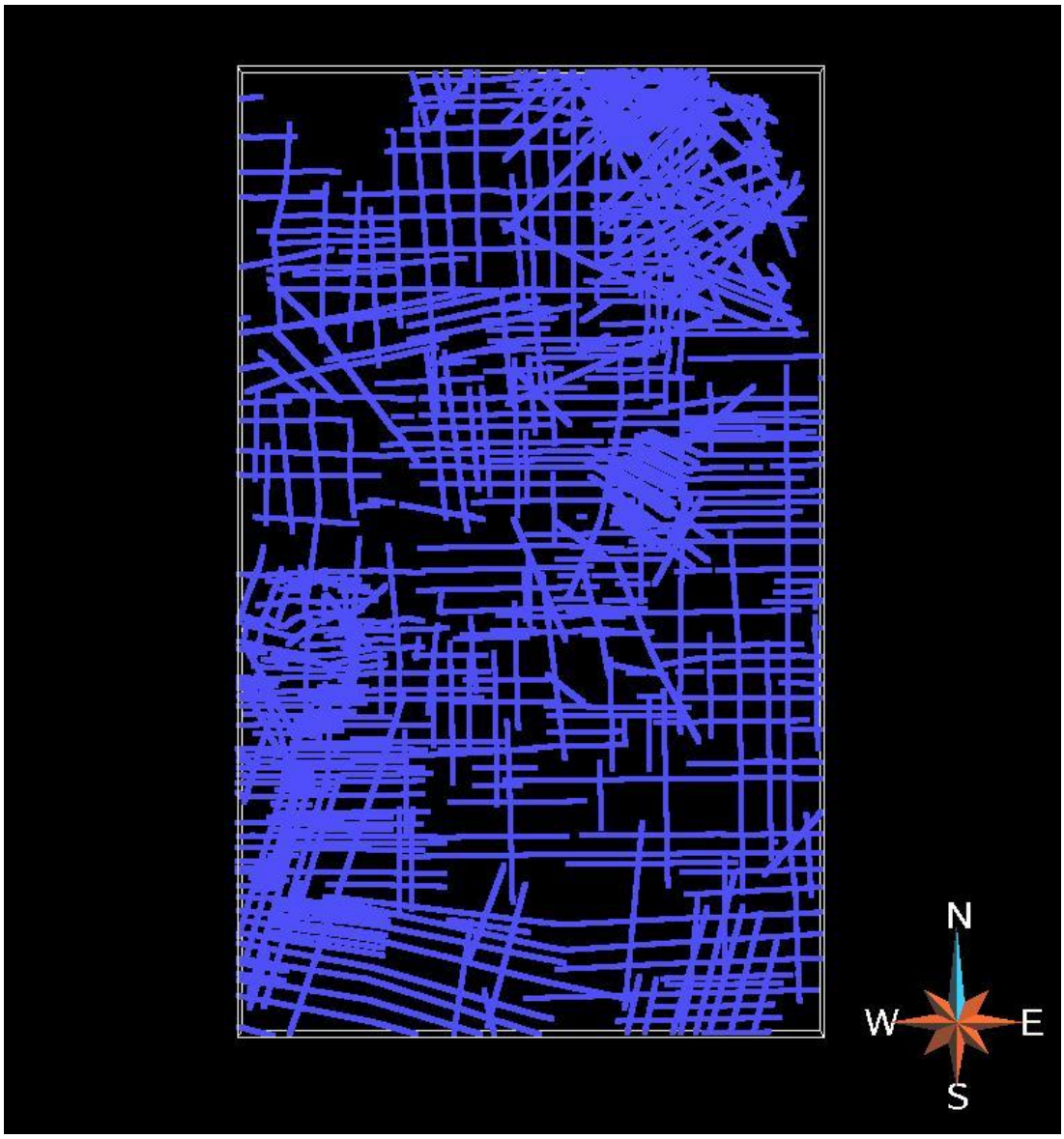

Figure 2.27. The collected time picks for Horizon 6

When color coding the Z axis to show the time picks distribution it becomes obvious that these picks dip east following a regional trend (Figure 2.28).

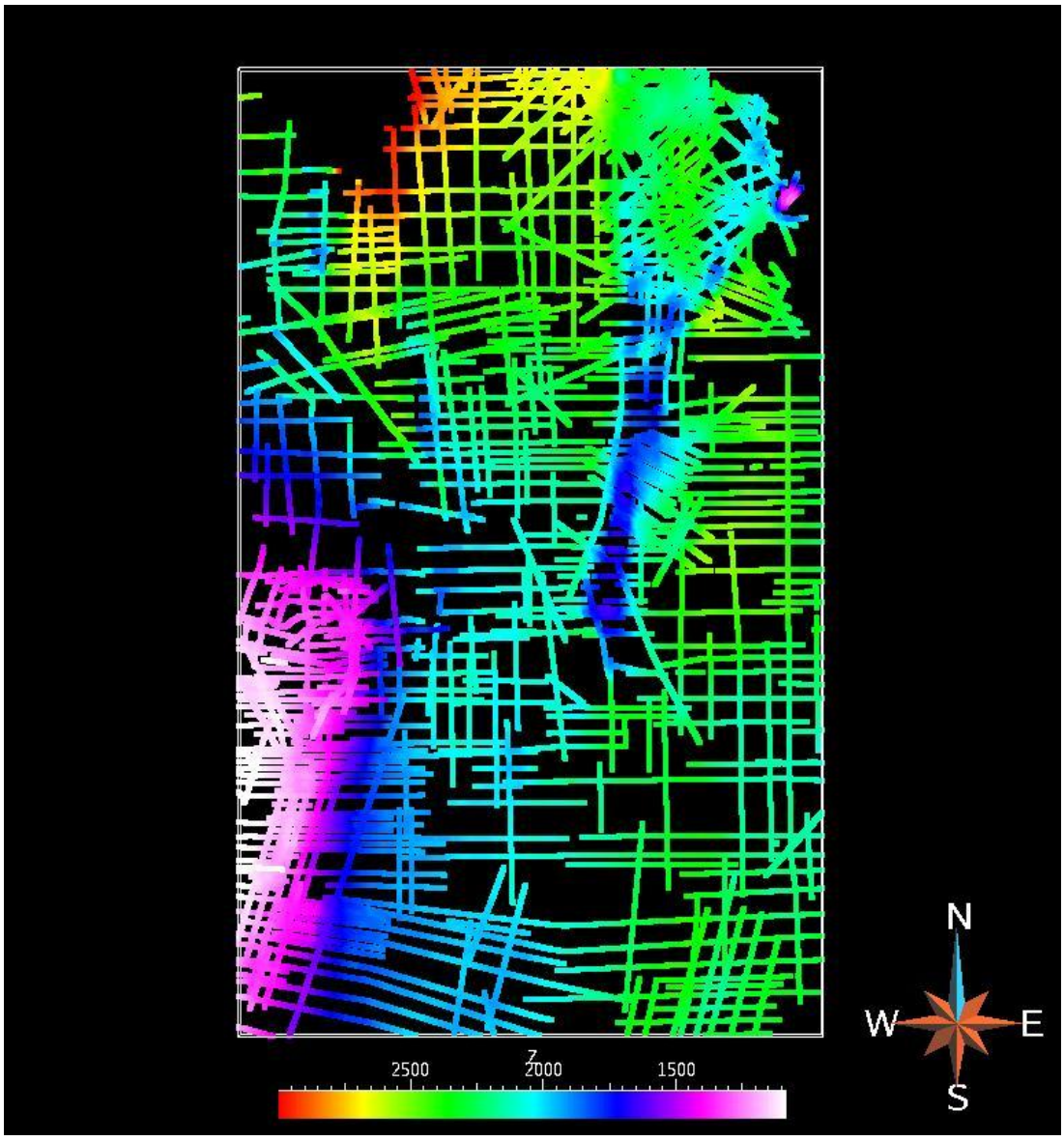

Figure 2.28. The collected time picks for Horizon 6 with the Z axis (time in ms) color coded

Horizon 7

A total number of 380,498 time picks corresponding to Horizon 7 were collected. Those picks are well distributed throughout the assigned region of study (Figure 2.29).

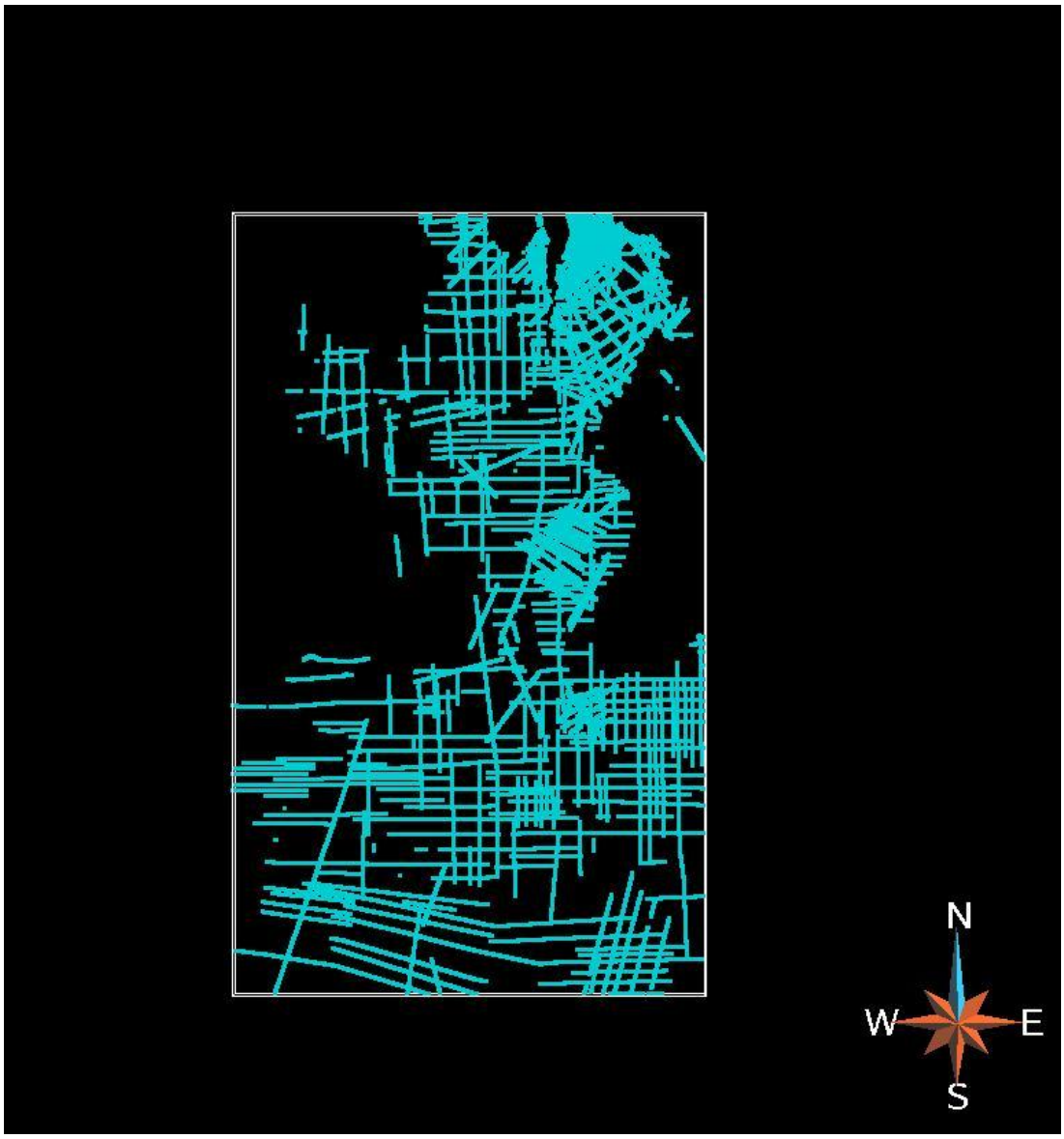

Figure 2.29. The collected time picks for Horizon 7

These picks dip east following a regional trend (Figure 2.30).

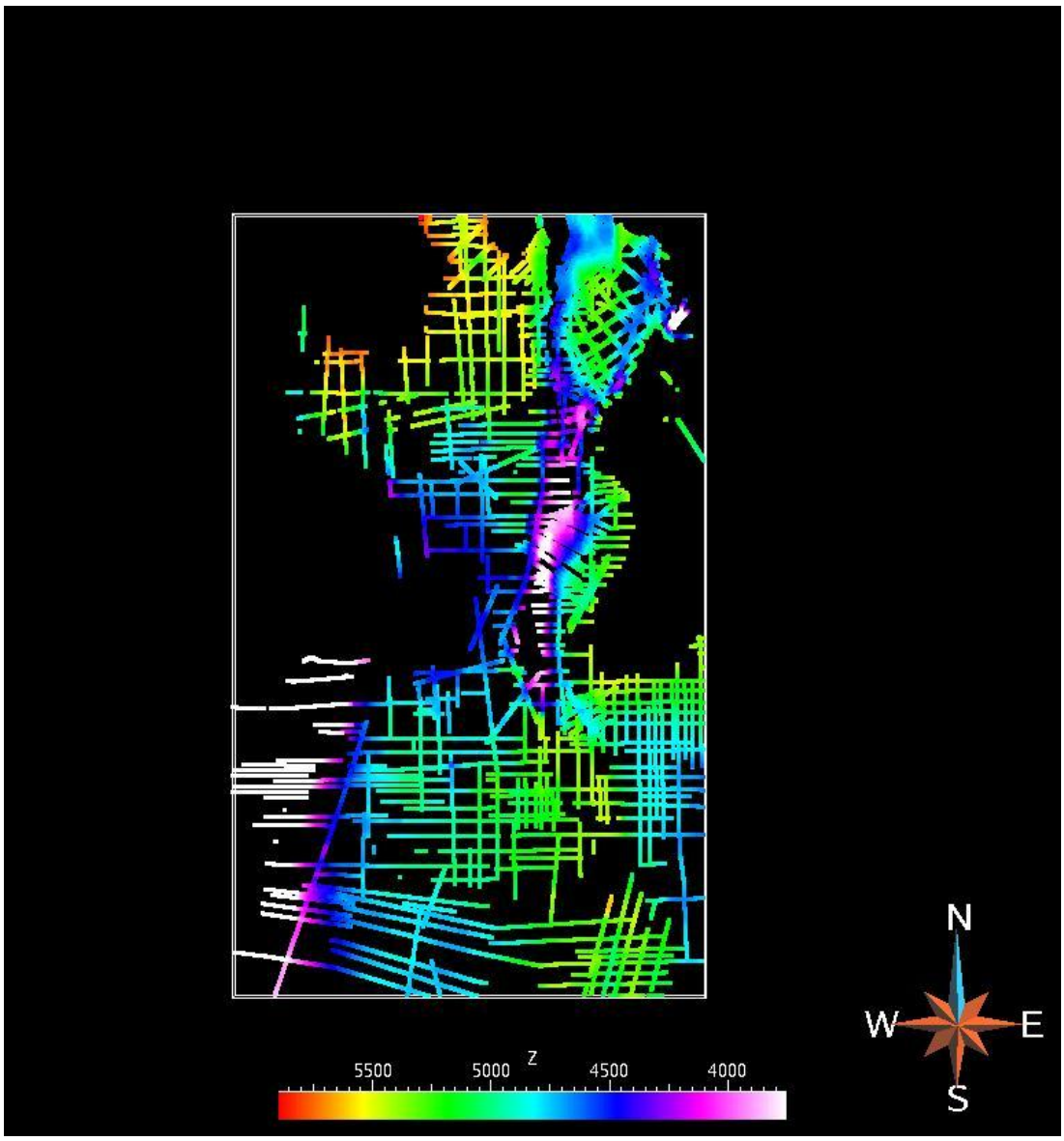

Figure 2.30 The collected time picks for Horizon 7 with the Z axis (time in ms) color coded

2.5.3 THE DATUM MODEL

Since the velocity picks are picked from CDPs that were referenced to surface and the seismic time picks were picked from seismic stacked that had the datum applied to them, it is important to maintain the datum model with the data. The datum model is generated from the datum grid that is 500 meter by 500 meter spaced, which is considered very dense especially if plotted on the large area of the study.

It is quite obvious that the grid is quite densely populated at 500 X 500 meters spacing. When color coding the time axis, the actual picture demonstrates the shape of the datum model with the difference in time between one place and another (Figure 2.31).

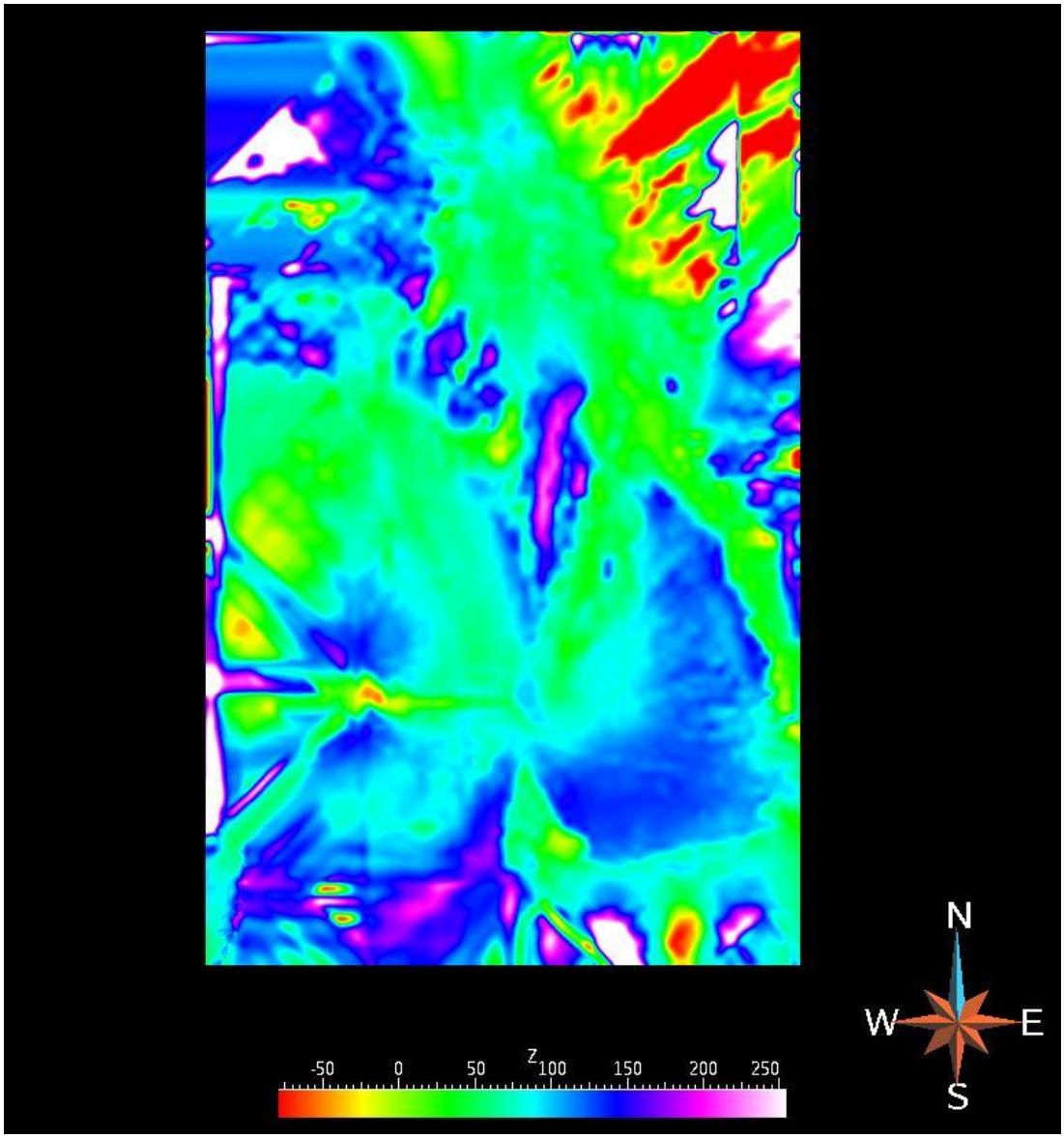

Figure 2.31 The datum model with the time (in ms)

CHAPTER 3

DATA INTEGRATION

3.1 ORDER OF THE METHOD

The order of the method has been followed as described previously in the introduction (Figure 1.8). Initially, the velocities were compiled, then the interpretation data which consists of seismic time picks from key regional horizons was also compiled. Following the compilation steps, each key regional horizon seismic time picks were interpolated into surfaces. Each surface was embedded into the velocity picks volume and the velocities were projected on the surfaces for their values. Each interpolated surface was then smoothed and was given the value in both velocity and time.

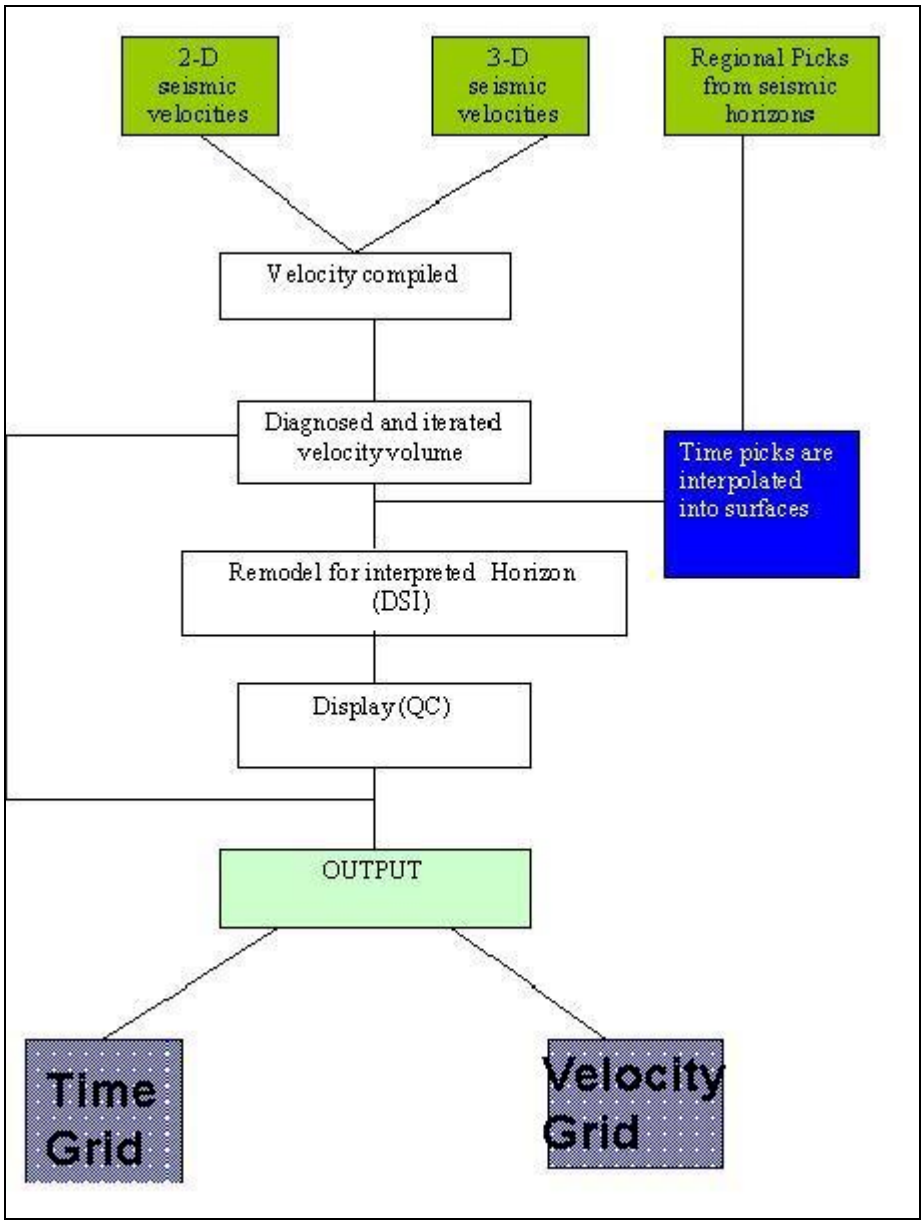

Figure 1.8: Flowchart indicating the steps of the proposed procedure.

3.1.1 THE DSI INTERPOLATOR

The interpolator used was the discrete smoothing interpolator (DSI) which is based on the concept of modeling geological objects. The DSI method considers a scalar continuous function ϕ (Figure 3.1)

Where ϕ is defined on segment Ω that has a step of 1 such that $\Omega = \{1,2,3,4,.,.,.,.,\alpha,.,.M\}$

The interpolation is done by the function ϕ which is a spline function minimizing the global roughness.

Roughness is defined here as $R(\phi) = \int_{\Omega} \mu(x) \cdot R(\Phi \mid x) \cdot dx$

$$R(\Phi \mid x) = \left| \frac{d^2\phi}{dx^2} \right|^2$$

and $\mu(x) > 0$ and it is the local stiffness constant (for example 1).

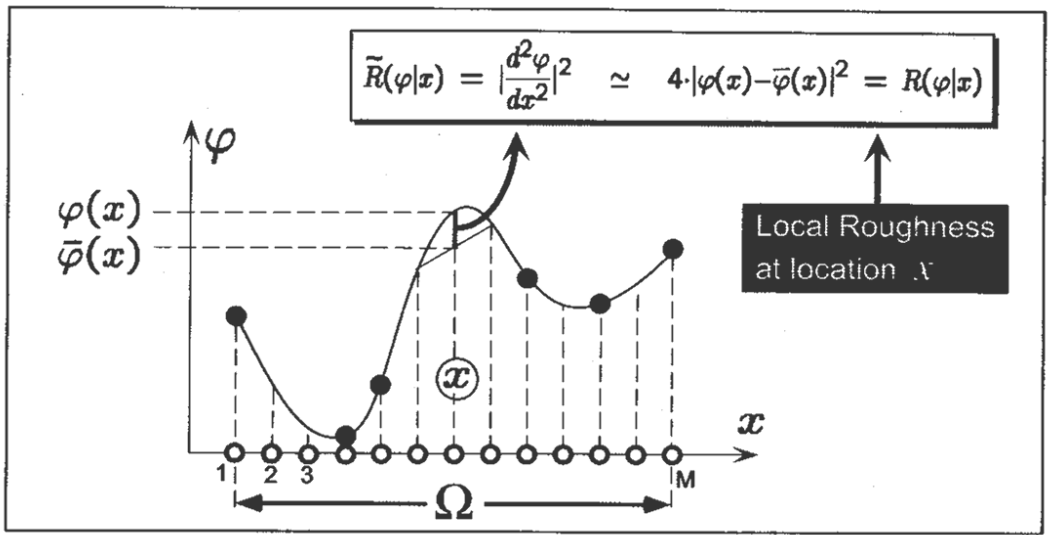

Figure 3.1. A sketch of how the DSI method represents data points in space (after Mallet, 2002). (Adopted from Mallet, 2001)

3.2 KEY HORIZON PICKS INTERPOLATED INTO SURFACES

The first step of the integration process is to interpolate the time picks of the key horizons that are represented in points in space into surfaces. This will require the use of the points as control points for the desired curvilinear triangulated surfaces.

3.2.1 Horizon 1 from points to surface

The method used the points of Horizon 1 and interpolated them into a surface (Figures 3.2-3.3).

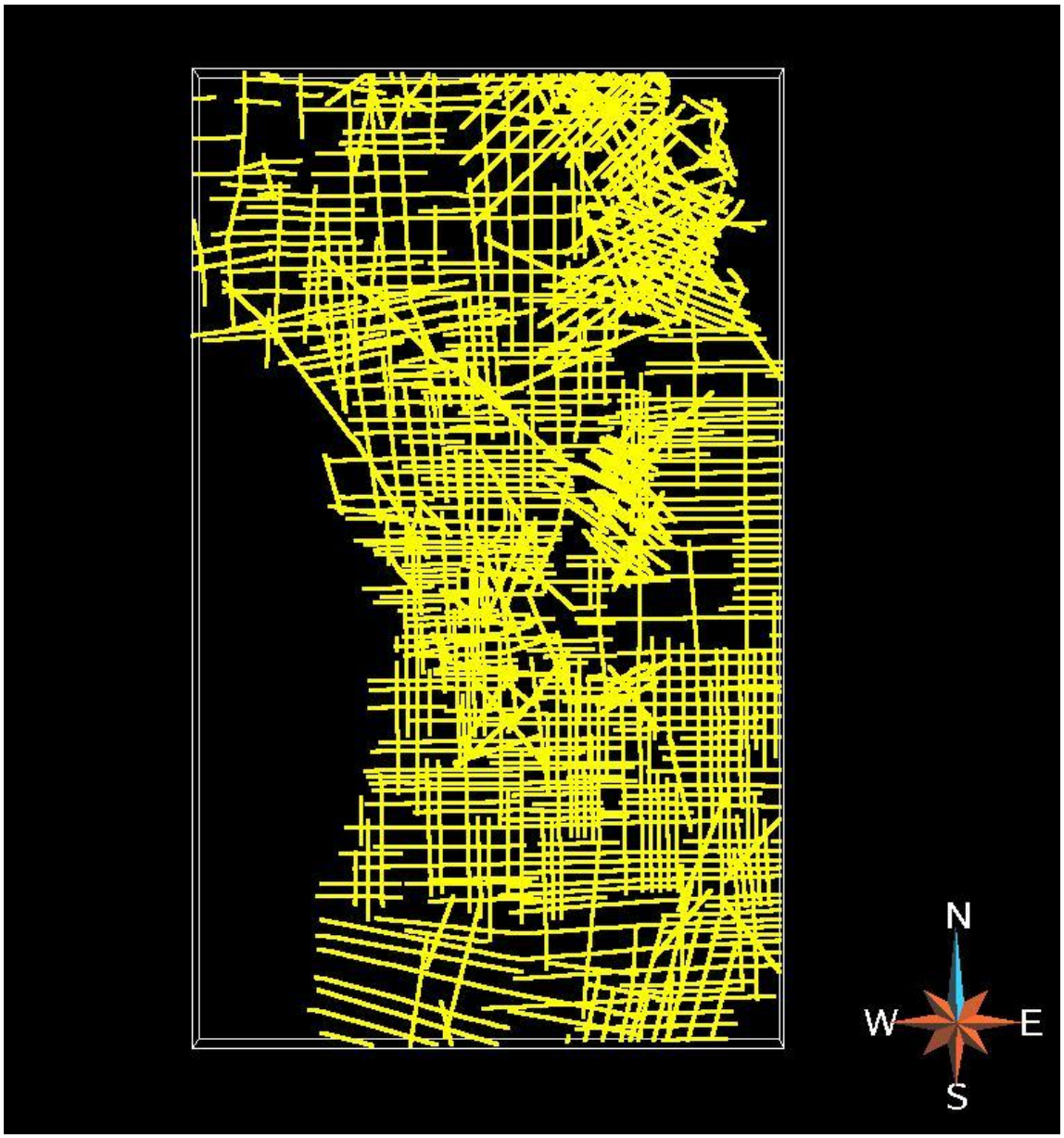

Figure 3.2. Horizon 1 as points

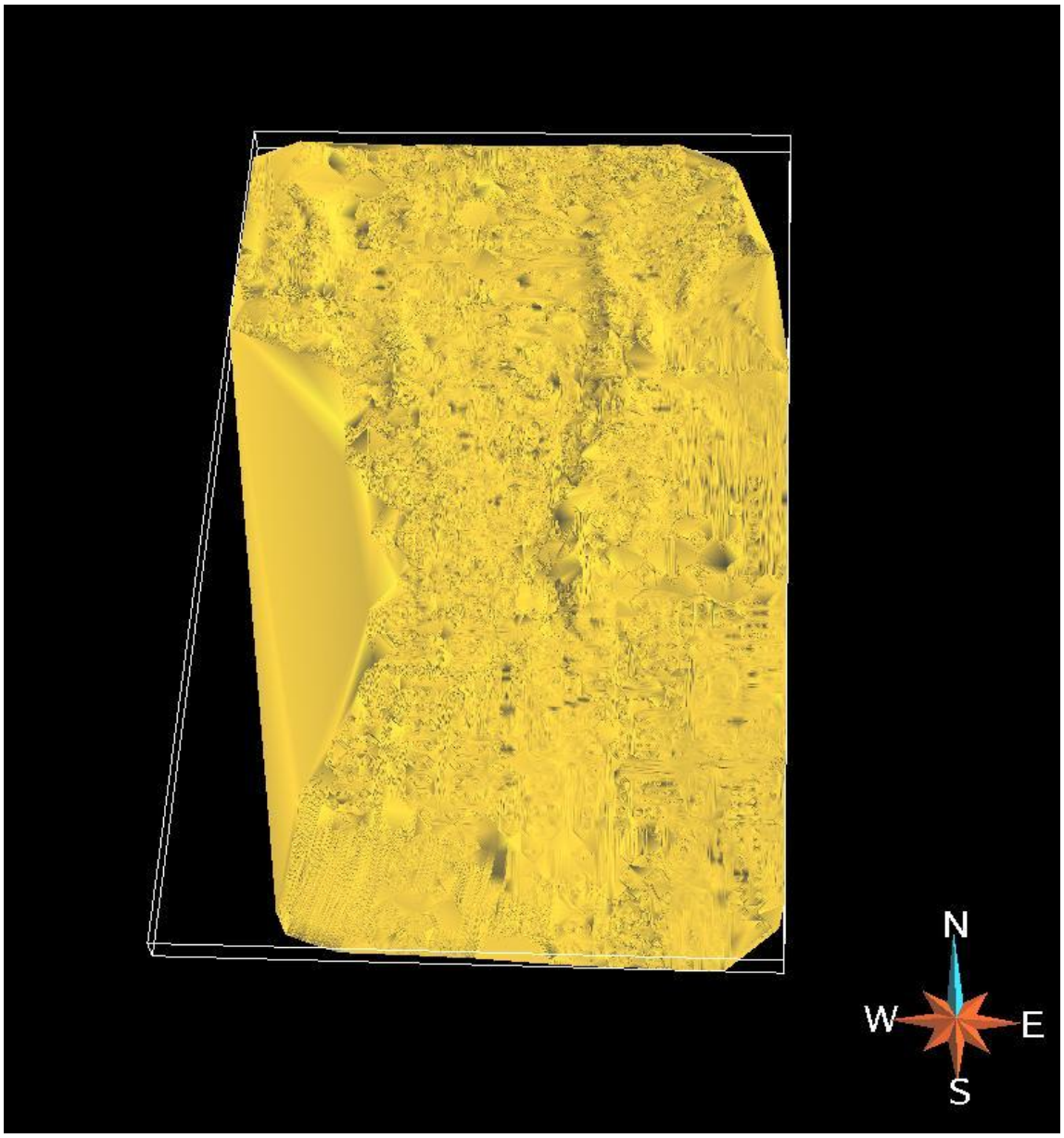

Figure 3.3. Horizon 1 interpolated into a surface

If the Z axis (represented in time) is exaggerated and color coded, it would make a more meaningful interpretation of the interpolated surface (Figure 3.4).

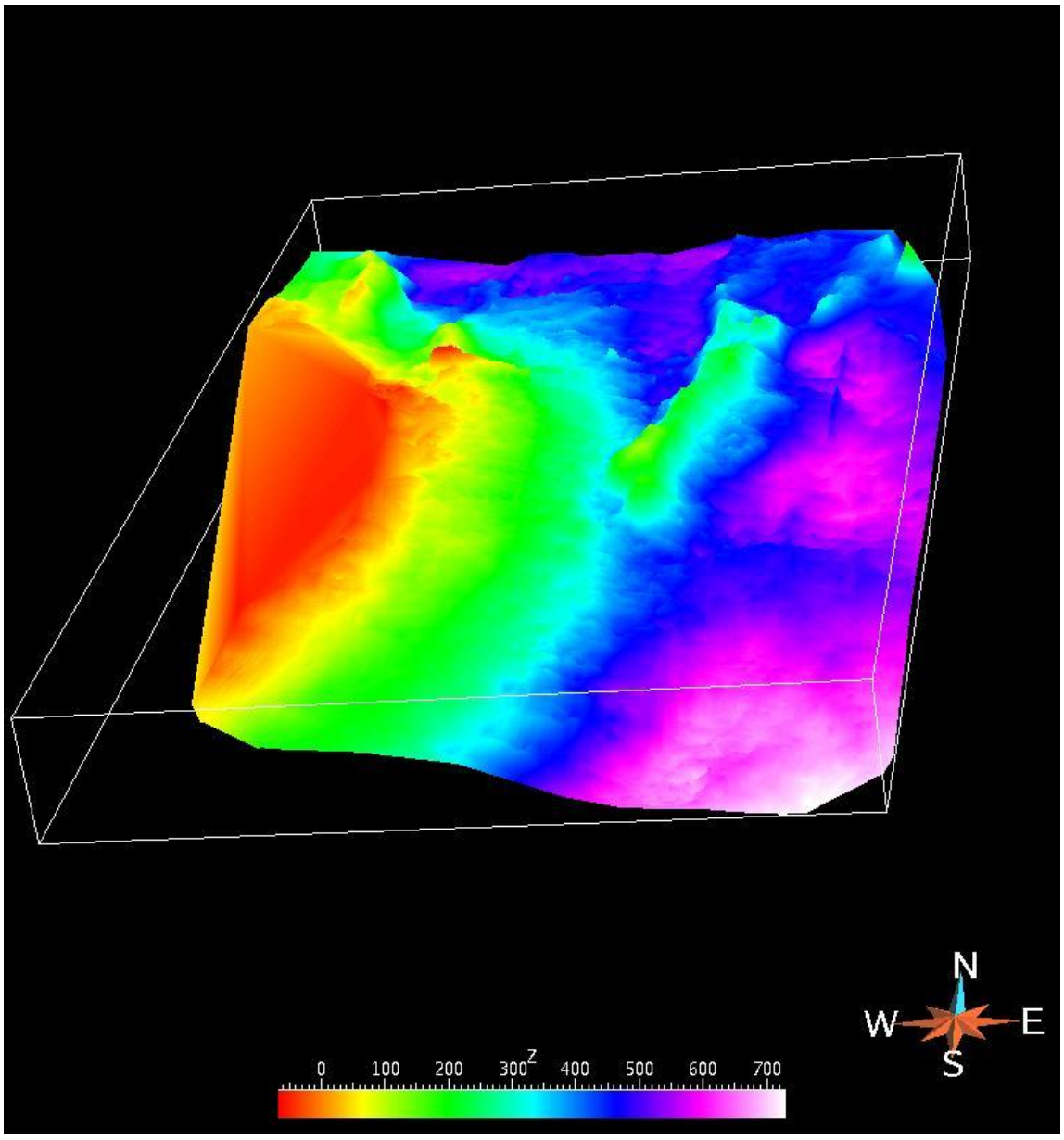

Figure 3.4. Horizon 1 surface exaggerated in the time axis and color coded (time in ms).

3.2.2 Horizon 2 from points to surface

The method used the points of Horizon 2 and interpolated them into a surface (Figures 3.5-3.6).

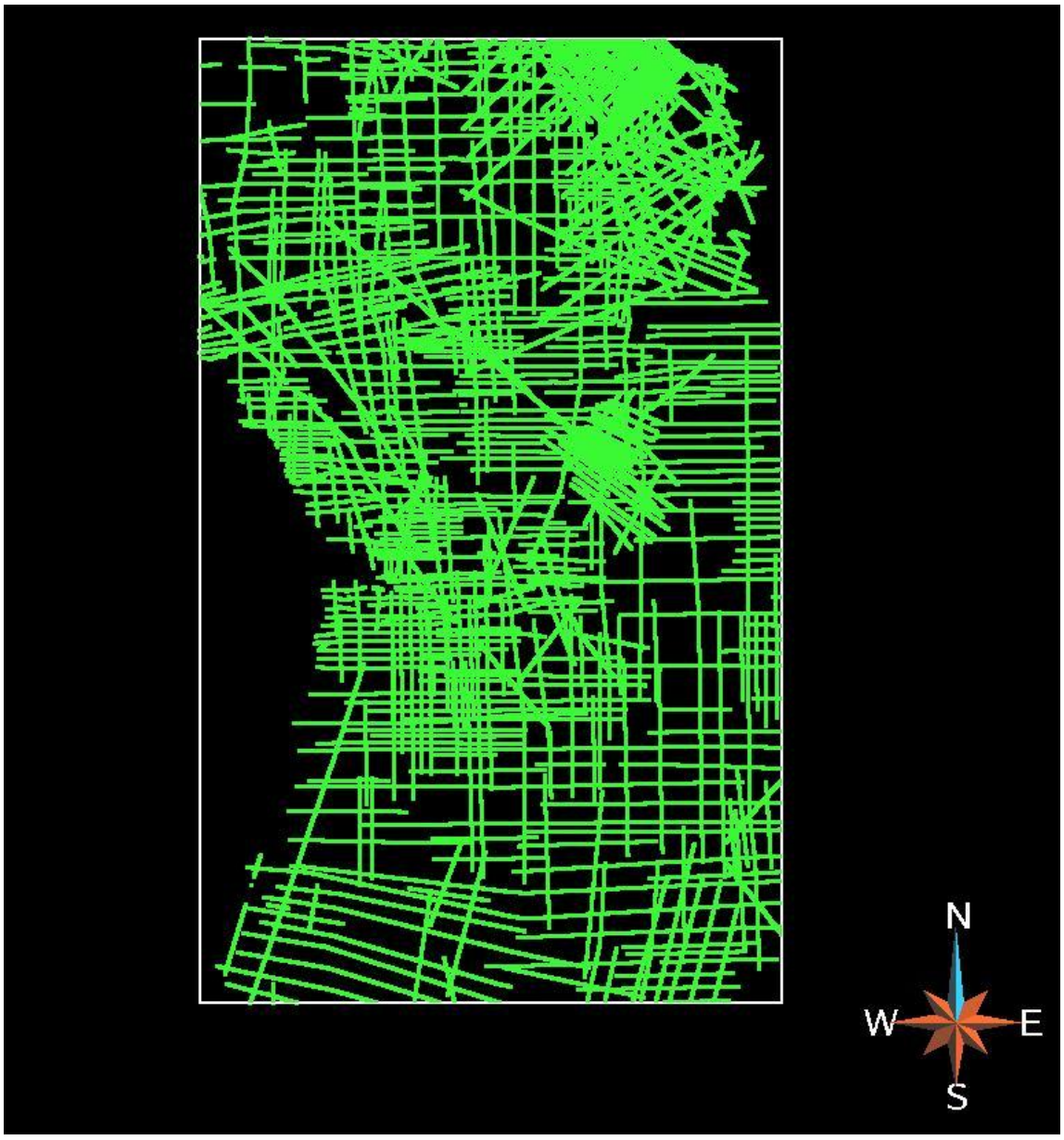

Figure 3.5. Horizon 2 as points

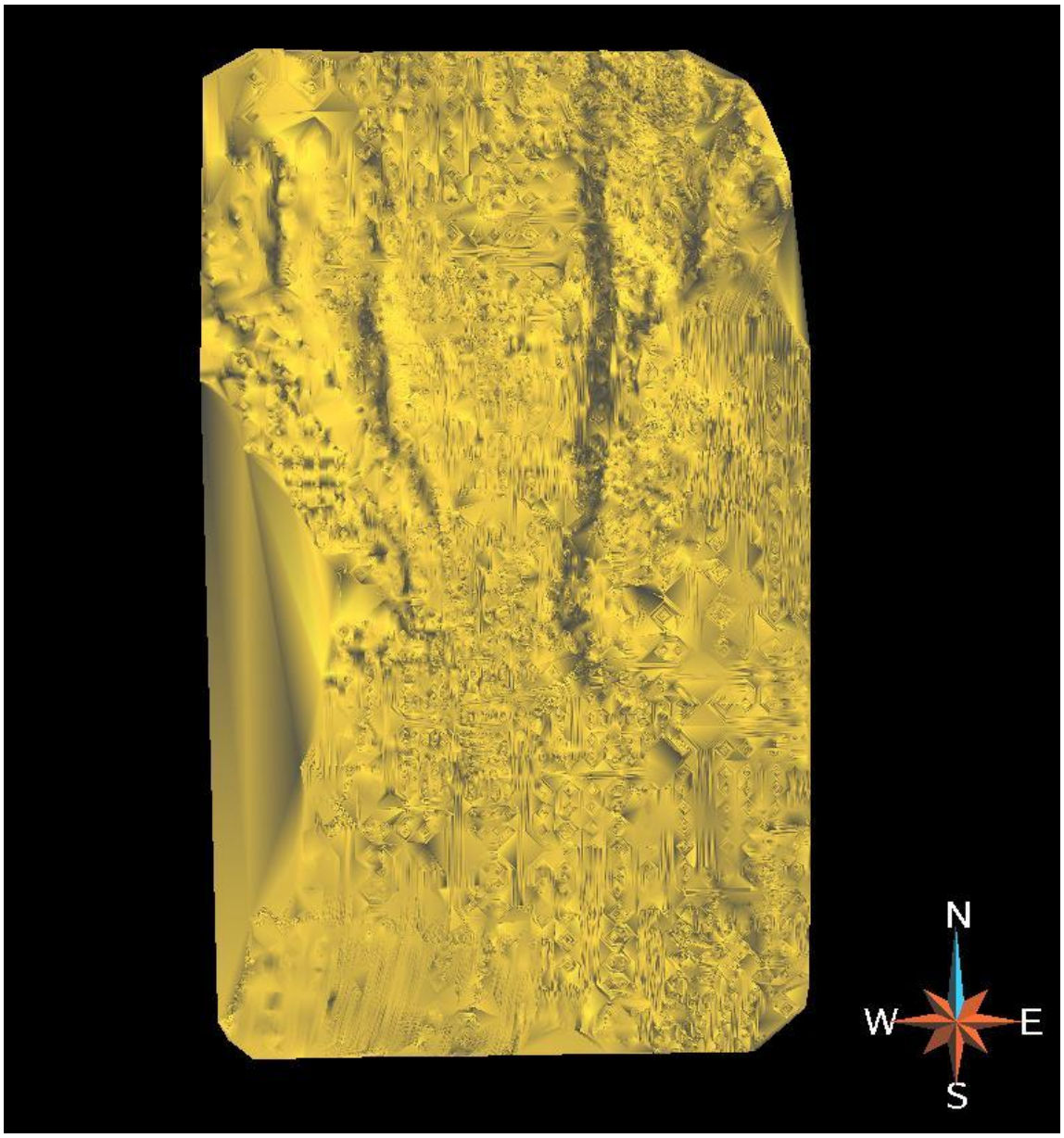

Figure 3.6. Horizon 2 interpolated into a surface

If the Z axis (represented in time) is exaggerated and color coded it makes a more meaningful interpretation of the interpolated surface (Figure 3.7).

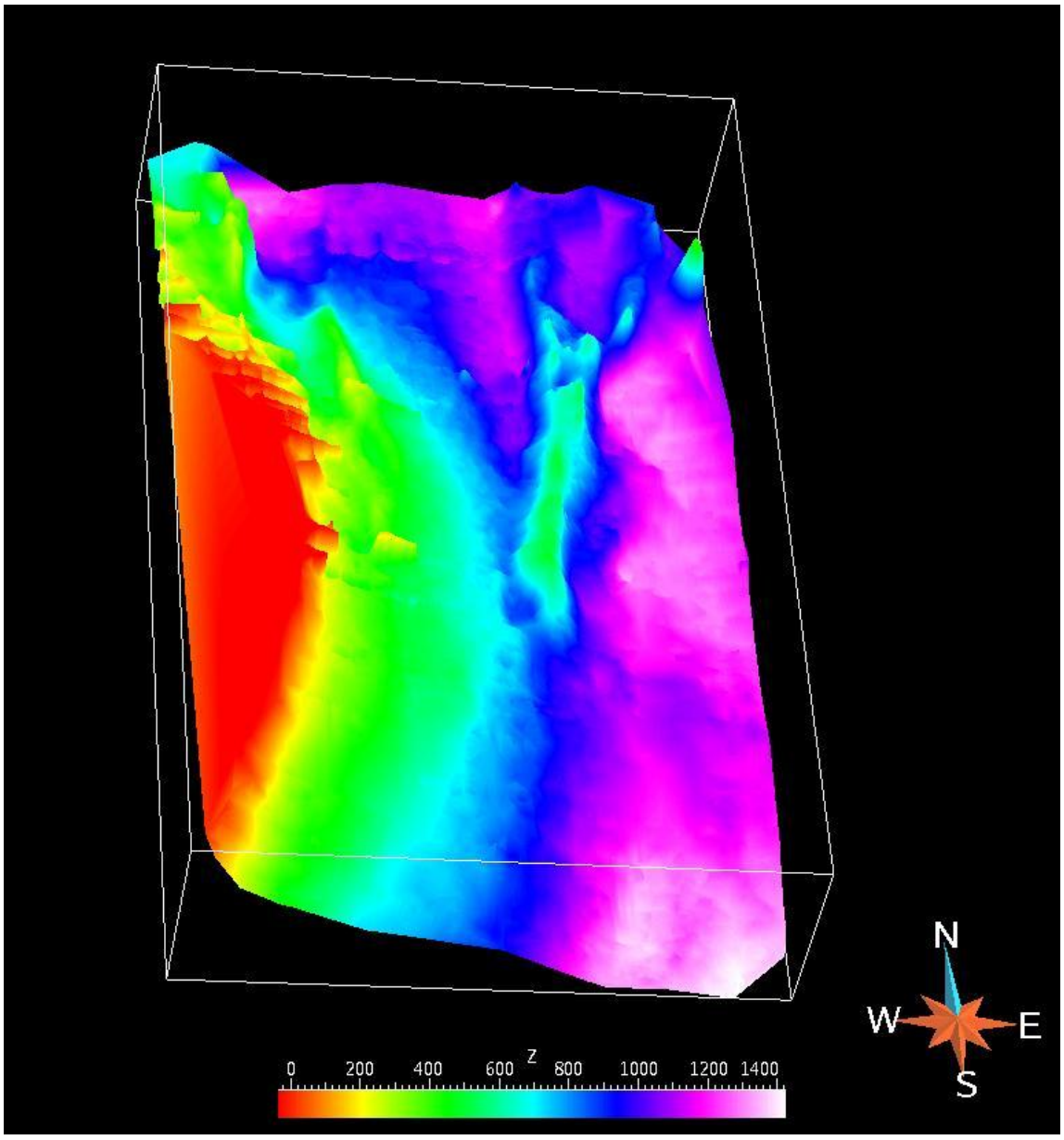

Figure 3.7. Horizon 2 surface exaggerated in the time axis and color coded (time in ms).

3.2.3 Horizon 3 from points to surface

The method used the points of Horizon 3 and interpolated them into a surface (Figures 3.8-3.9).

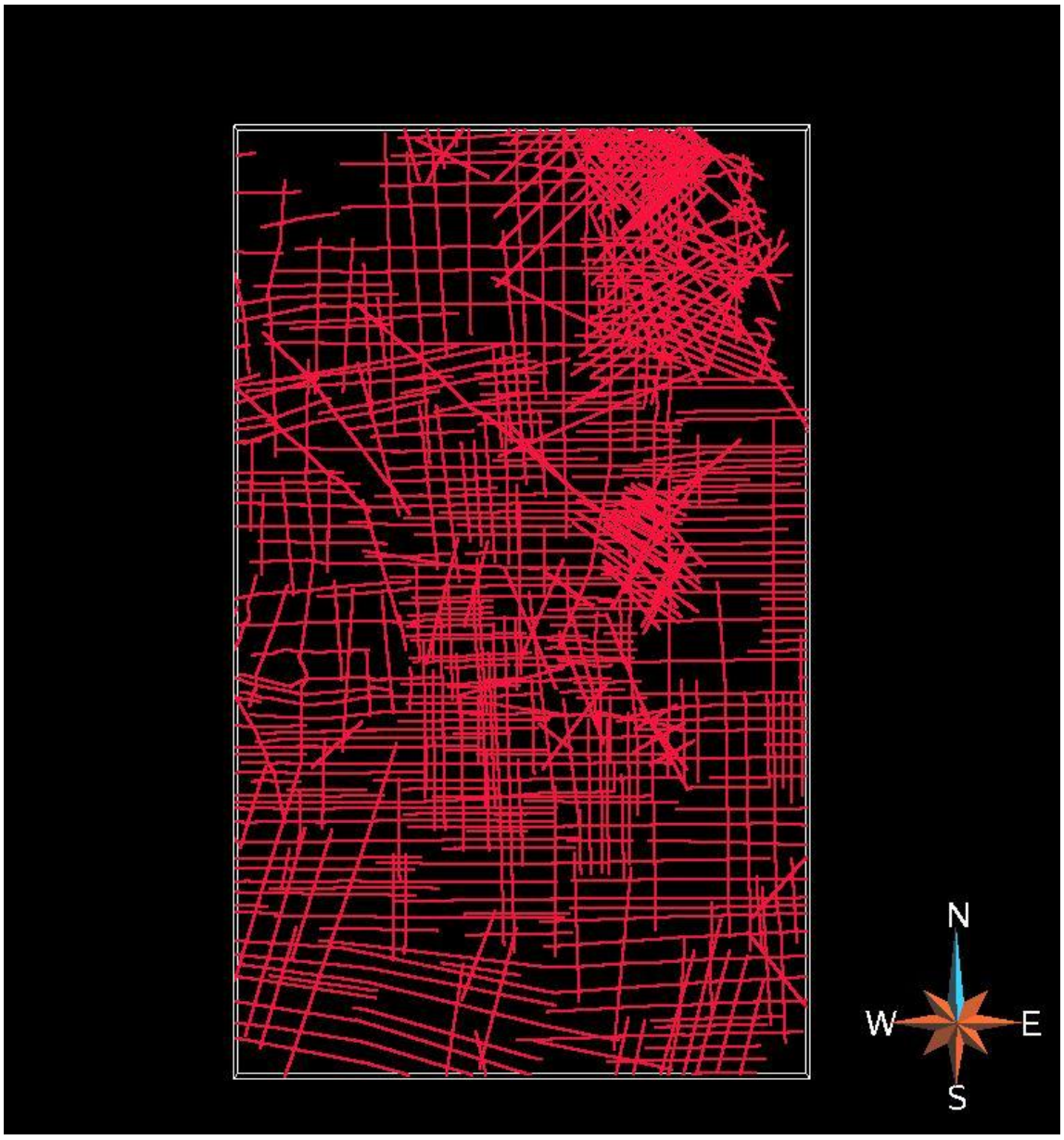

Figure 3.8. Horizon 3 as points

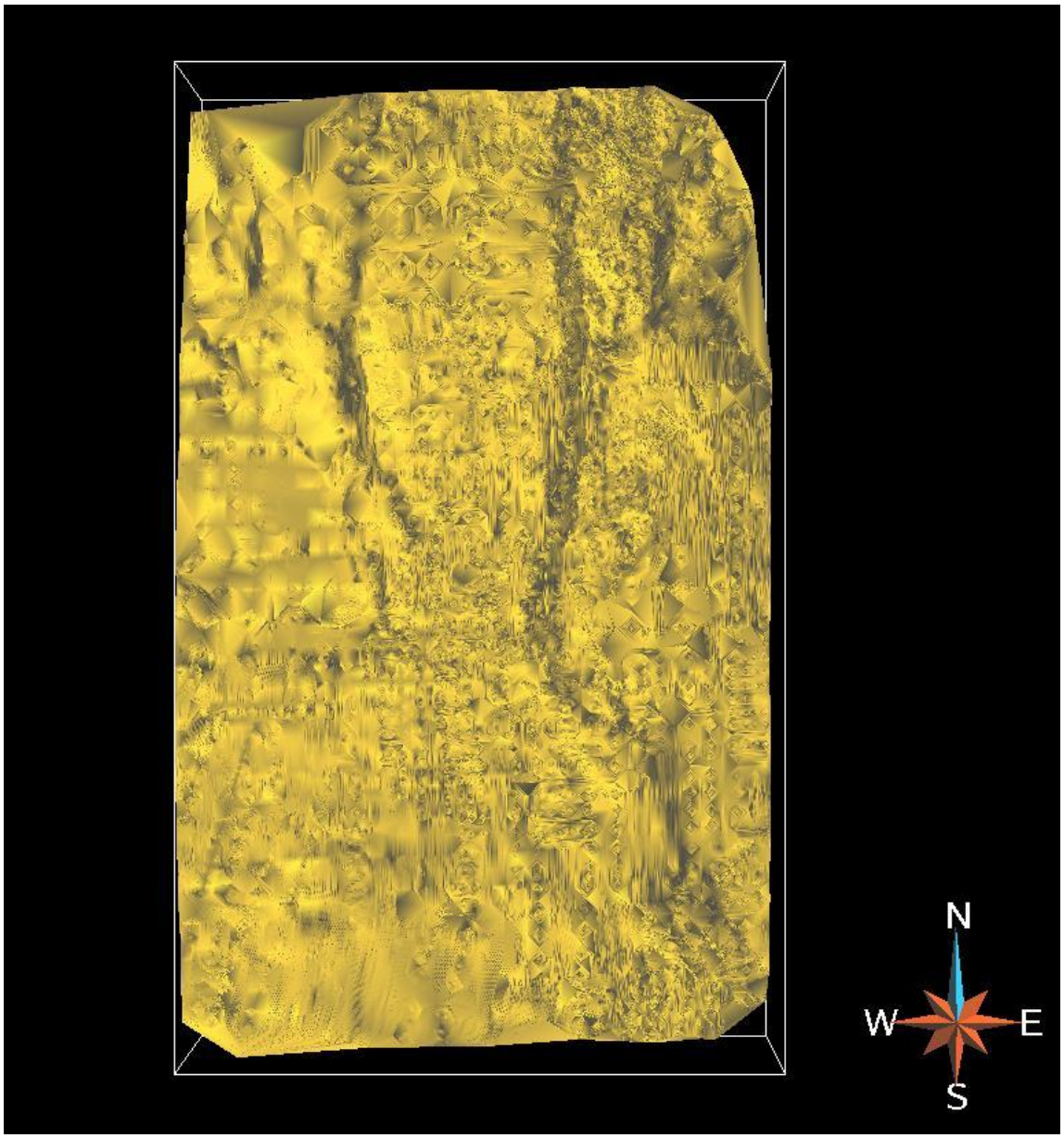

Figure 3.9. Horizon 3 interpolated into a surface

If the Z axis (represented in time) is exaggerated and color coded, it makes a more meaningful interpretation of the interpolated surface (Figure 3.10).

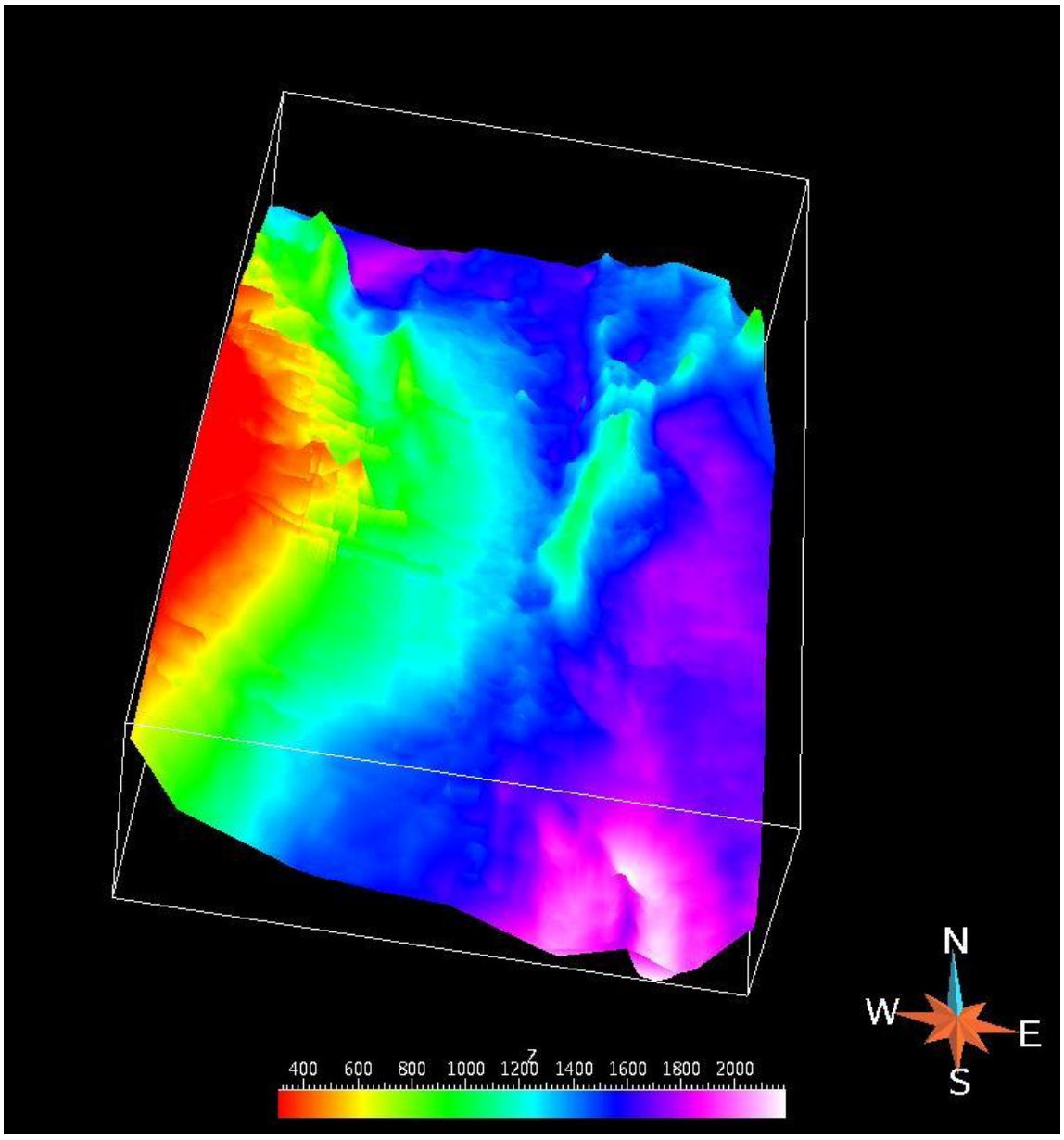

Figure 3.10. Horizon 3 surface exaggerated in the time axis and color coded (time in ms).

3.2.4 Horizon 4 from points to surface

The method used the points of Horizon 4 and interpolated them into a surface (Figures 3.11-3.12).

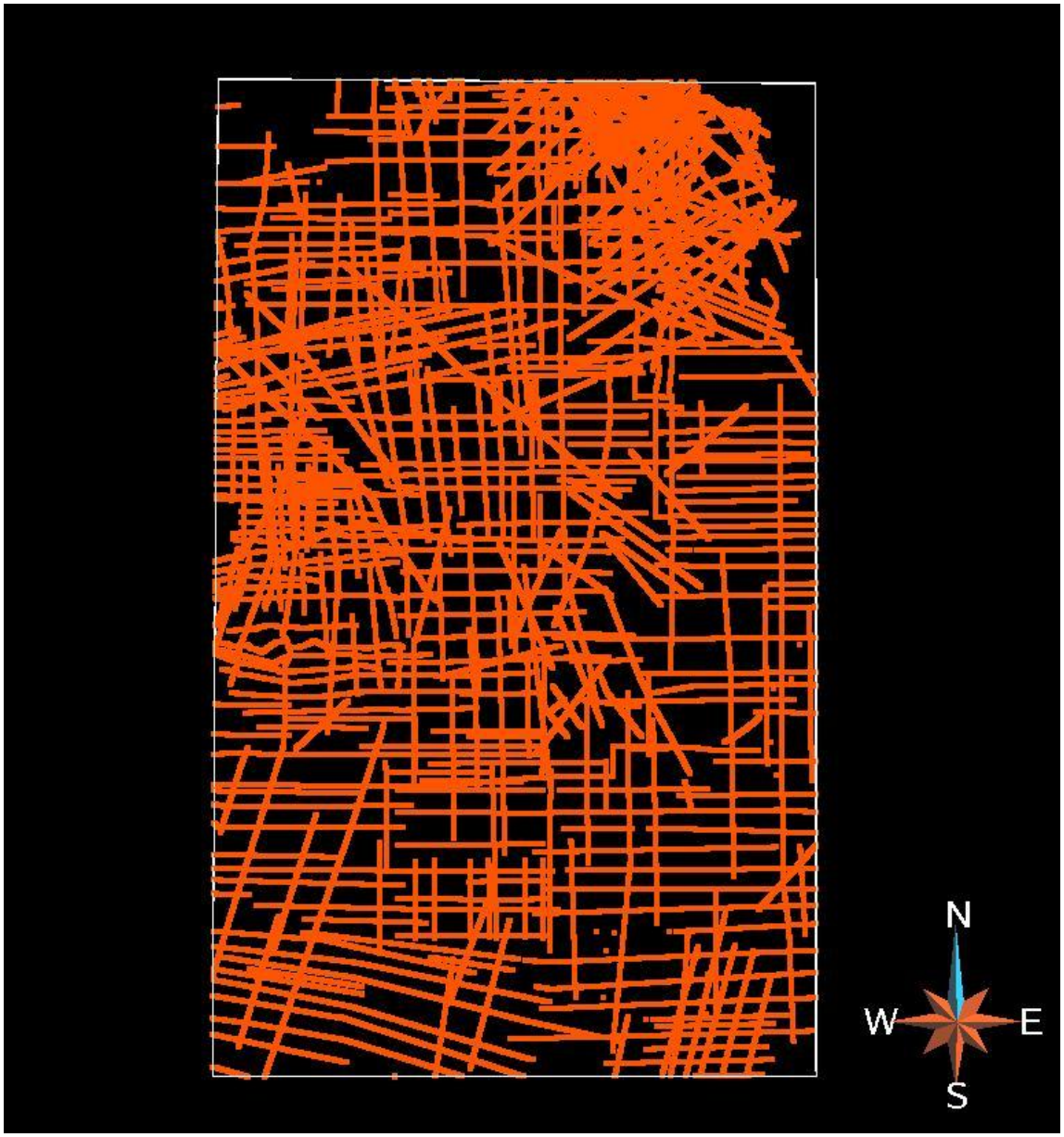

Figure 3.11. Horizon 4 as points

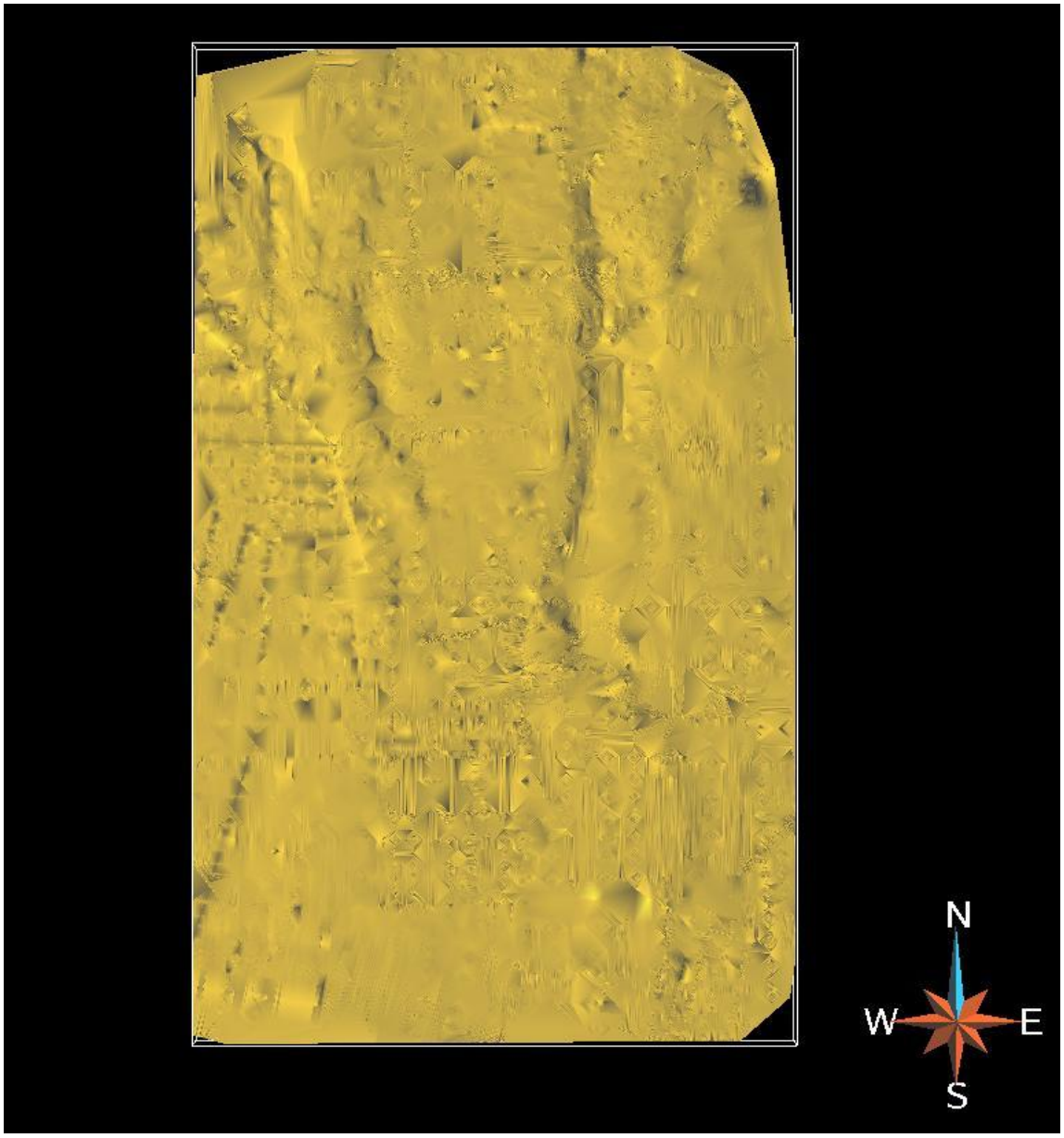

Figure 3.12. Horizon 4 interpolated into a surface

If the Z axis (represented in time) is exaggerated and color coded, it makes a more meaningful interpretation of the interpolated surface (Figure 3.13).

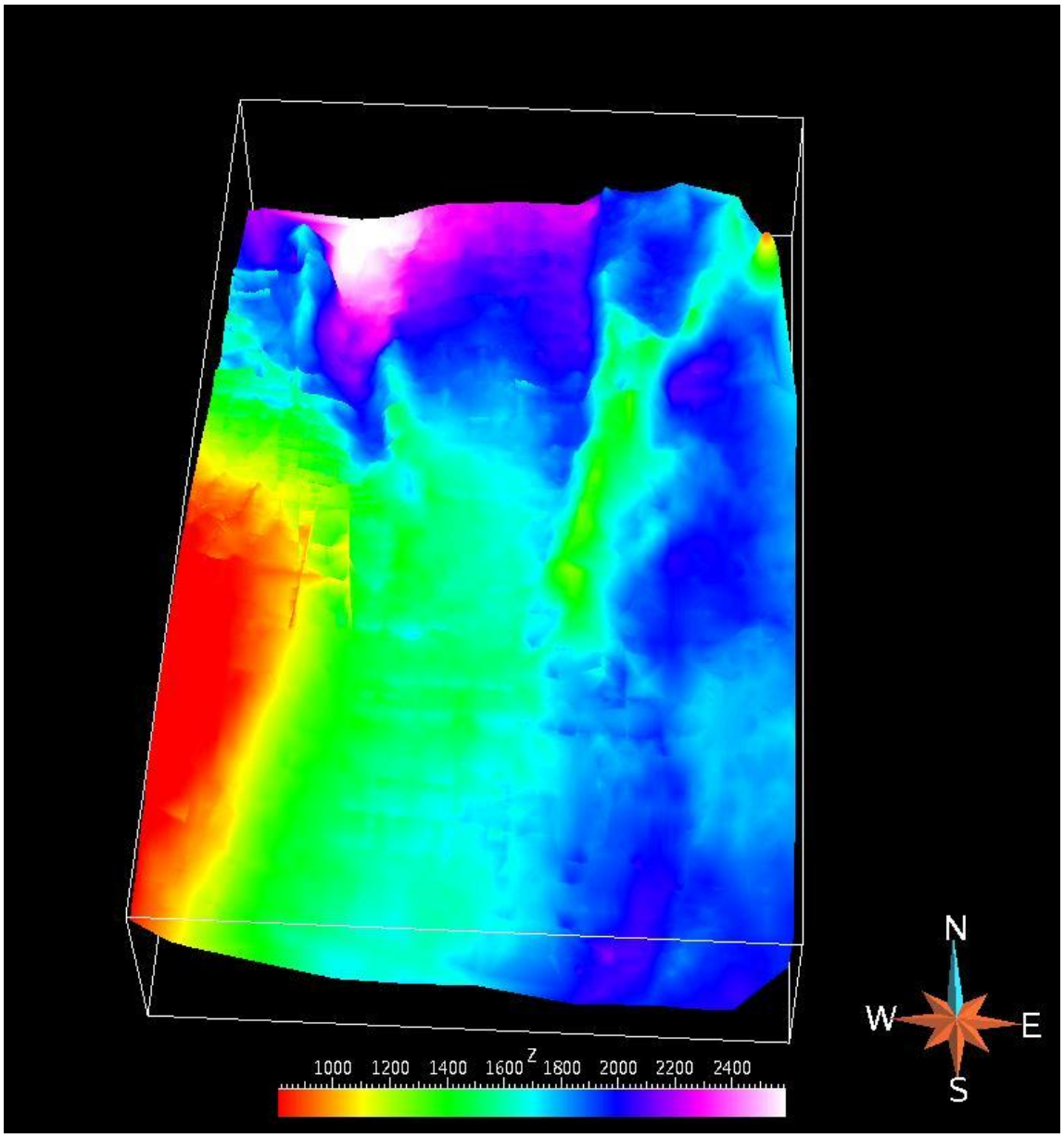

Figure 3.13. Horizon 4 surface exaggerated in the time axis and color coded (time in ms).

3.2.5 Horizon 5 from points to surface

The method used the points of Horizon 5 and interpolated them into a surface (Figures 3.14-3.15).

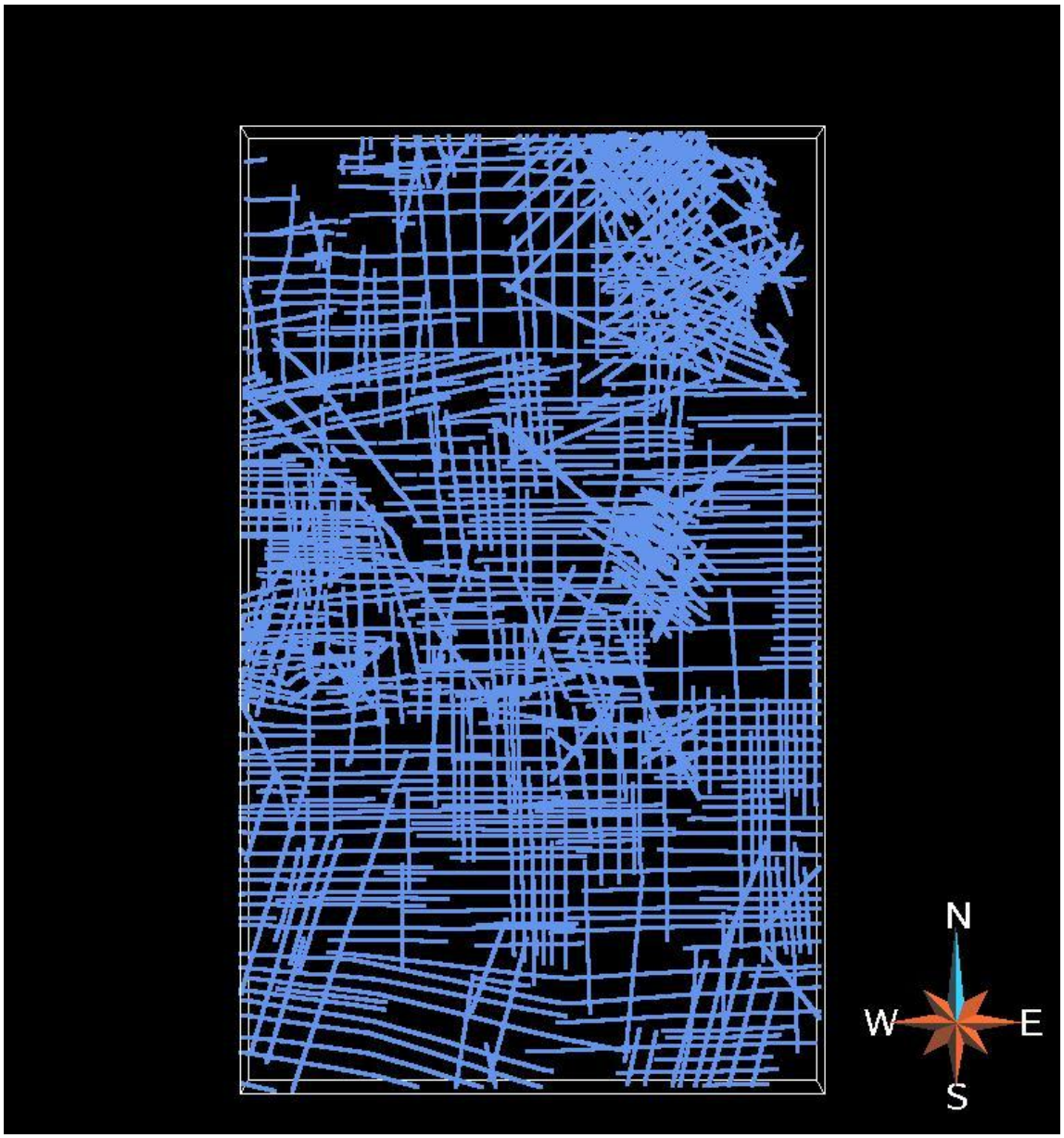

Figure 3.14. Horizon 5 as points

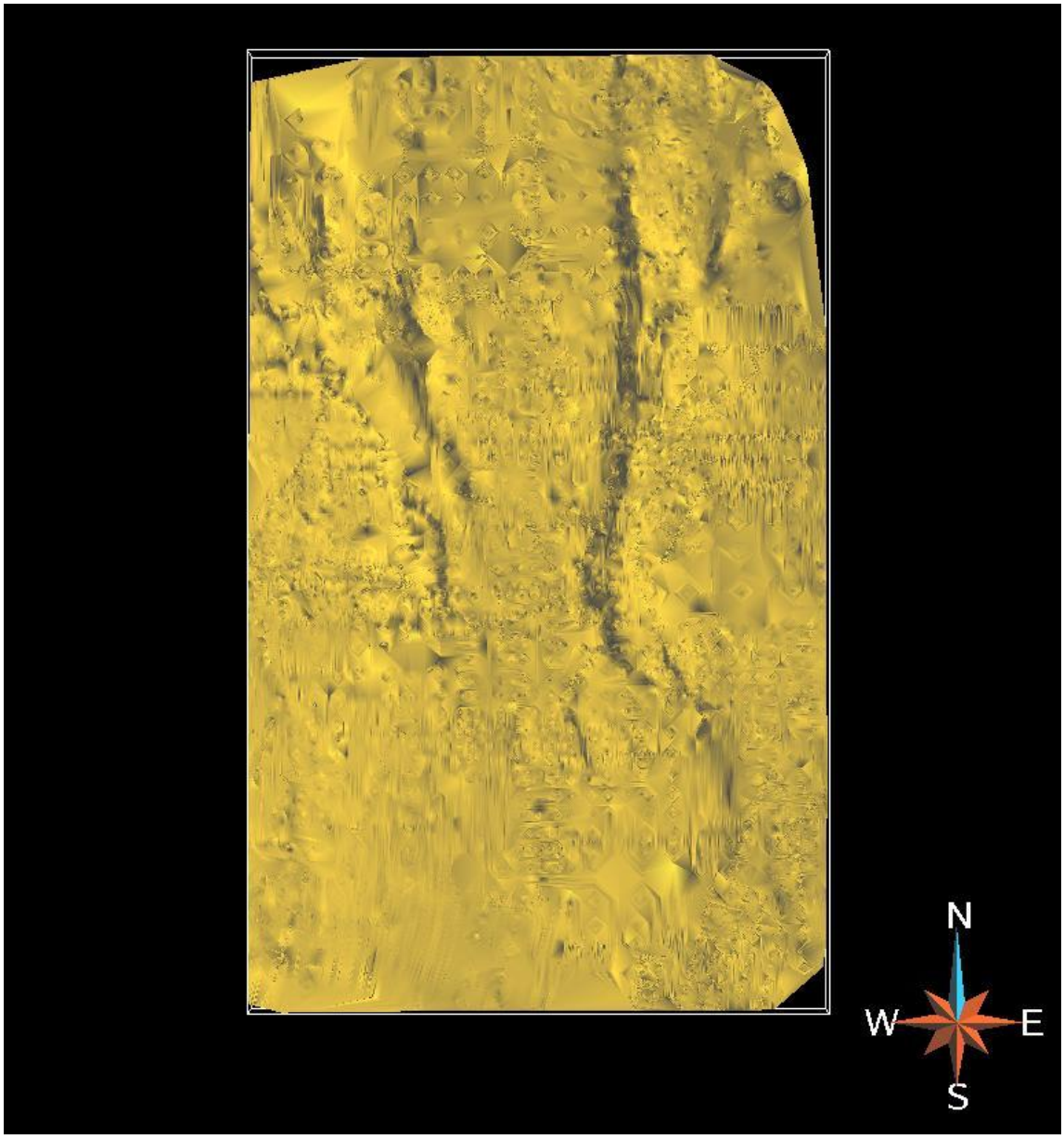

Figure 3.15. Horizon 5 interpolated into a surface

If the Z axis (represented in time) is exaggerated and color coded it makes a more meaningful interpretation of the interpolated surface (Figure 3.16).

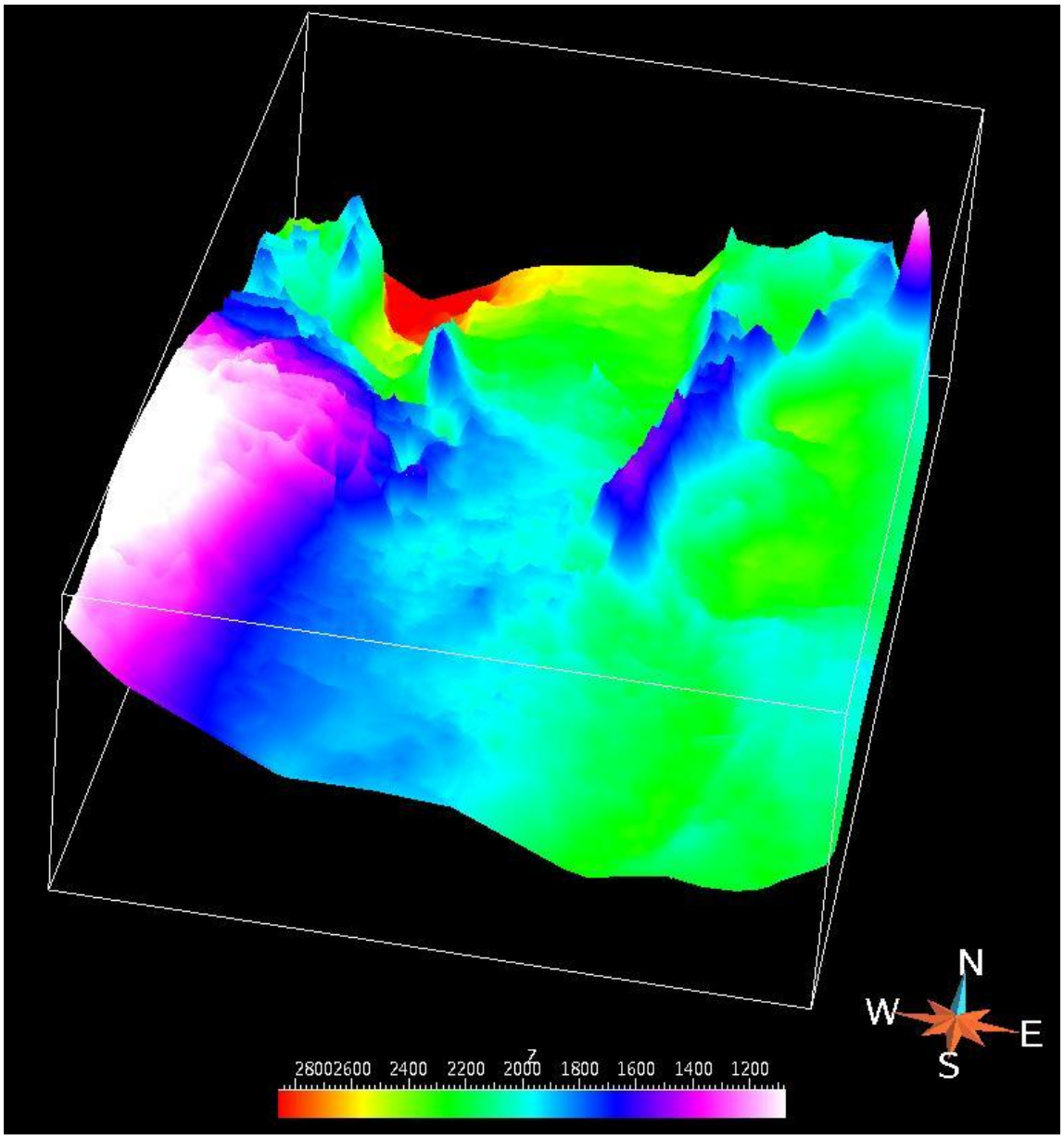

Figure 3.16. Horizon 5 surface exaggerated in the time axis and color coded (time in ms).

3.2.6 Horizon 6 from points to surface

The method used the points of Horizon 6 and interpolated them into a surface (Figures 3.17- 3.18).

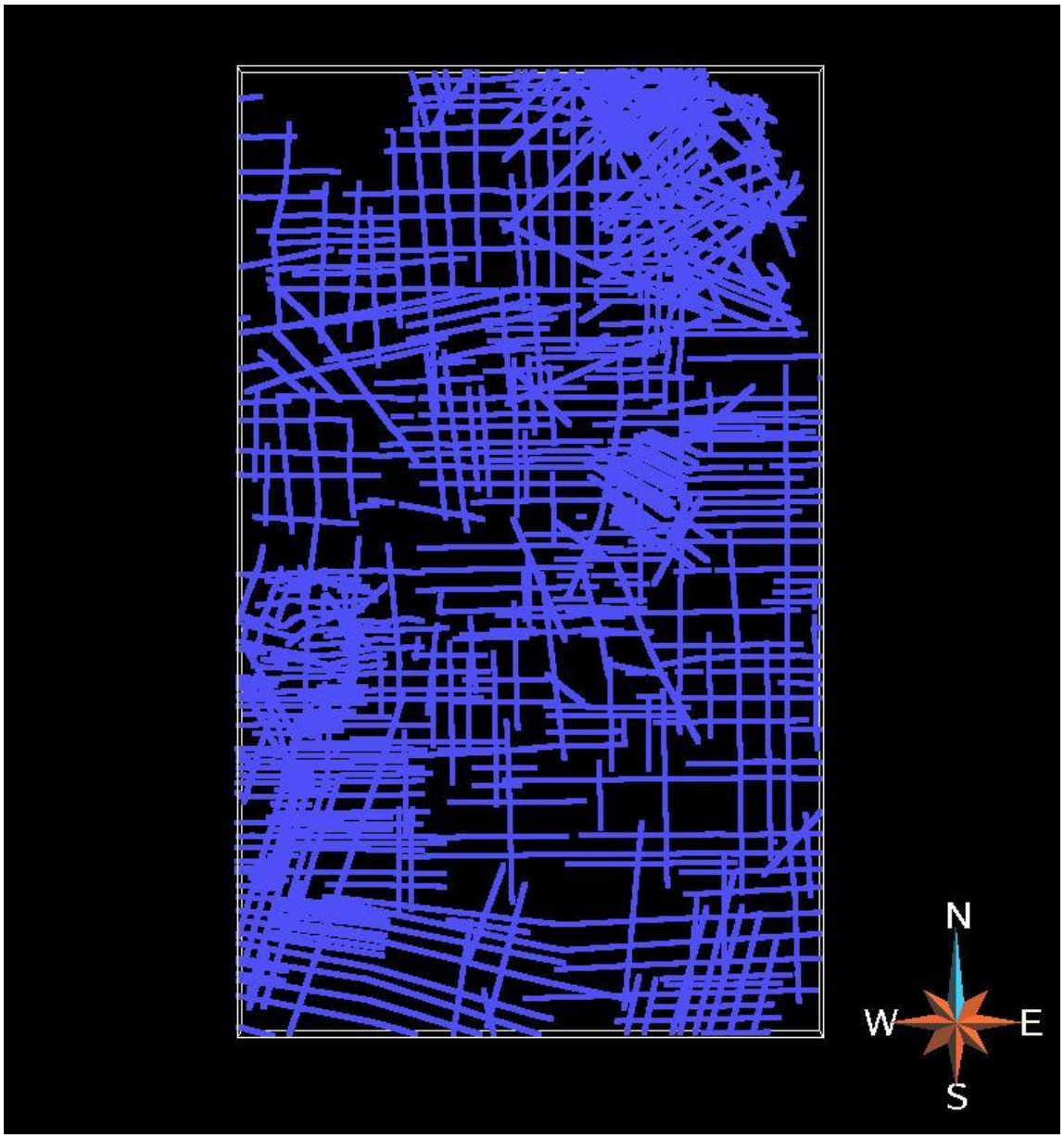

Figure 3.17. Horizon 6 as points

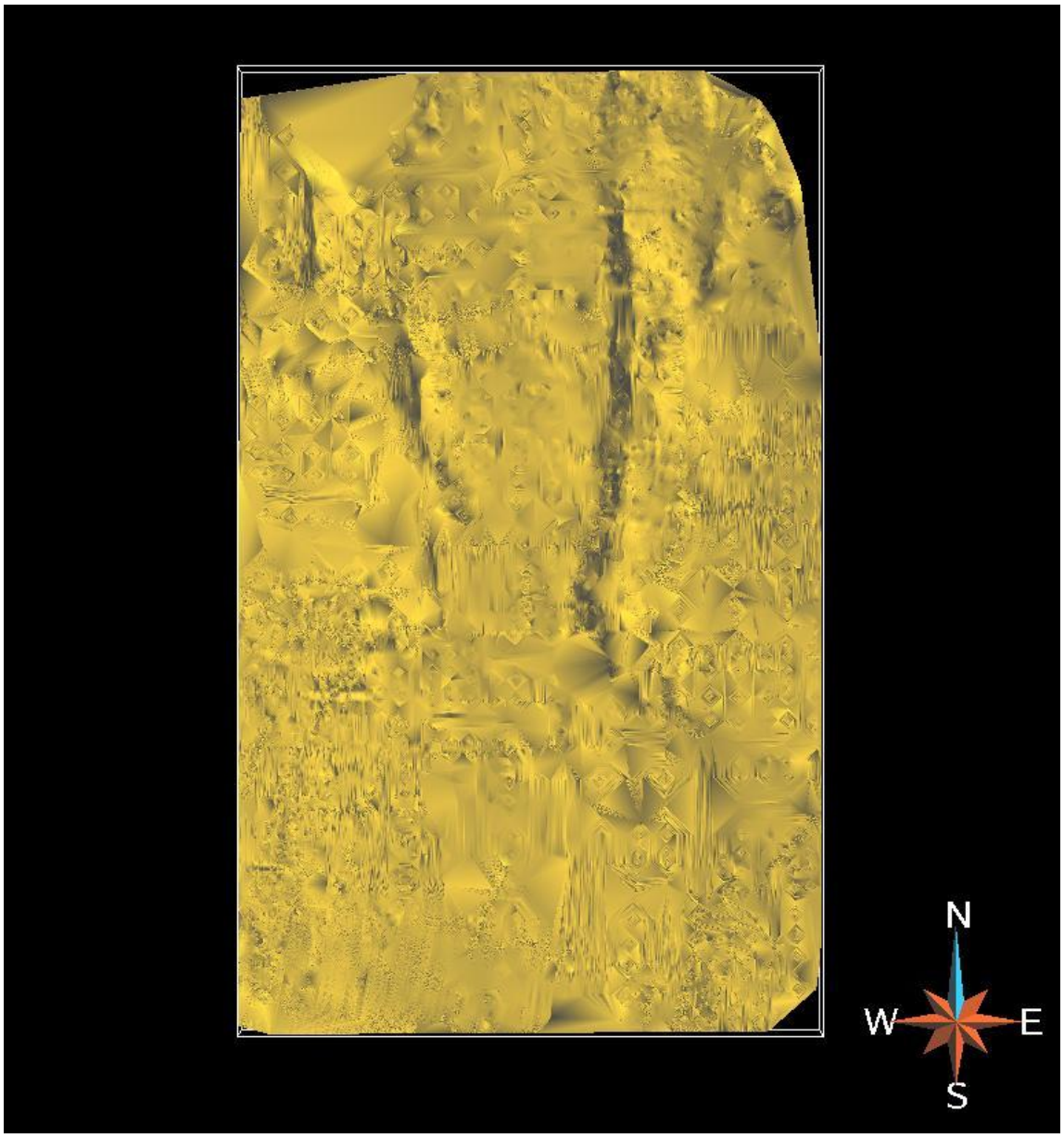

Figure 3.18. Horizon 6 interpolated into a surface

If the Z axis (represented in time) is exaggerated and color coded it makes a more meaningful interpretation of the interpolated surface (Figure 3.19).

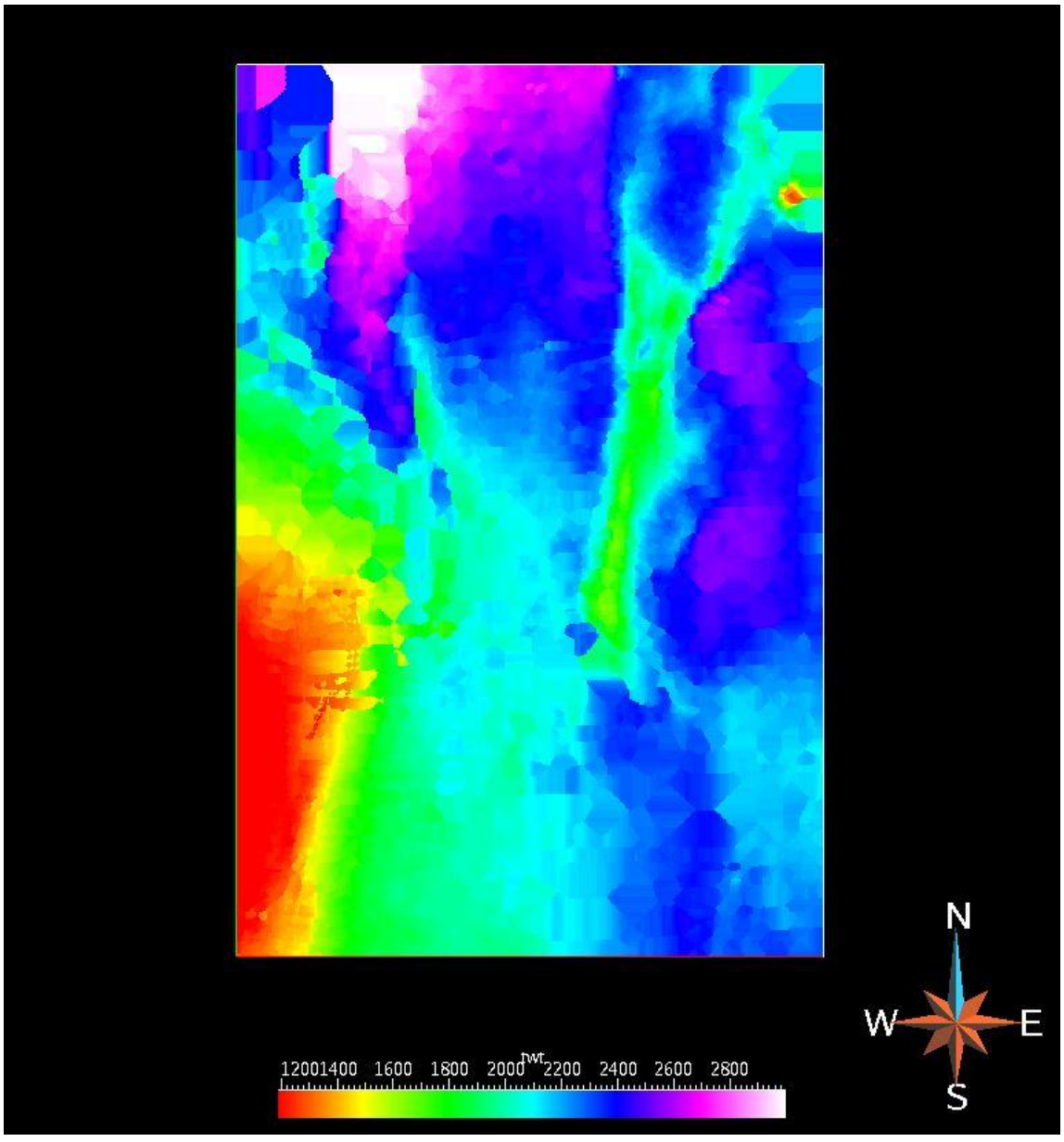

Figure 3.19. Horizon 6 surface exaggerated in the time axis and color coded (time in ms).

3.2.7 Horizon 7 from points to surface

The method used the points of Horizon 7 and interpolated them into a surface (Figures 3.20-.21).

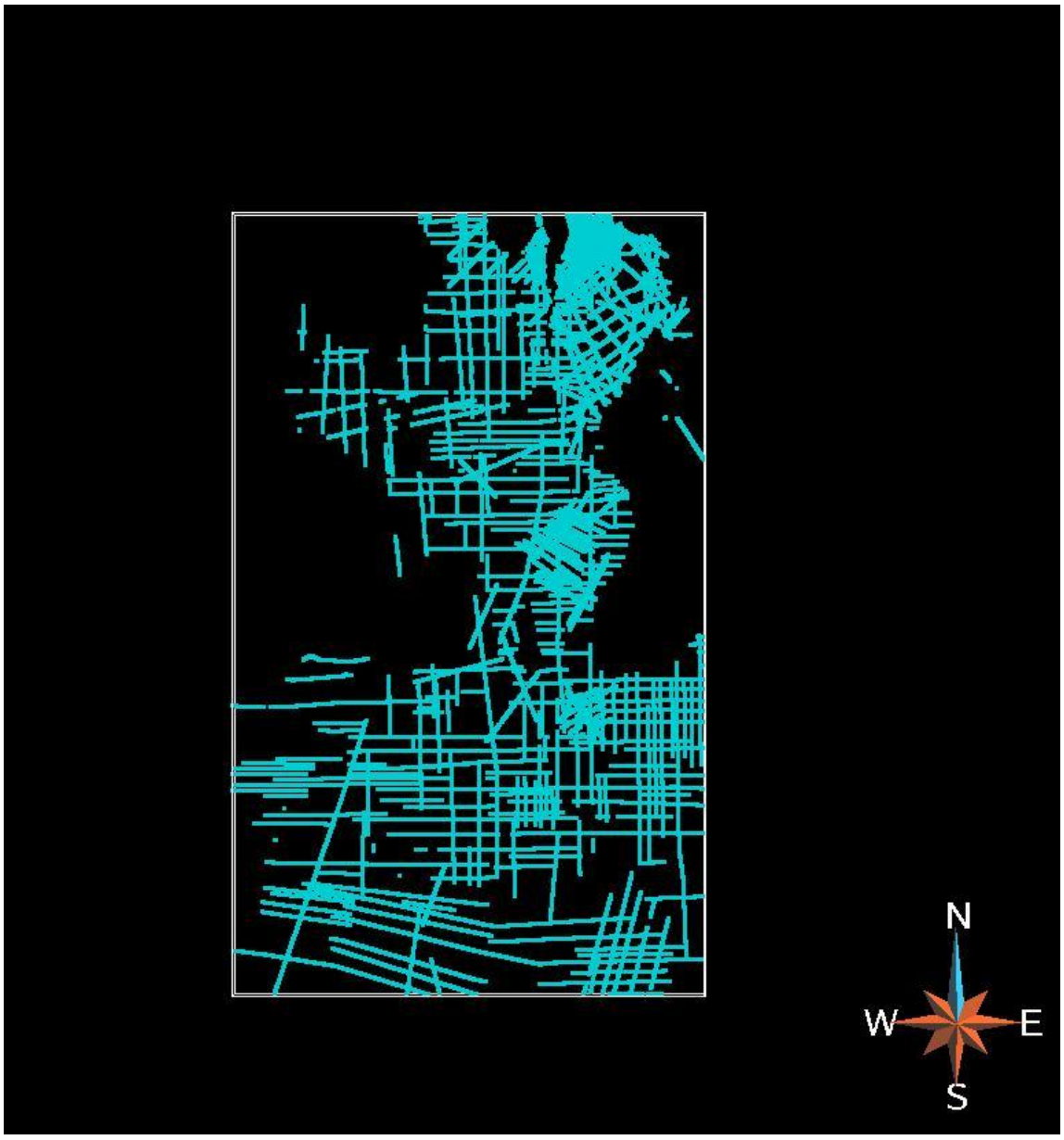

Figure 3.20. Horizon 7 as points

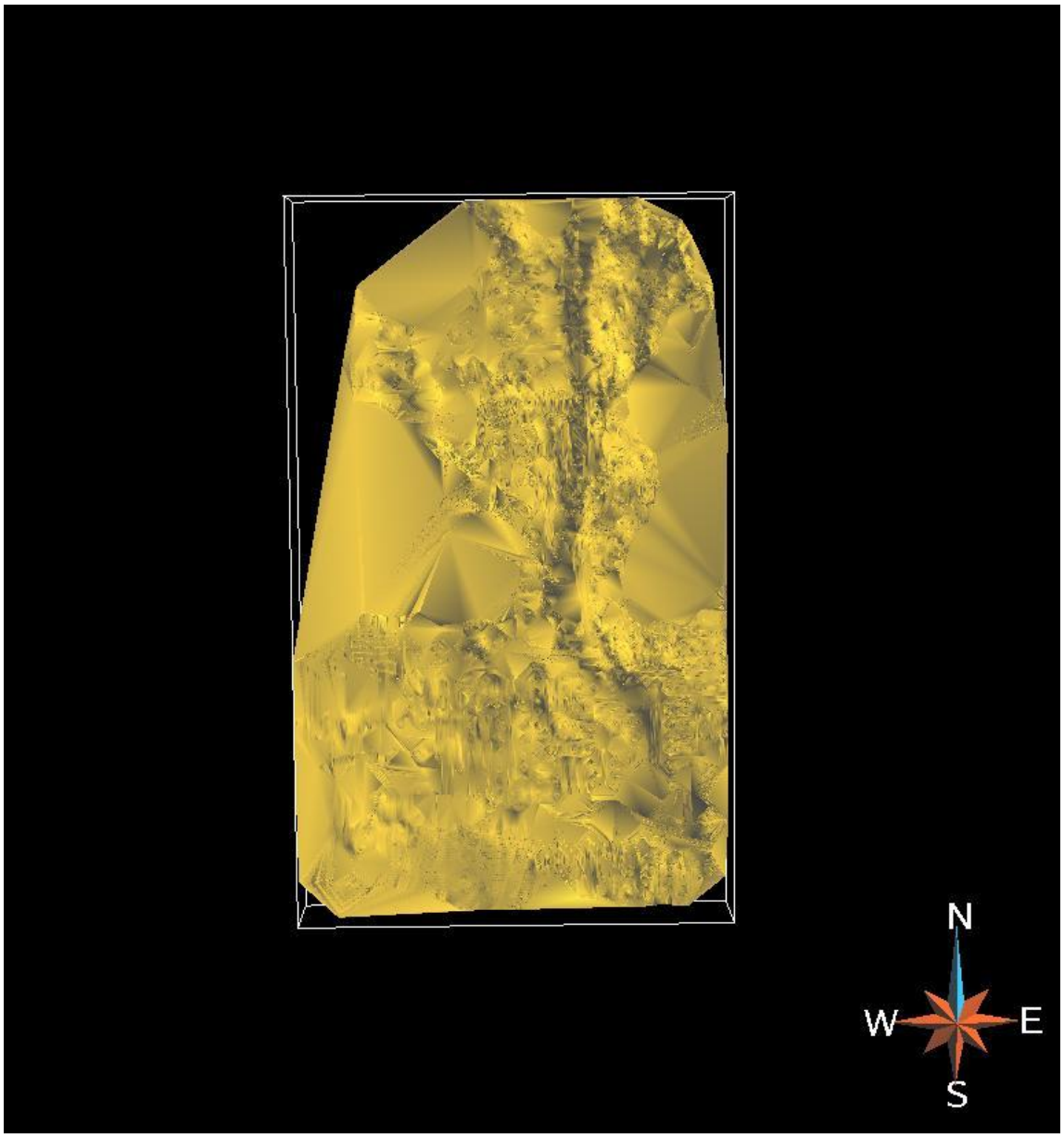

Figure 3.21. Horizon 7 interpolated into a surface

If the Z axis (represented in time) is exaggerated and color coded, it makes a more meaningful interpretation of the interpolated surface (Figure 3.22).

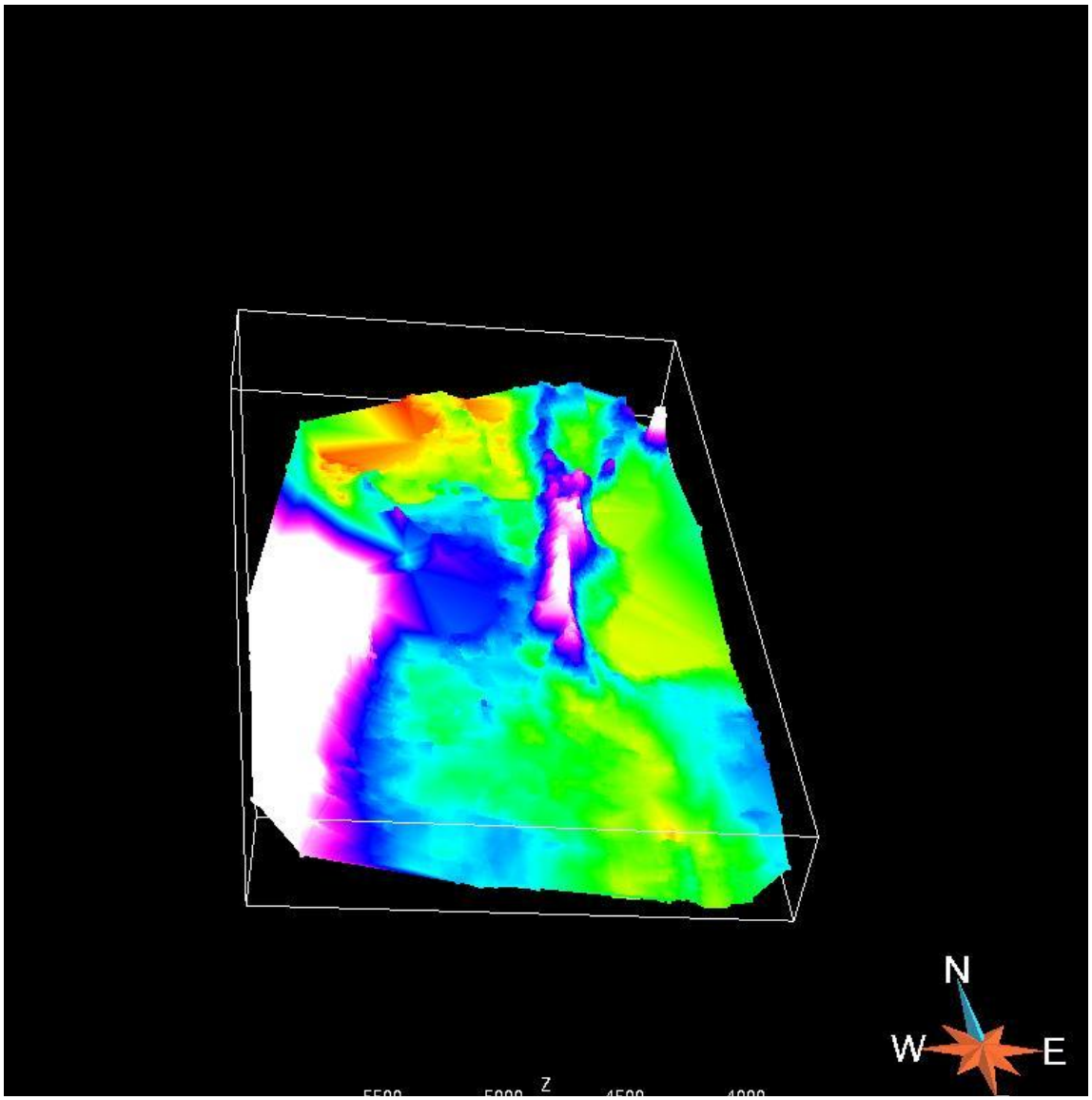

Figure 3.22. Horizon 7 surface exaggerated in the time axis and color coded (time in ms).

All the time information has been carried from the regional lines to a set of surfaces with regional extents. However, the velocity information needs to be projected on these surfaces. That way both time and velocity information would be available for use in a more practical way.

3.3 EMBEDDING THE SURFACES INTO THE VELOCITY VOLUME

Since the surfaces are ready and the velocity picks volume is already compiled (Figure 3.23) The surfaces will be embed into the velocity picks volume (Figures 3.24-3.26).

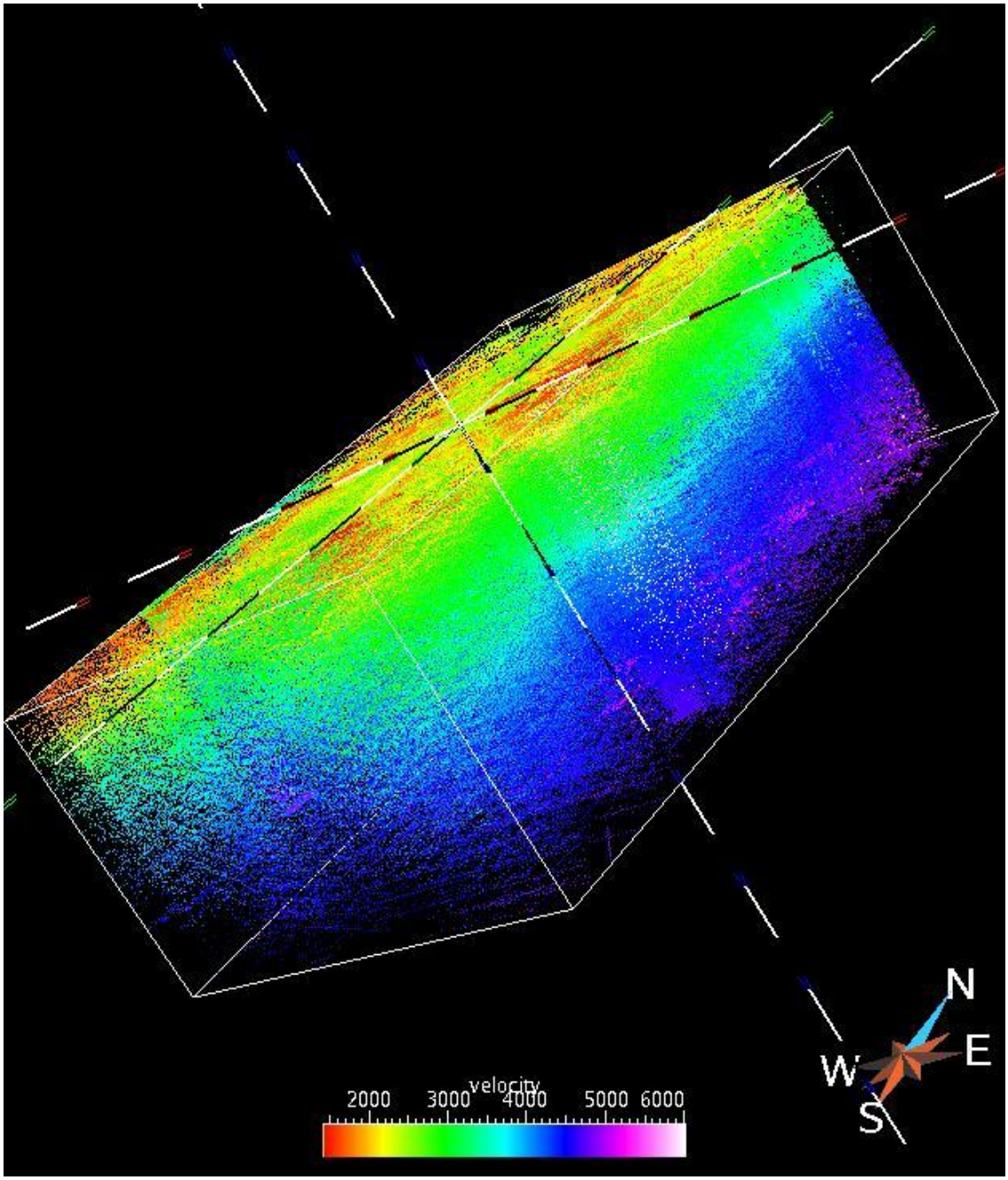

Figure 3.23. The velocity volume of compiled picks.

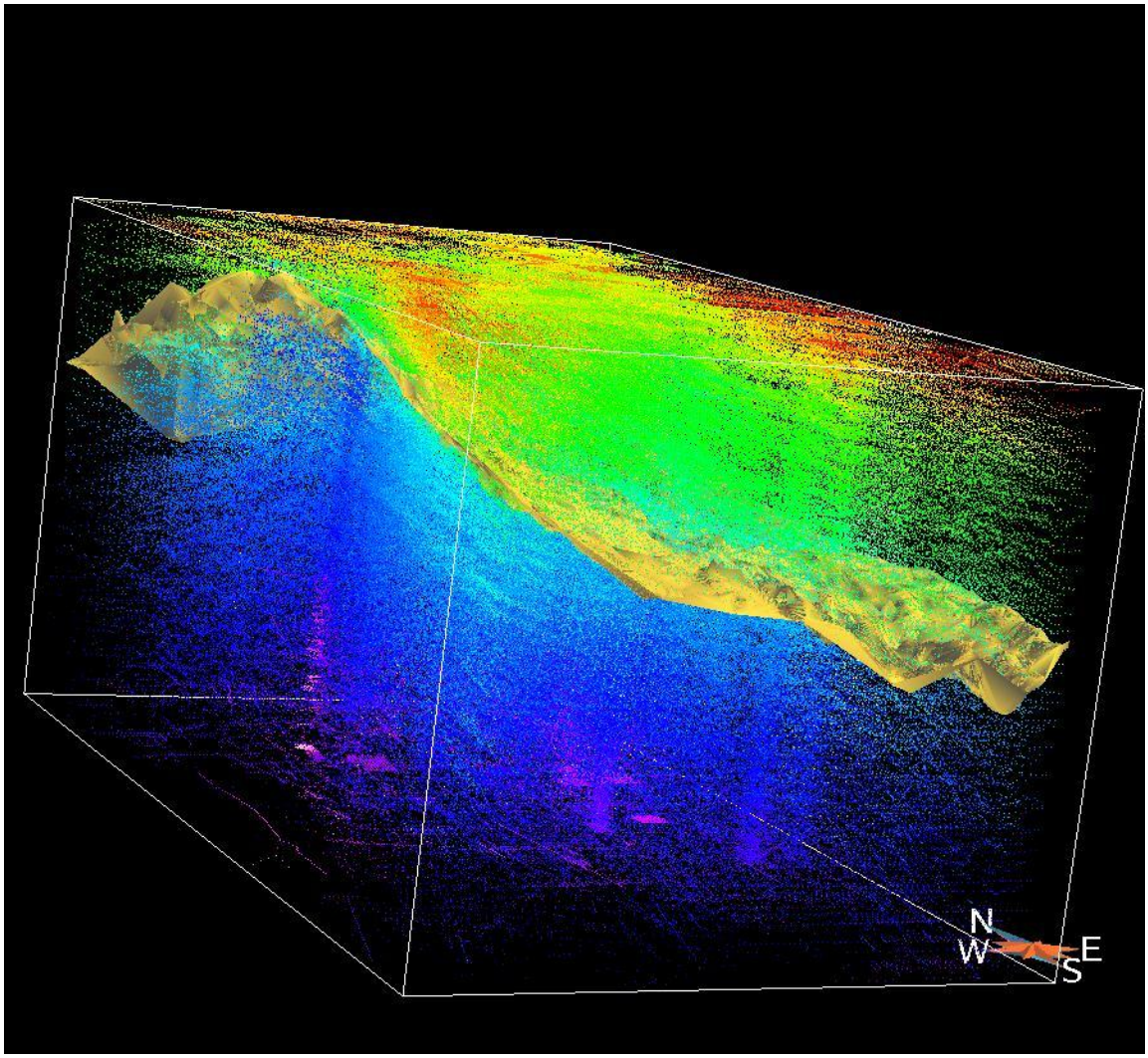

Figure 3.24. The velocity volume of compiled picks with one surface embedded into the volume. A view from the south west.

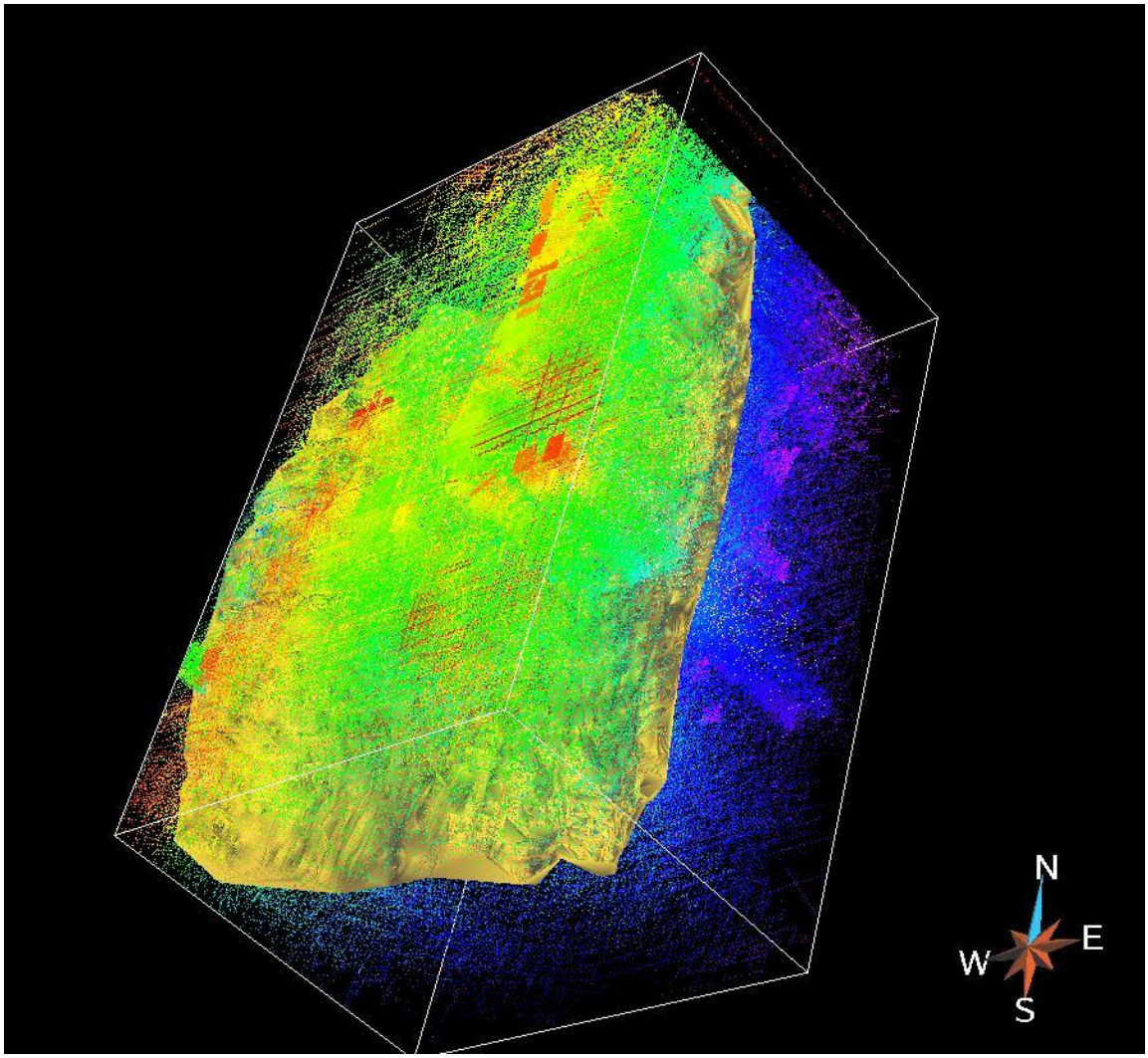

Figure 3.25. The velocity volume of compiled picks with one surface embedded into the volume. A view from the south east.

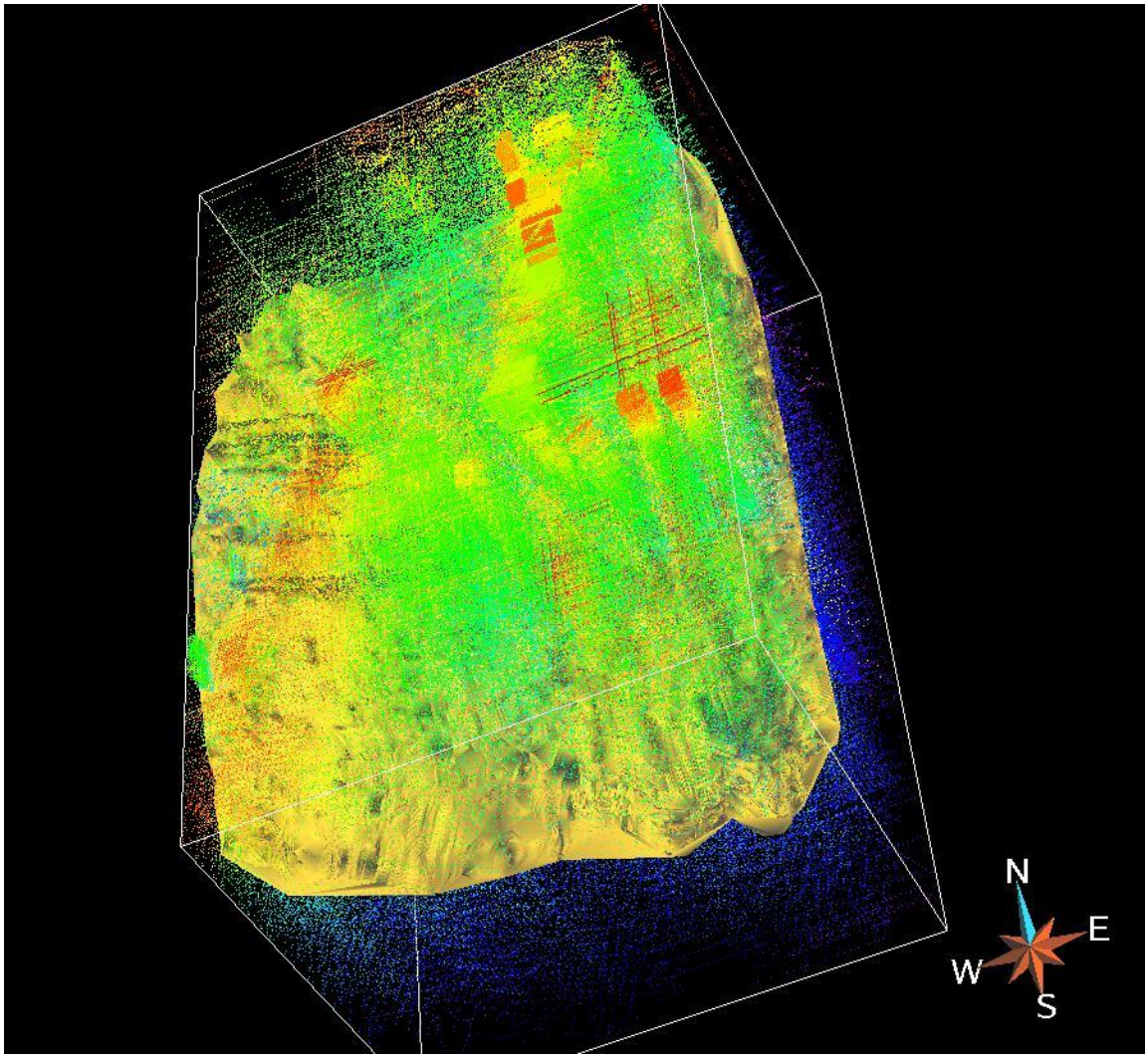

Figure 3.26 The velocity volume of compiled picks with one surface embedded into the volume. A view from the top.

3.4 PROJECTING THE VELOCITY VALUES INTO THE SURFACES

The velocity values from the velocity volume need to be projected on the surfaces that are carrying the time information. A consideration is made on the size of the window in time in milliseconds. This window is equivalent to the dominant frequency of that surface (Figure 3.27). For most horizons in this region, the dominant frequencies are between 47 Hz to 60 Hz, and thus the width of the window is between 21.2 milliseconds to 16.7 milliseconds. A conservative 25 millisecond window was set on all the interpolations done on all the surfaces. 25 milliseconds from the interpretation surface to the top of the window and 25 milliseconds from the interpretation surface to the bottom of the window. The total size in milliseconds of the window is 50 milliseconds.

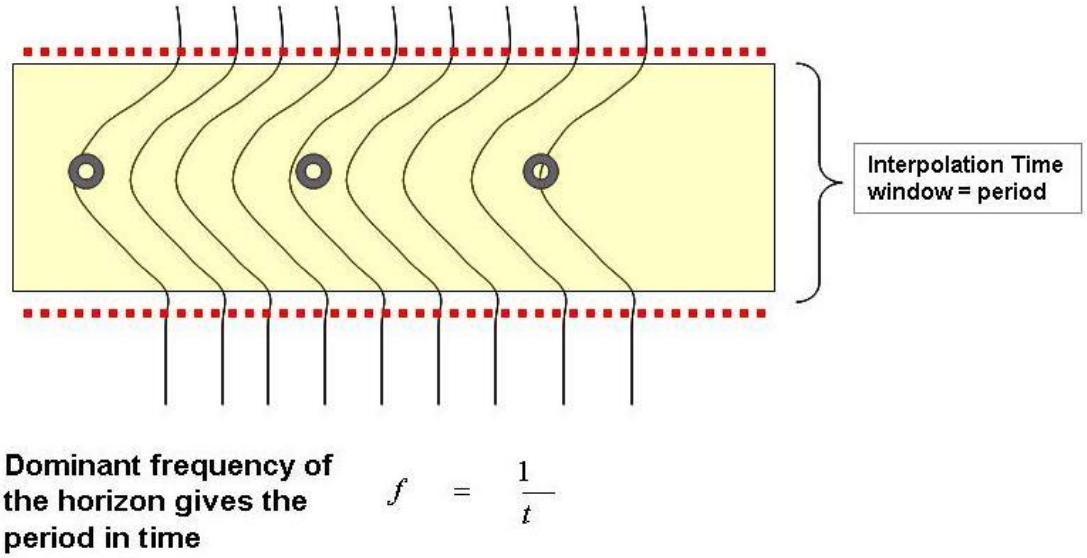

Figure 3.27. The three grey rings are assumed as the horizon time picks of the surface and a window of interpolation is set equivalent to the dominant frequency of that horizon.

3.5 GENERATED GRIDS

Now that a surface was generated with both velocity and time information, two grids were generated for each surface, one for velocity (Figures 3.28-3.34) and the other for time (Figures 3.35-3.41).

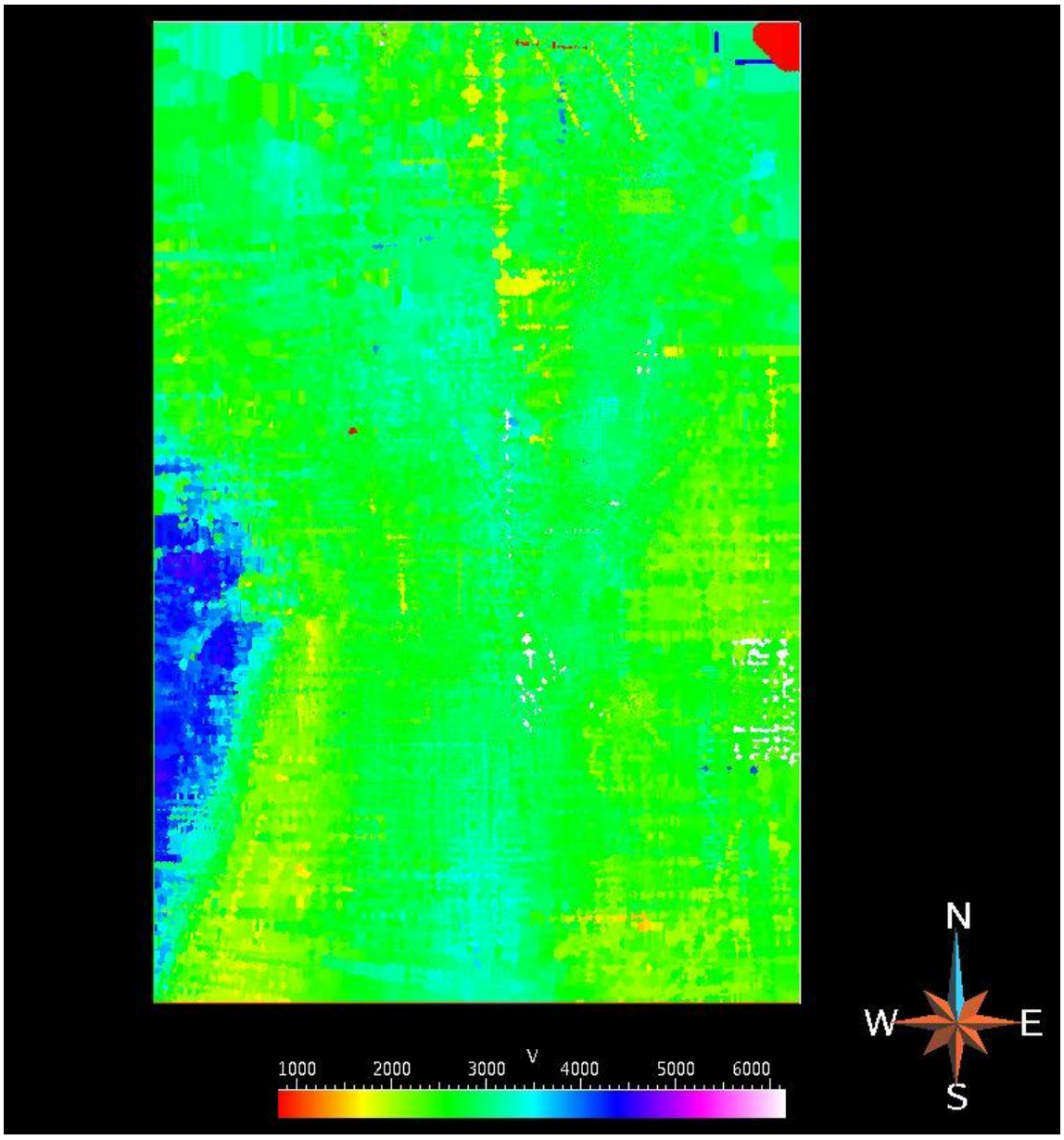

Figure 3.28. The generated velocity grid for Horizon 1.

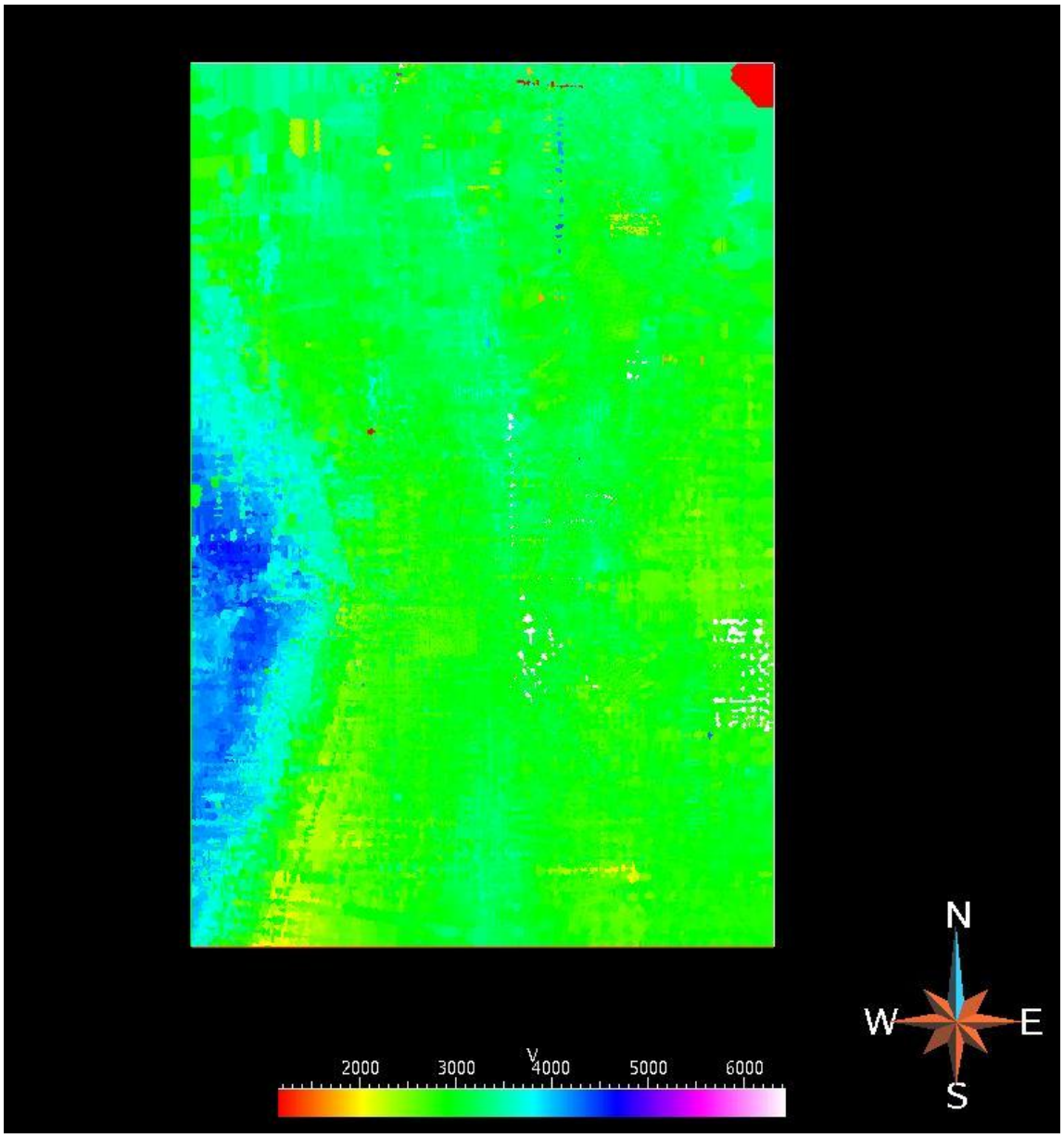

Figure 3.29. The generated velocity grid for Horizon 2.

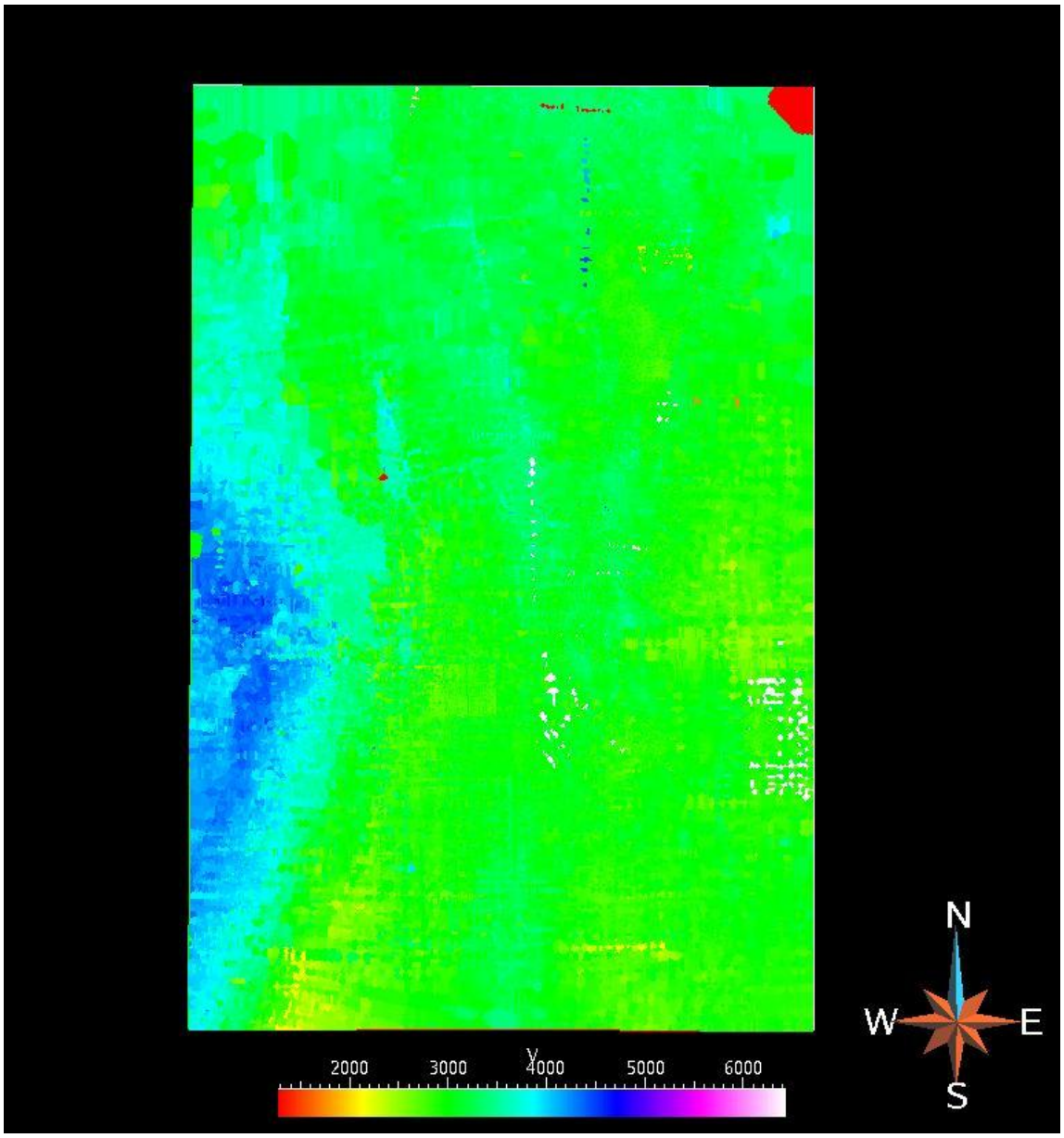

Figure 3.30. The generated velocity grid for Horizon 3.

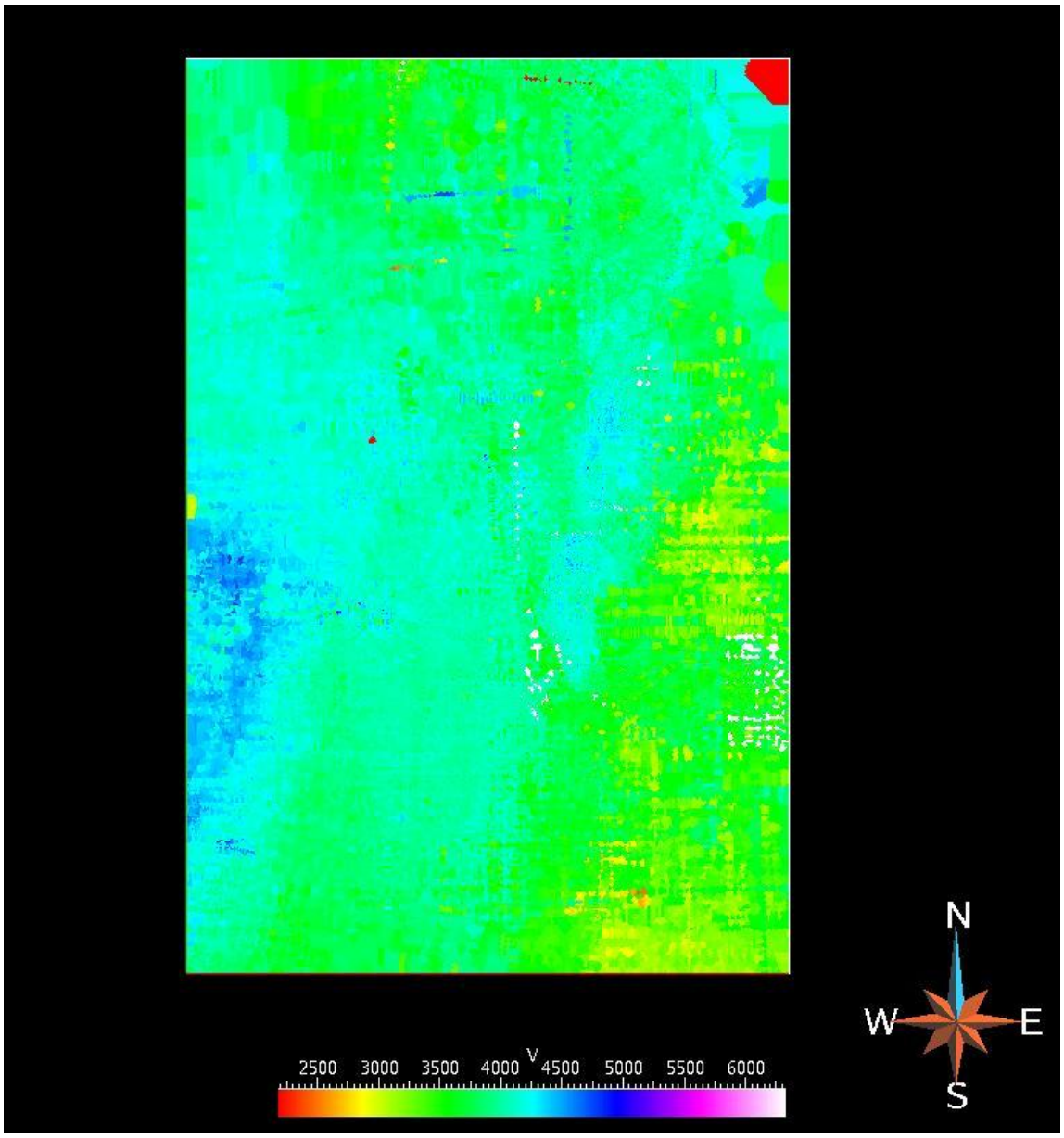

Figure 3.31. The generated velocity grid for Horizon 4.

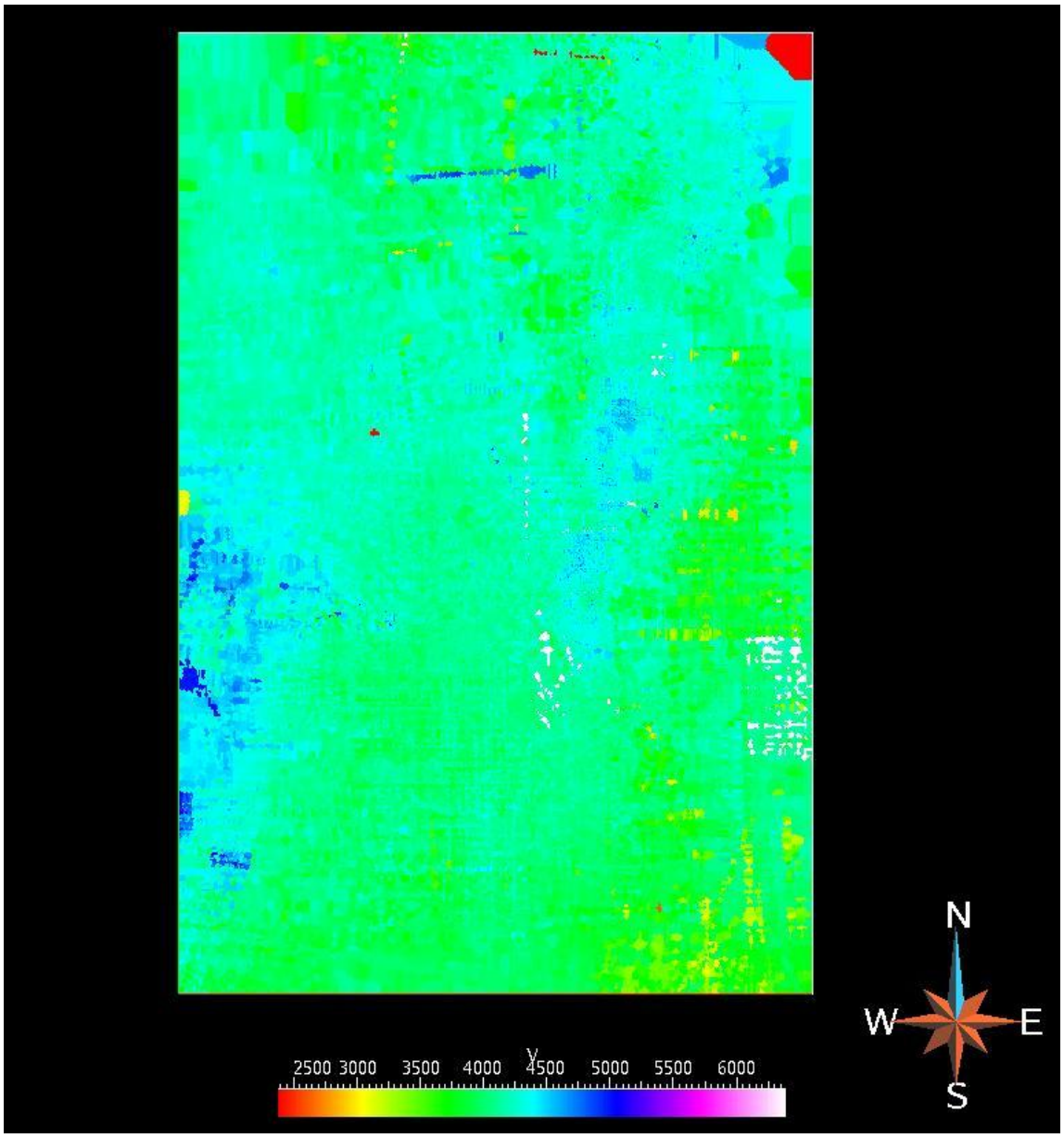

Figure 3.32. The generated velocity grid for Horizon 5.

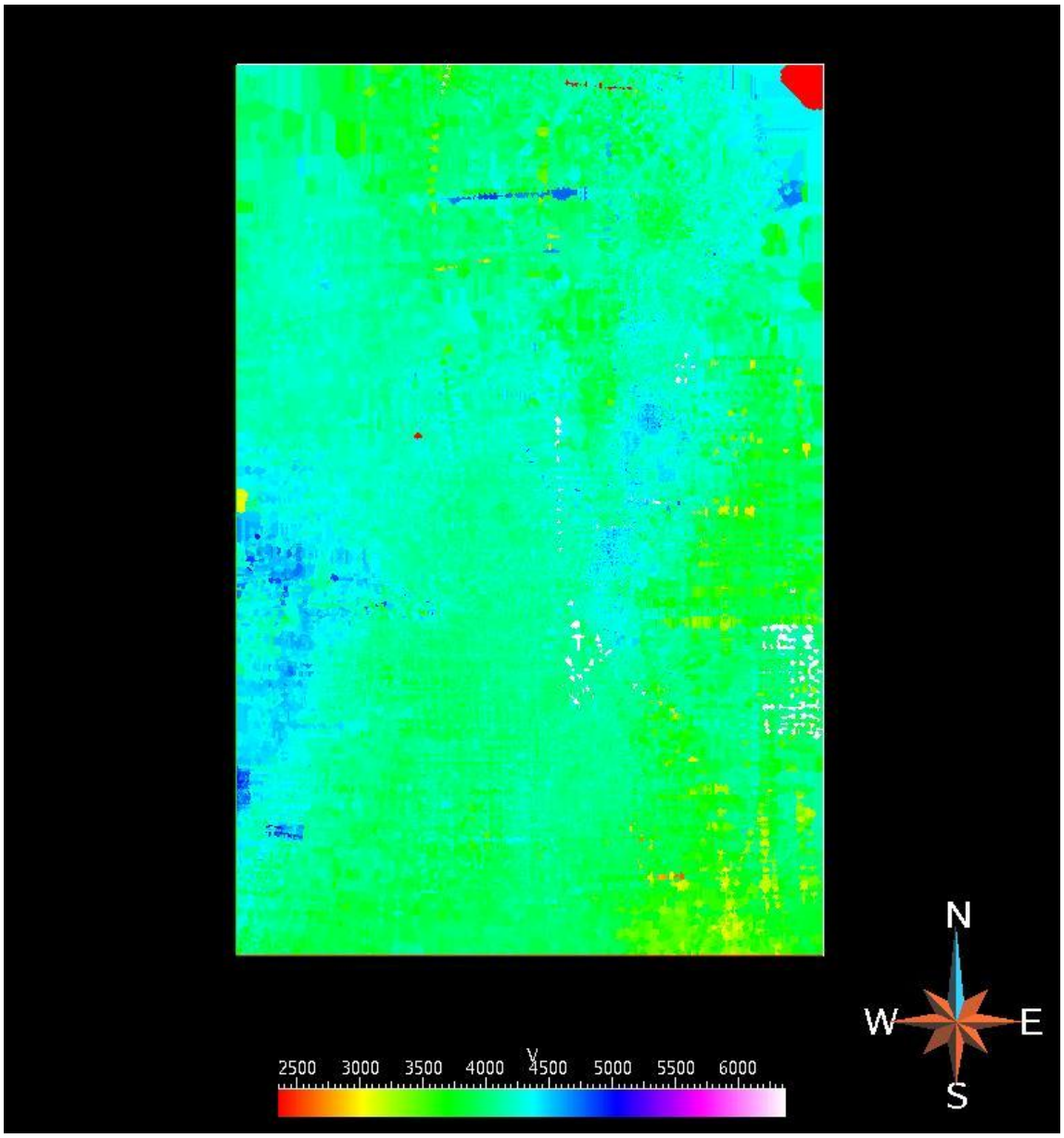

Figure 3.33. The generated velocity grid for Horizon 6.

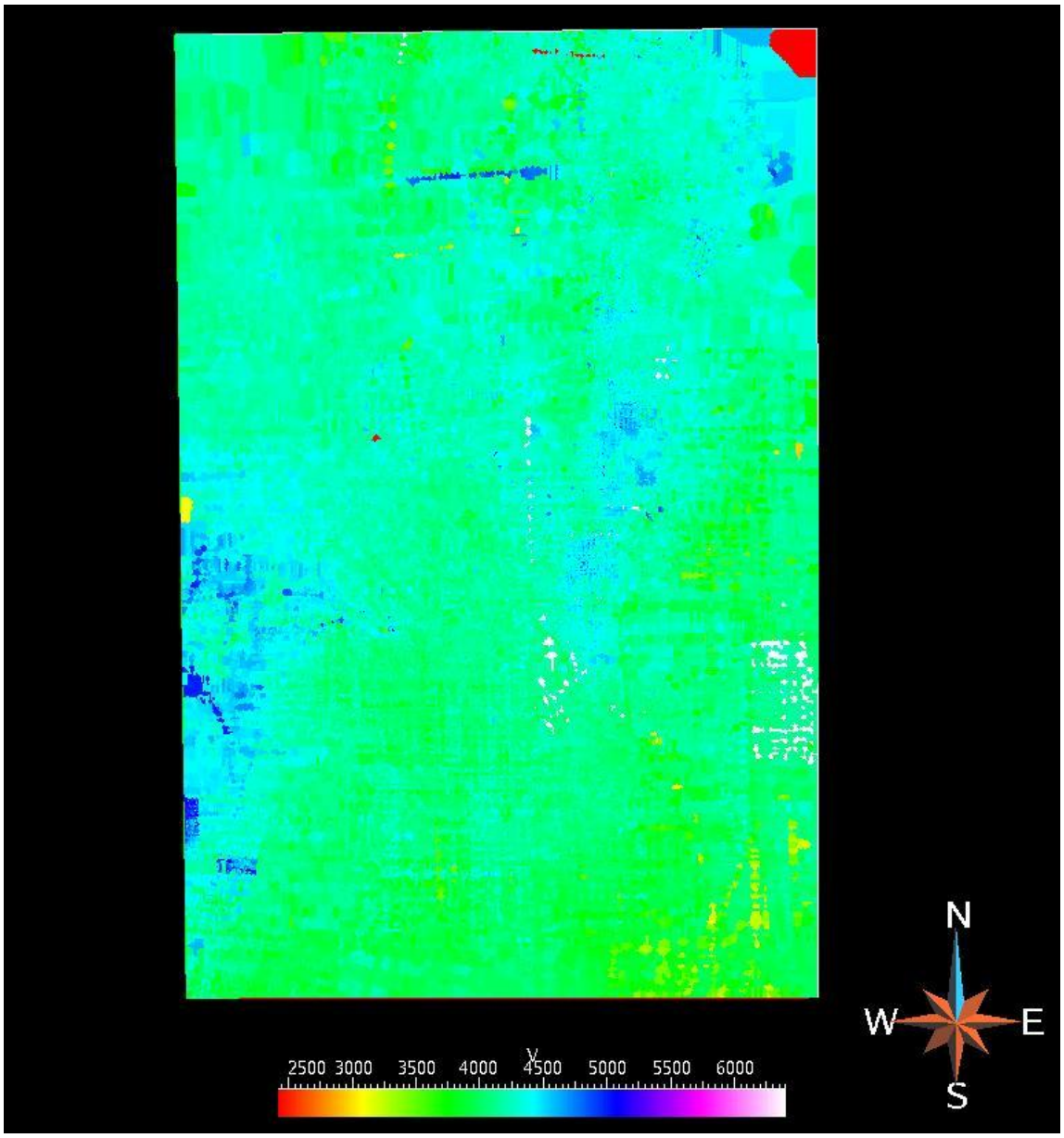

Figure 3.34. The generated velocity grid for Horizon 7.

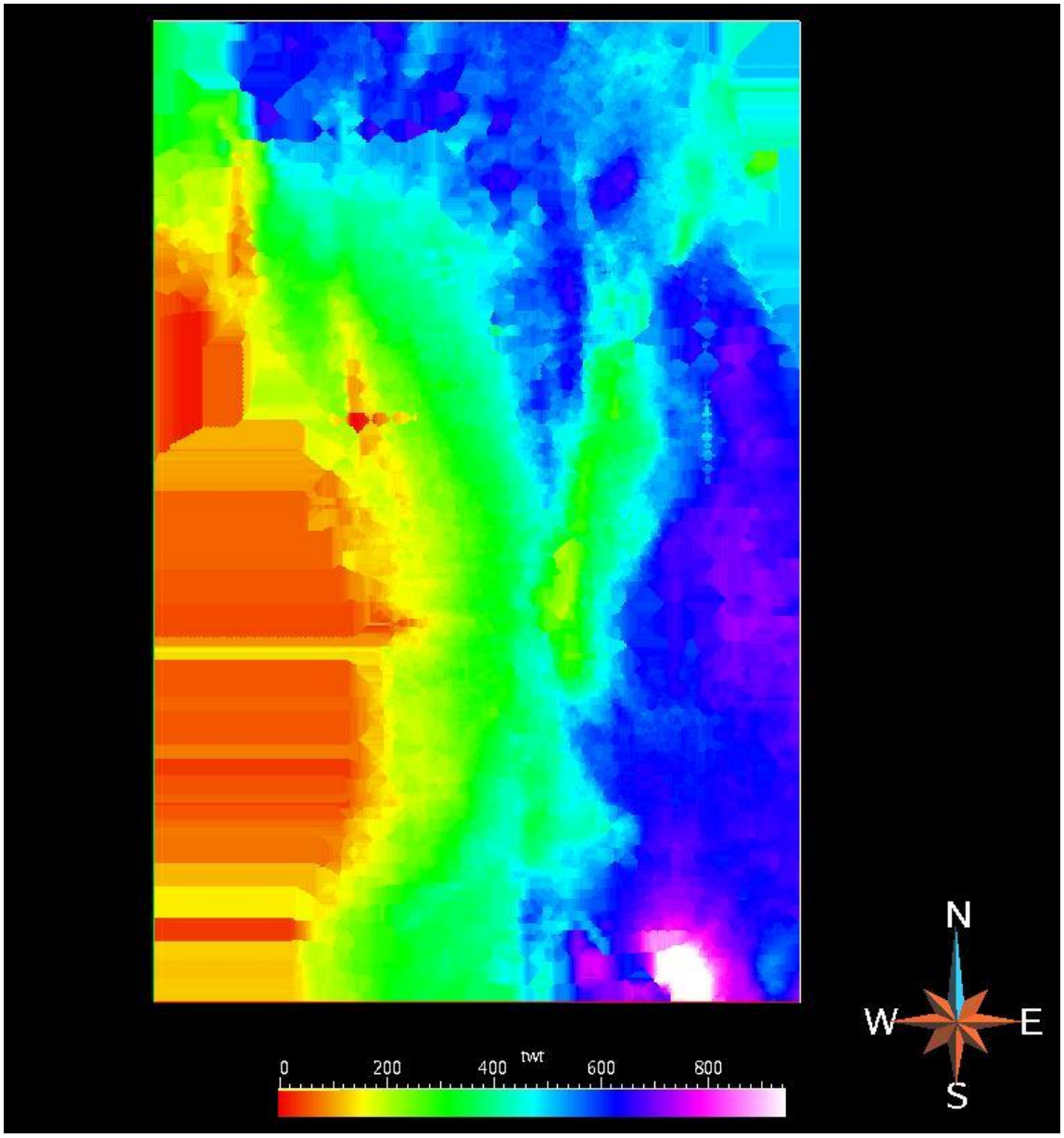

Figure 3.35. The generated time grid for Horizon 1 (twt is in ms).

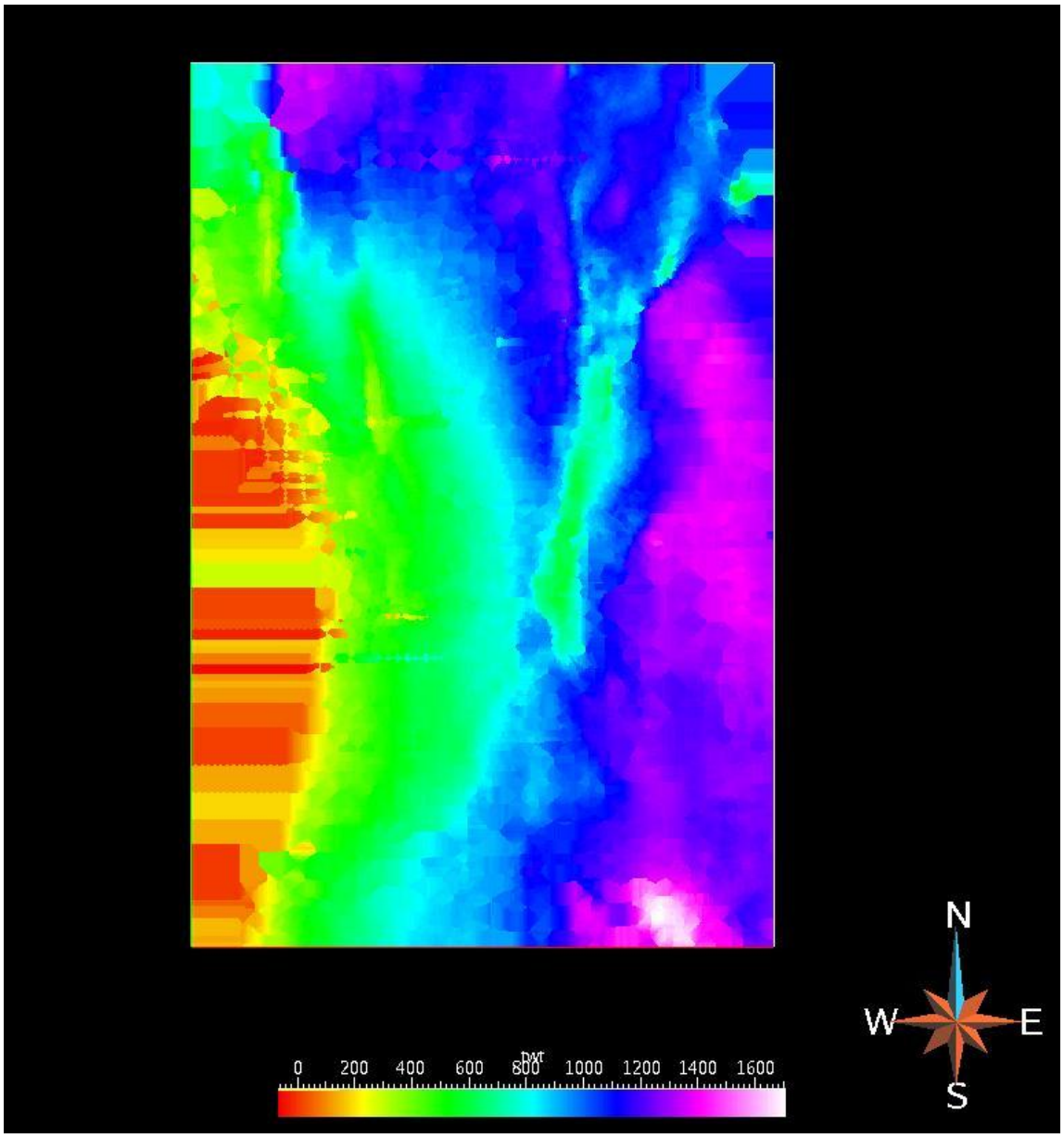

Figure 3.36. The generated time grid for Horizon 2 (twt is in ms).

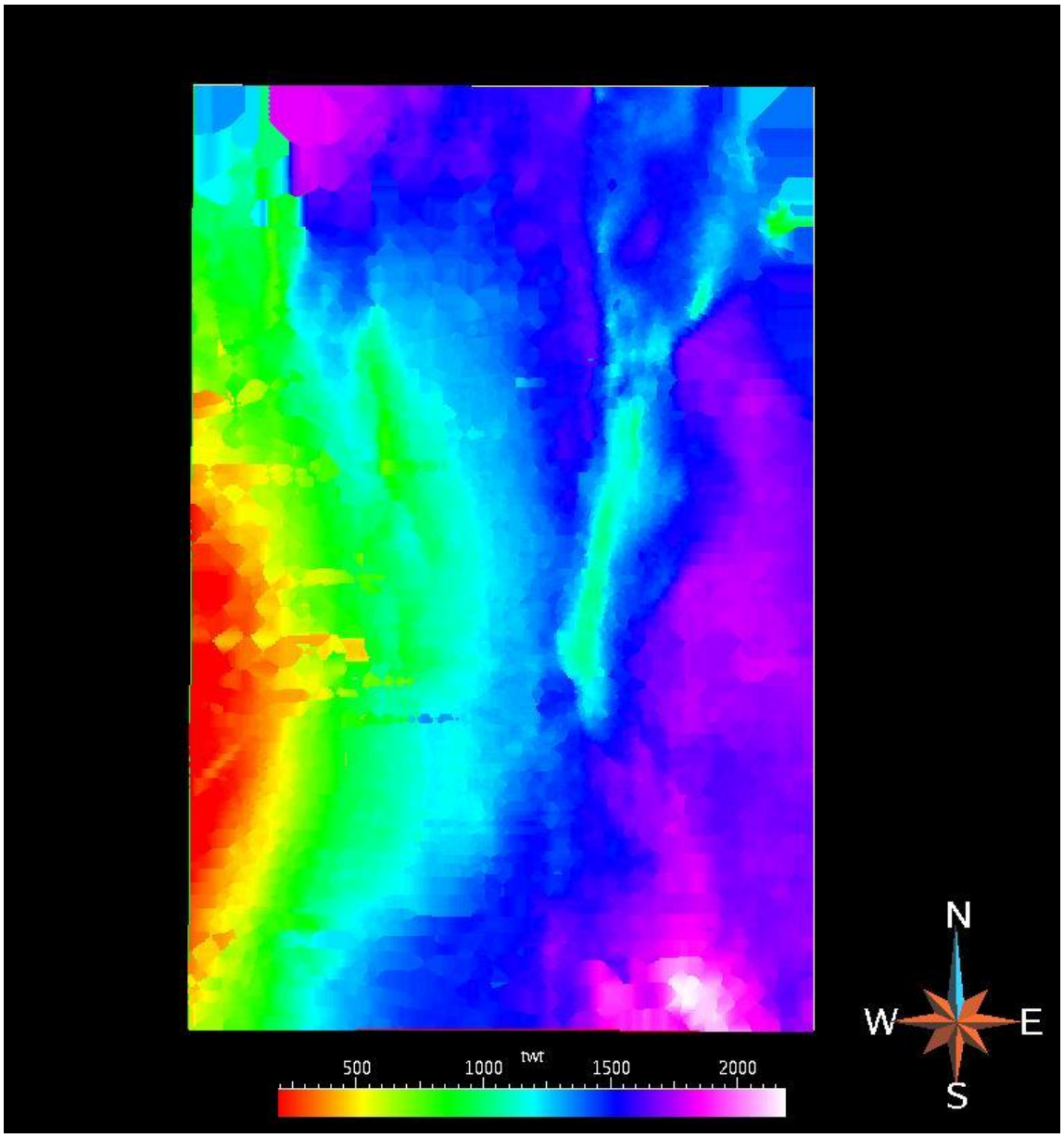

Figure 3.37. The generated time grid for Horizon 3 (twt is in ms).

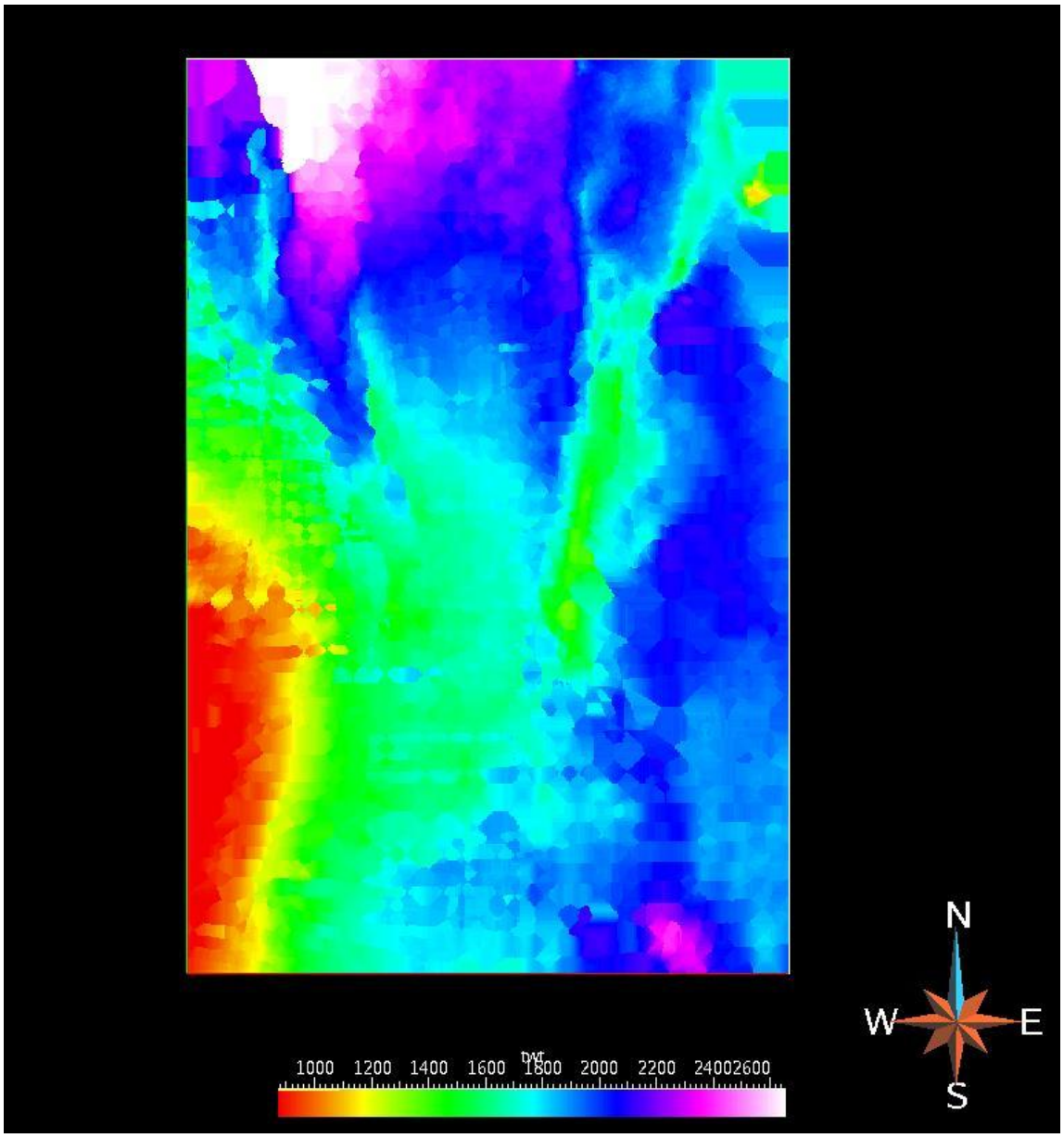

Figure 3.38. The generated time grid for Horizon 4 (twt is in ms).

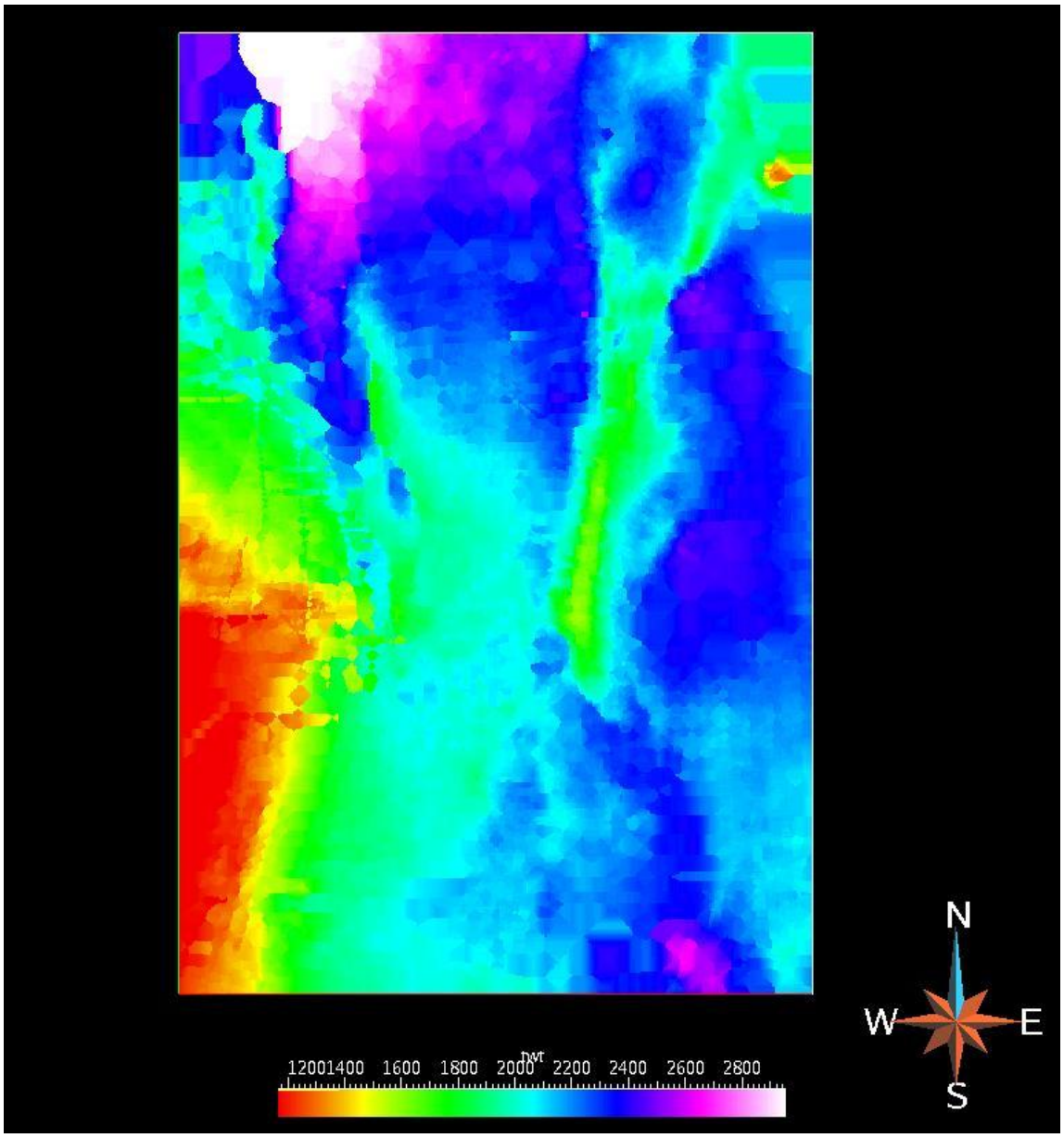

Figure 3.39. The generated time grid for Horizon 5 (twt is in ms).

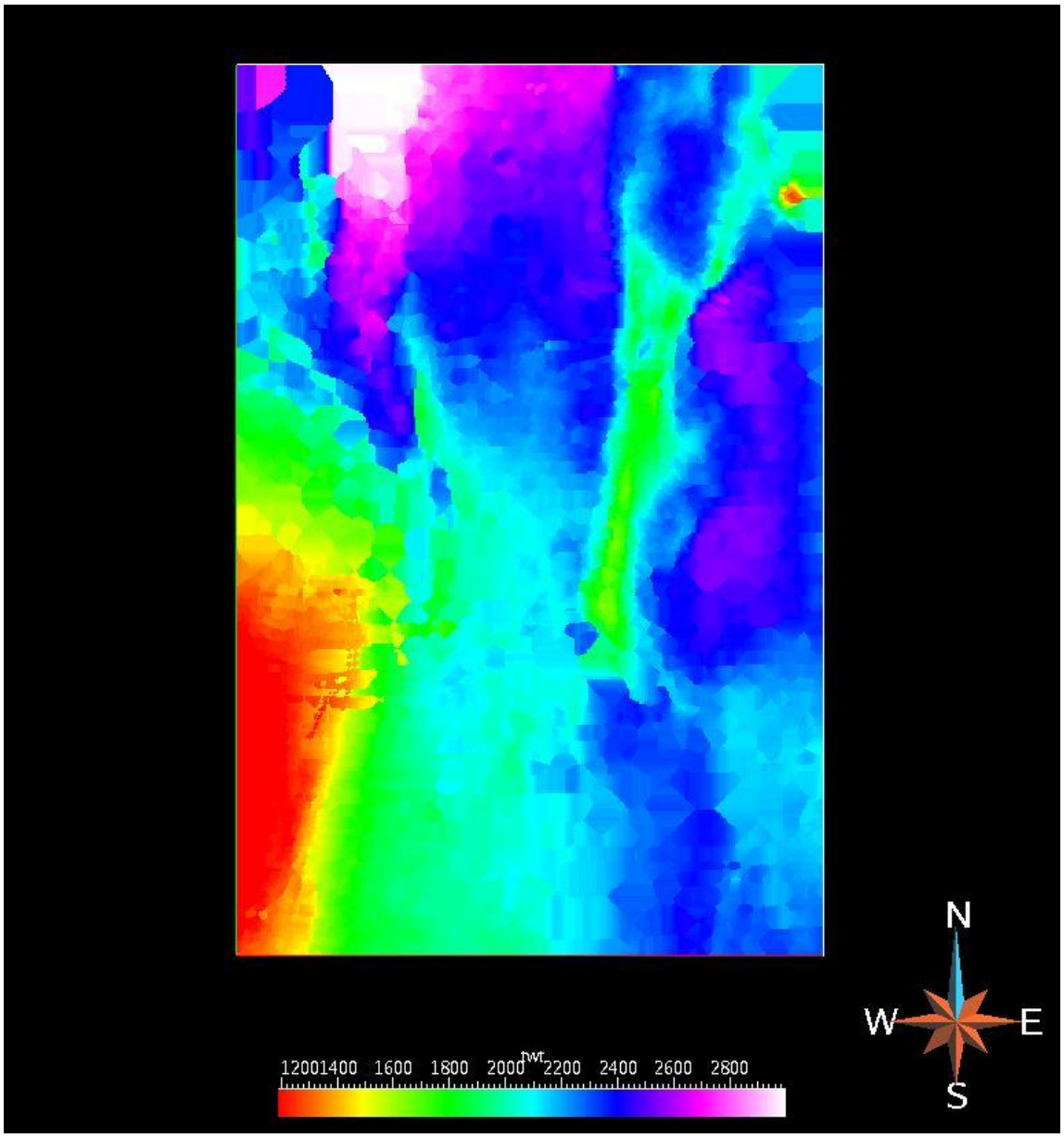

Figure 3.40. The generated time grid for Horizon 6 (twt is in ms).

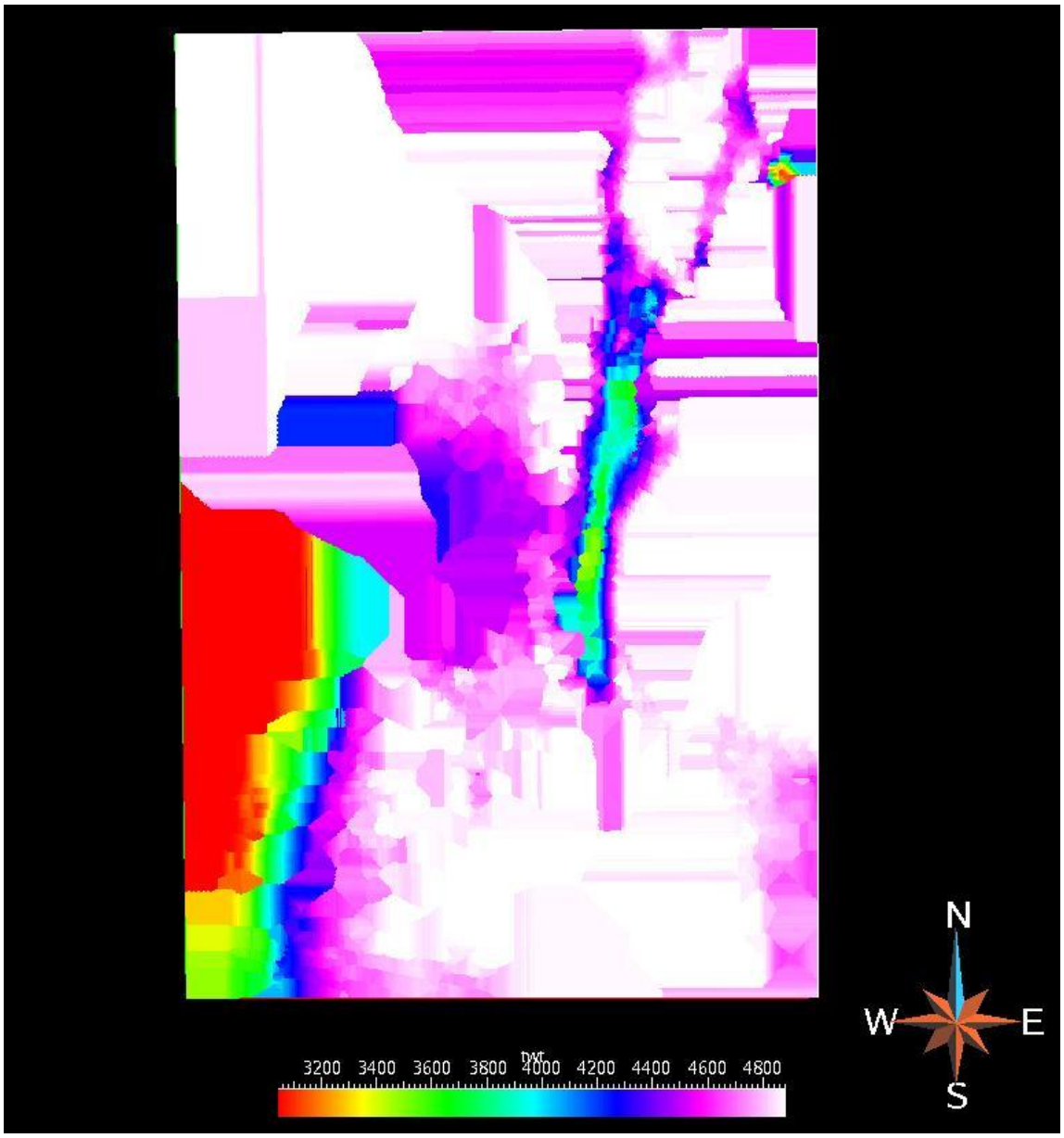

Figure 3.41. The generated time grid for Horizon 7 (twt is in ms).

CHAPTER 4

RESULTS

For every key Horizon, both time and velocity values were made available at all locations of the horizon. At any point of the area of study a time value as well as a velocity value can be obtained for every subsurface horizon at that point. The results of the study was tested on various cases to evaluate its validity (Table 4.1).

Horizon	Time	Velocity
Horizon1	T-h1	V-h1
Horizon2	T-h2	V-h2
Horizon3	T-h3	V-h3
Horizon4	T-h4	V-h4
Horizon5	T-h5	V-h5
Horizon6	T-h6	V-h6
Horizon7	T-h7	V-h7

Table 4.1 A sample table demonstrating the kind of result data that will be used into the stacks.

4.1 CASE ONE: Various possible points of maximum coherency at a wide range of velocity

In this case the coherency semblance has two potential problems. The first problem is that certain maximum coherency semblances indicate wide ranges of possible coherency at a wide range of velocities (Figure 4.1). This problem is clear in the figure at 630 milliseconds as well as another location at 840 milliseconds. This can mean that the offset is greatly varying, which indicates that the actual subsurface location of the horizon is varying.

The second problem with this location is that there are many possible picks if you consider maximum coherency semblances throughout the time scale but it is unknown which one of the maximum coherency semblances is actually a representation of an actual subsurface horizon (Figure 4.1). This problem is clear in the figure for the semblances between 1000 milliseconds to 2000 milliseconds as well as between 2400 milliseconds to 3400 milliseconds.

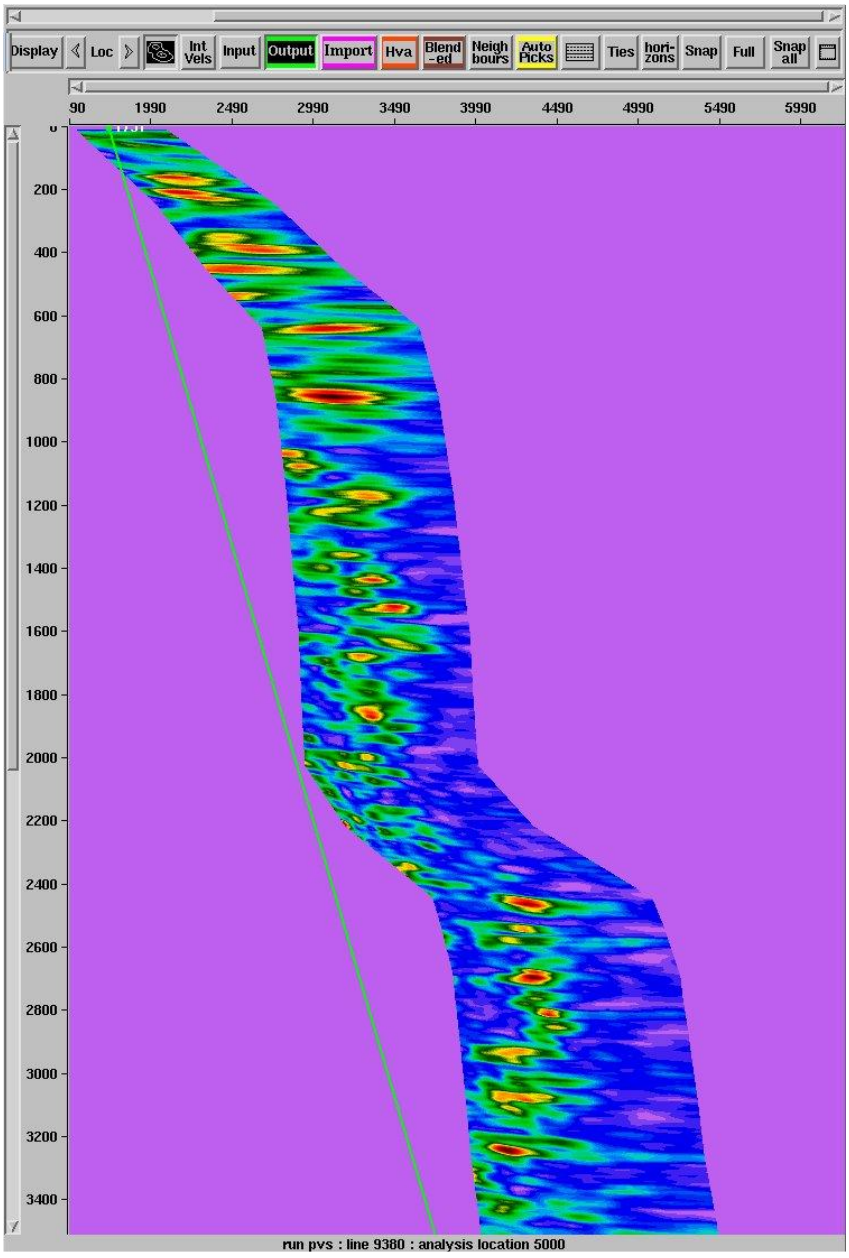

Figure 4.1 The semblance shows maximum coherency at a wide range of offset at 650 milliseconds and at 820 milliseconds. The figure also shows many possible time picks between 1000 milliseconds to 2000 milliseconds as well as between 2400 milliseconds to 3400 milliseconds, but which one of those maximum coherency points represents a valid pick of a horizon?

The study can provide time and velocity values for the seven key horizons that were compiled, interpolated, and integrated. The time values and velocity values were posted on the semblances as indicated in the figure (Figure 4.2).

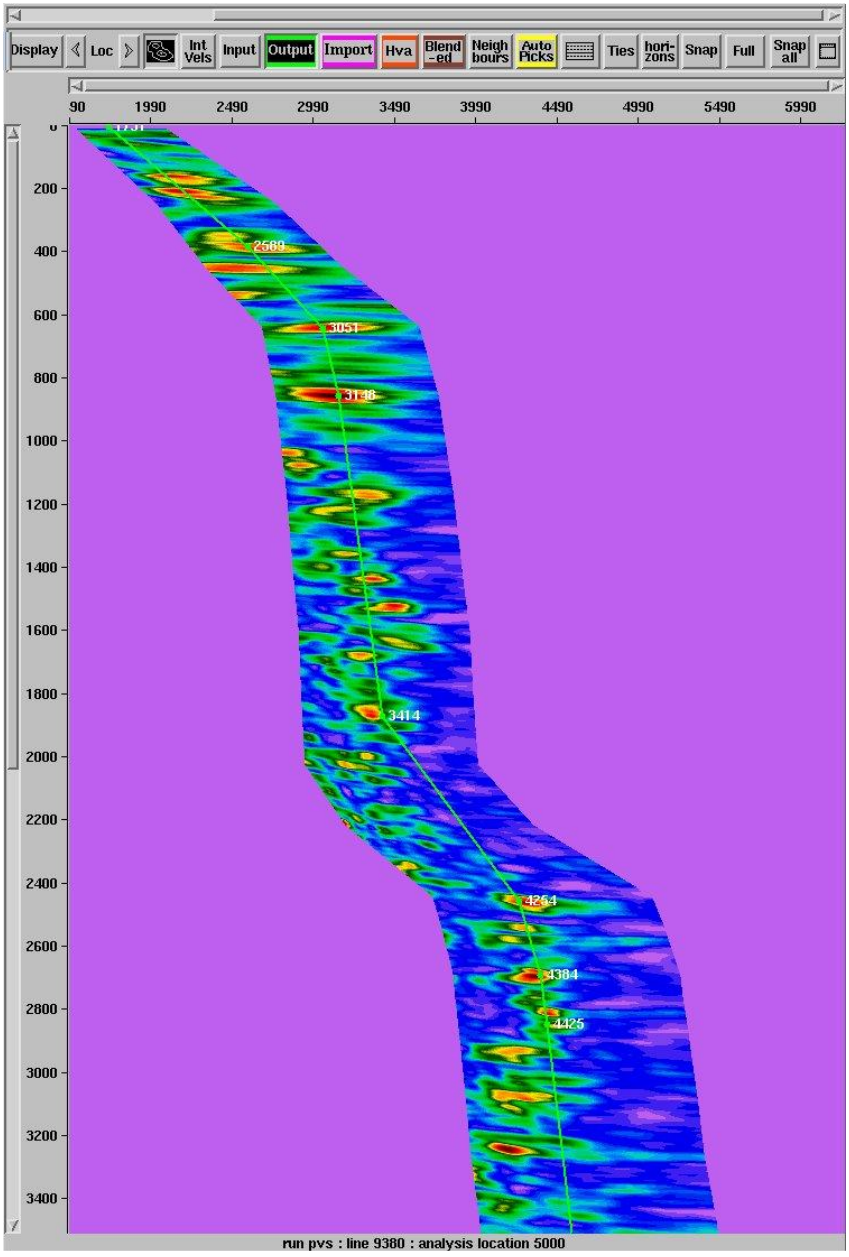

Figure 4.2. The same semblance as in Figure 4.1 with the time picks and velocity values applied for the 7 Horizons.

The stack response is quite indicative of the effectiveness of the method, major improvements in the signal to noise ratio are obvious throughout the time scale on the location of the seismic line where the semblance is reading (Figure 4.3 versus Figure 4.4).

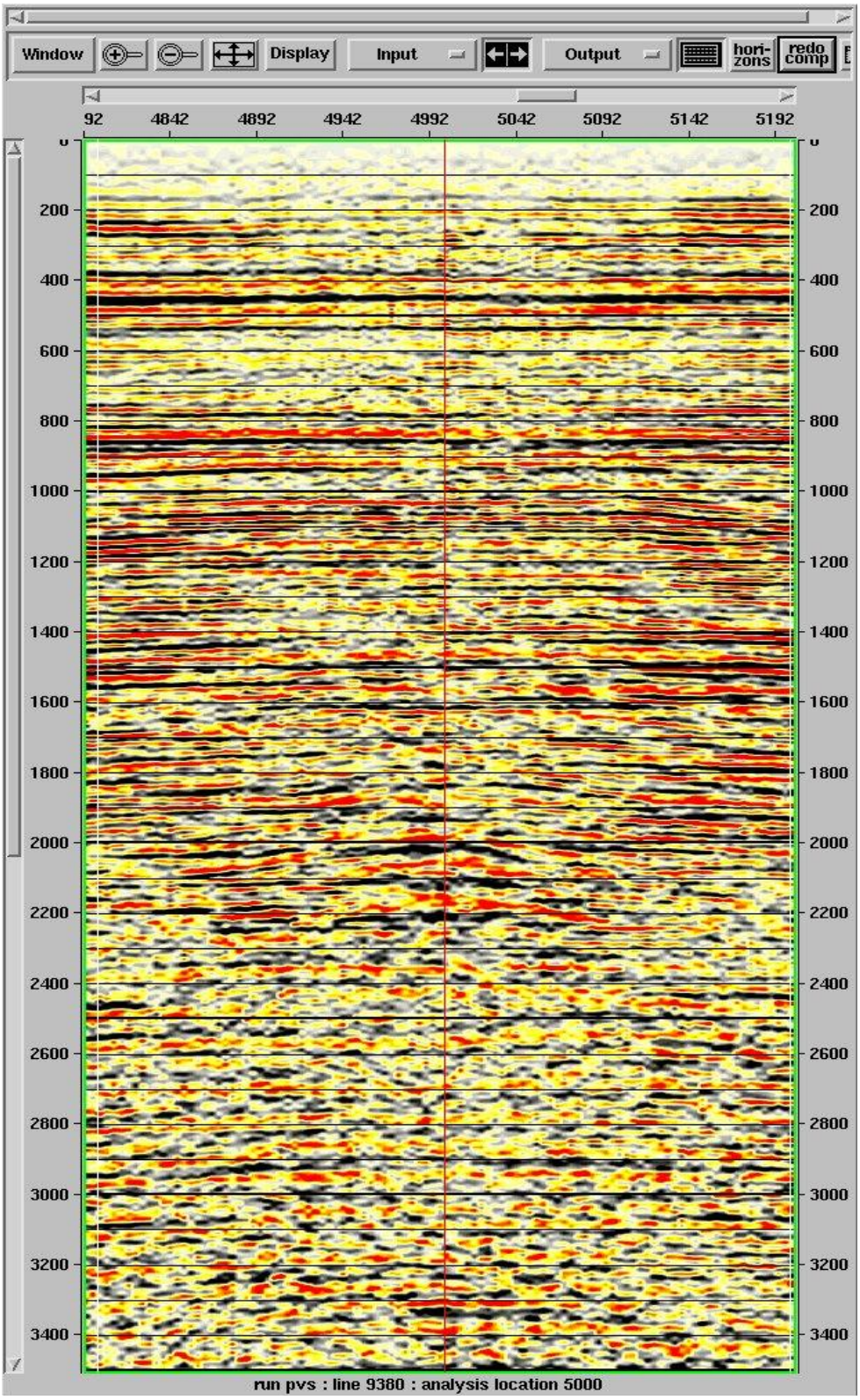

Figure 4.3. The stack response before applying the model-derived velocities for the seven key horizons.

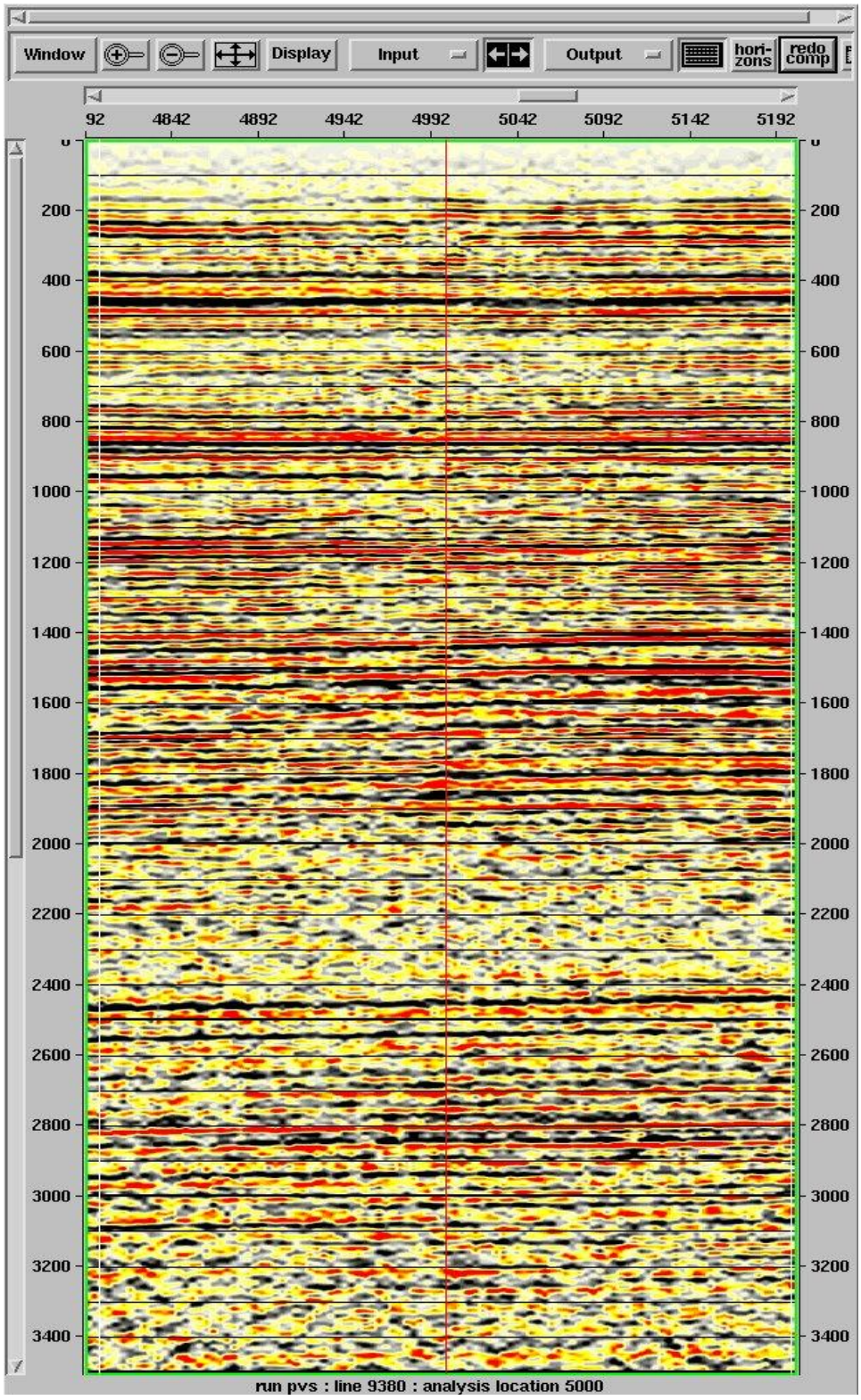

Figure 4.4. The stack response after applying the model-derived velocities for the seven key horizons.

4.2 CASE TWO: Poor coherency throughout the semblance

This case presents a coherency semblance that has poor indications of possible subsurface horizons throughout the time scale. Semblances from 1400 (ms) to 2400(ms) show poor coherencies making the coherency color as light as yellow but never makes a hot dark color which is a result of high coherencies if it existed. It does not provide any unique indication of where the subsurface horizons might be (Figure 4.5).

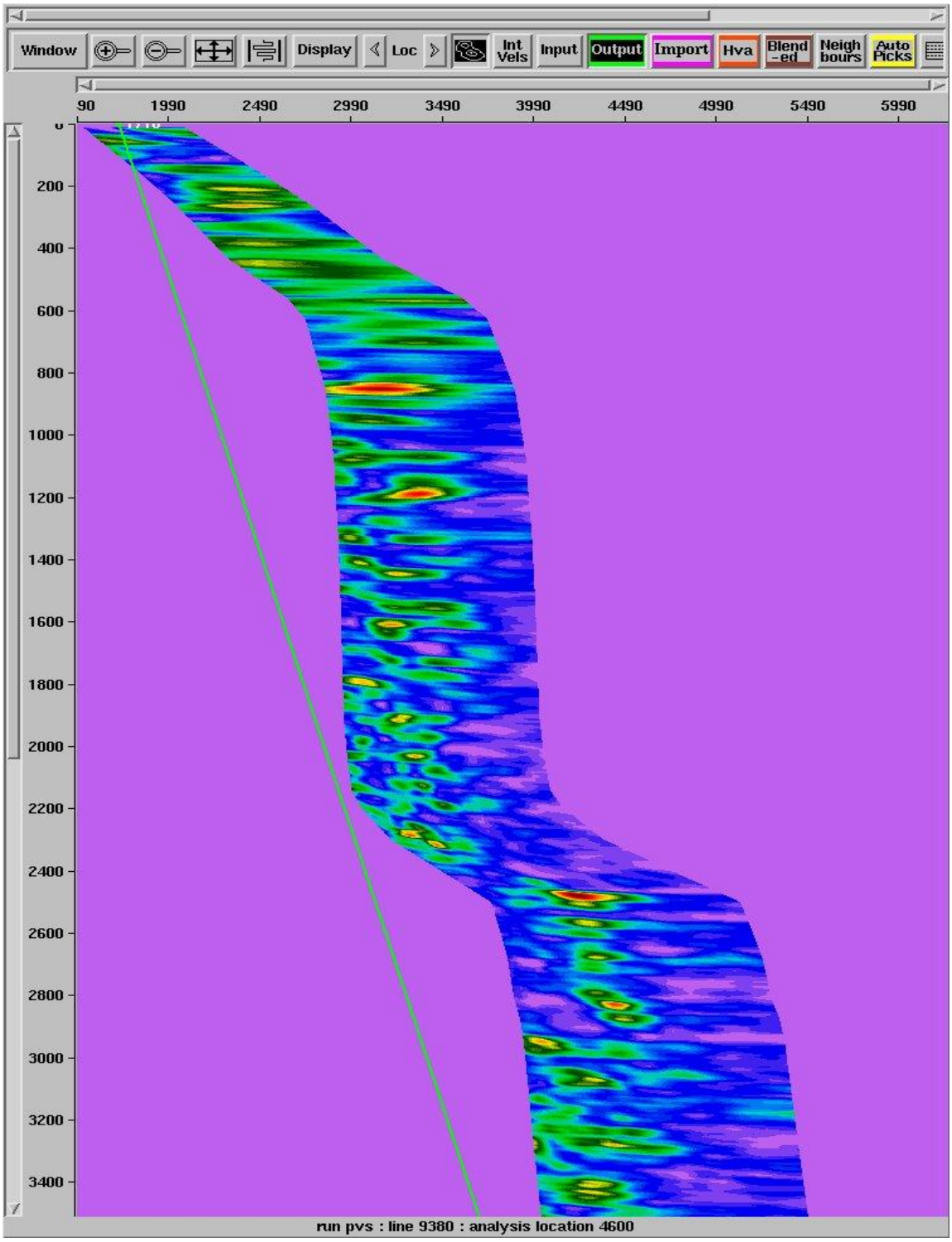

Figure 4.5. The semblance shows maximum coherency that is very poor. It makes it confusing to know where to pick throughout the semblance.

The study can provide time and velocity values for the seven key horizons that were compiled, interpolated, and integrated. In this case, the study tremendously helps to know where the key horizons are. The time values and velocity values were posted on the semblances as indicated in the Figure 4.6

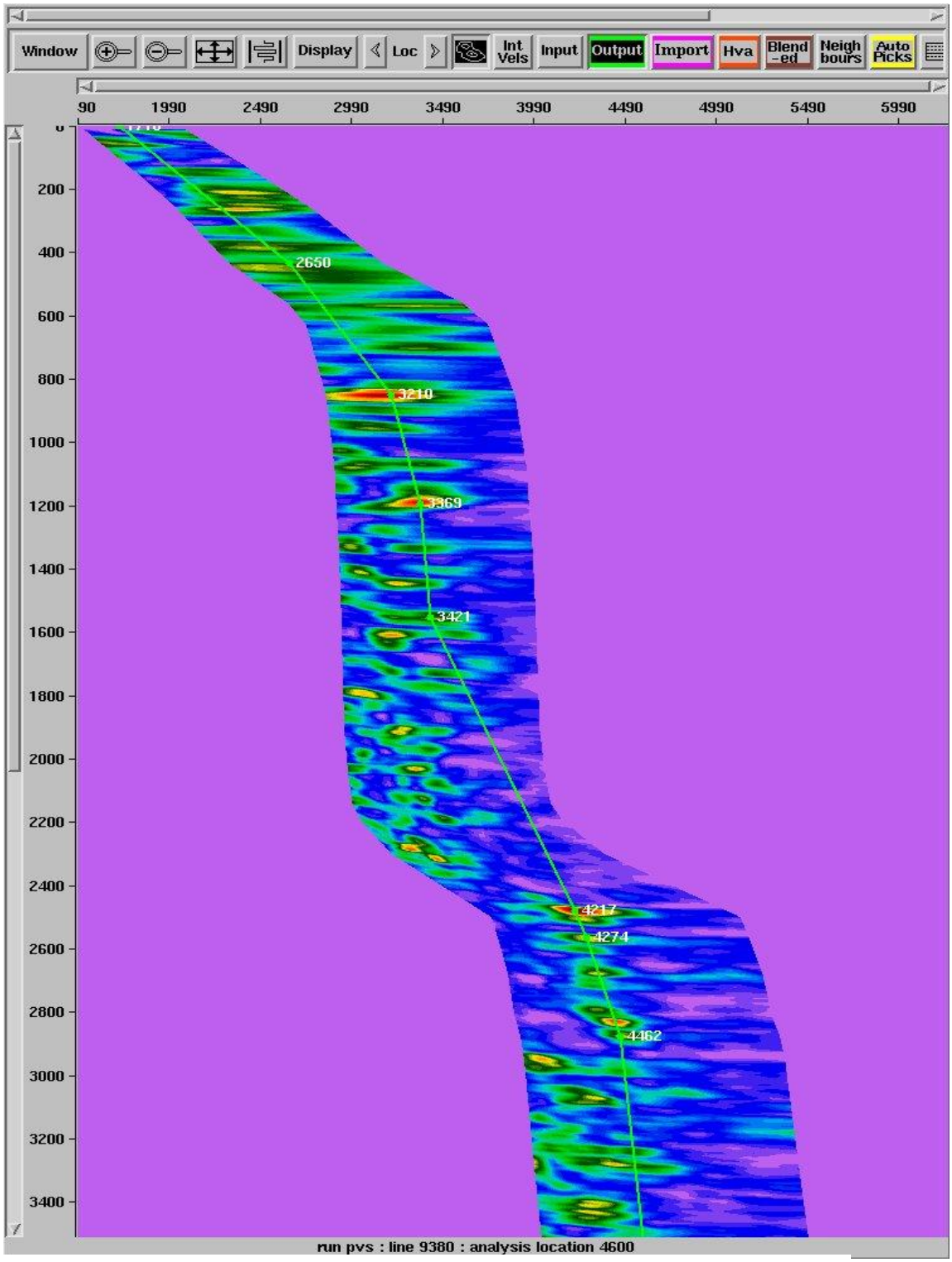

Figure 4.6. The same semblance as in Figure 4.5 with the time picks and velocity values applied for the 7 Horizons.

The stack response is quite indicative of the effectiveness of the method, major improvements in the signal to noise ratio are obvious throughout the time scale on the location of the seismic line where the red line passes. (Figure 4.7 versus Figure 4.8).

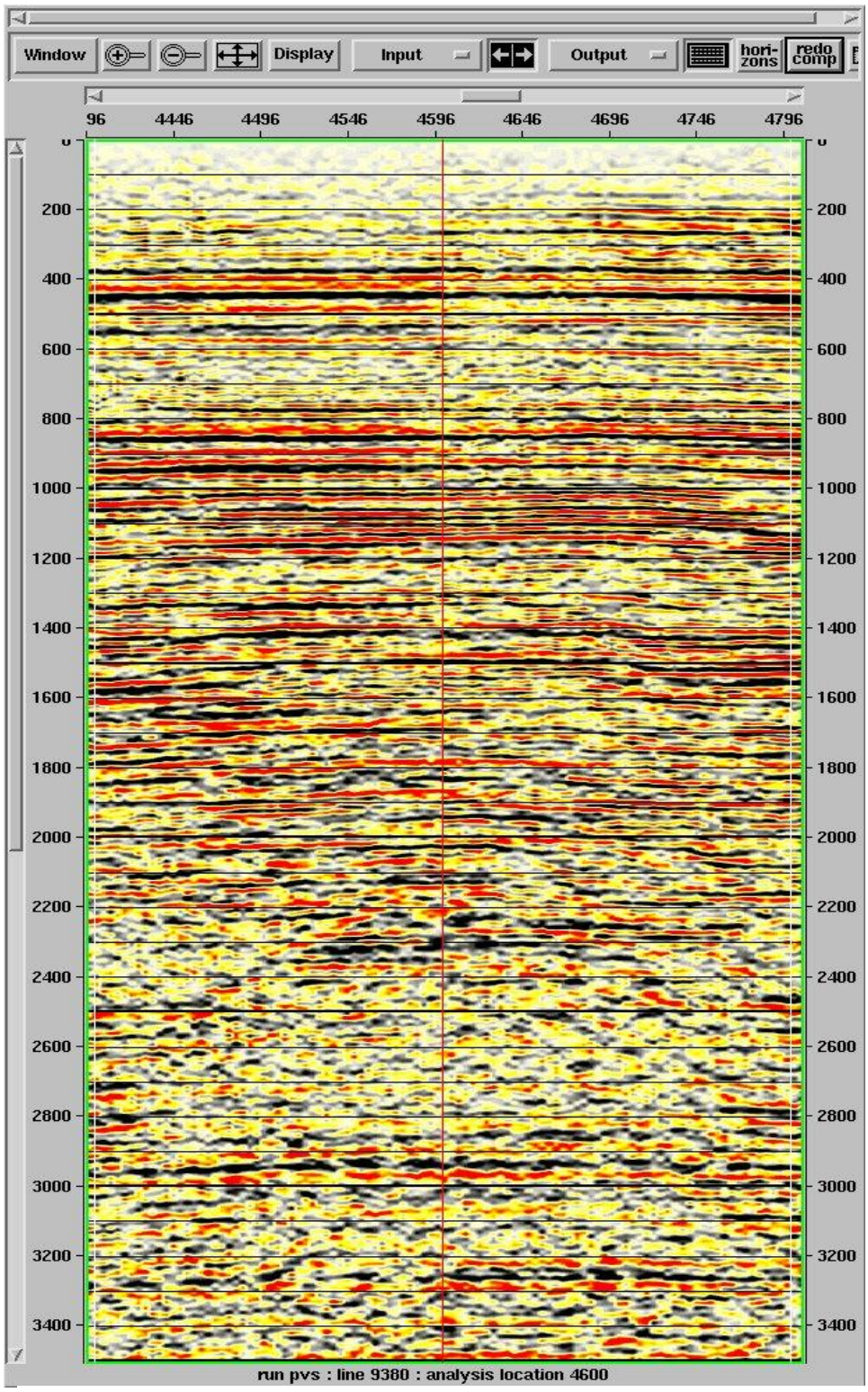

Figure 4.7. The stack response before applying the velocities

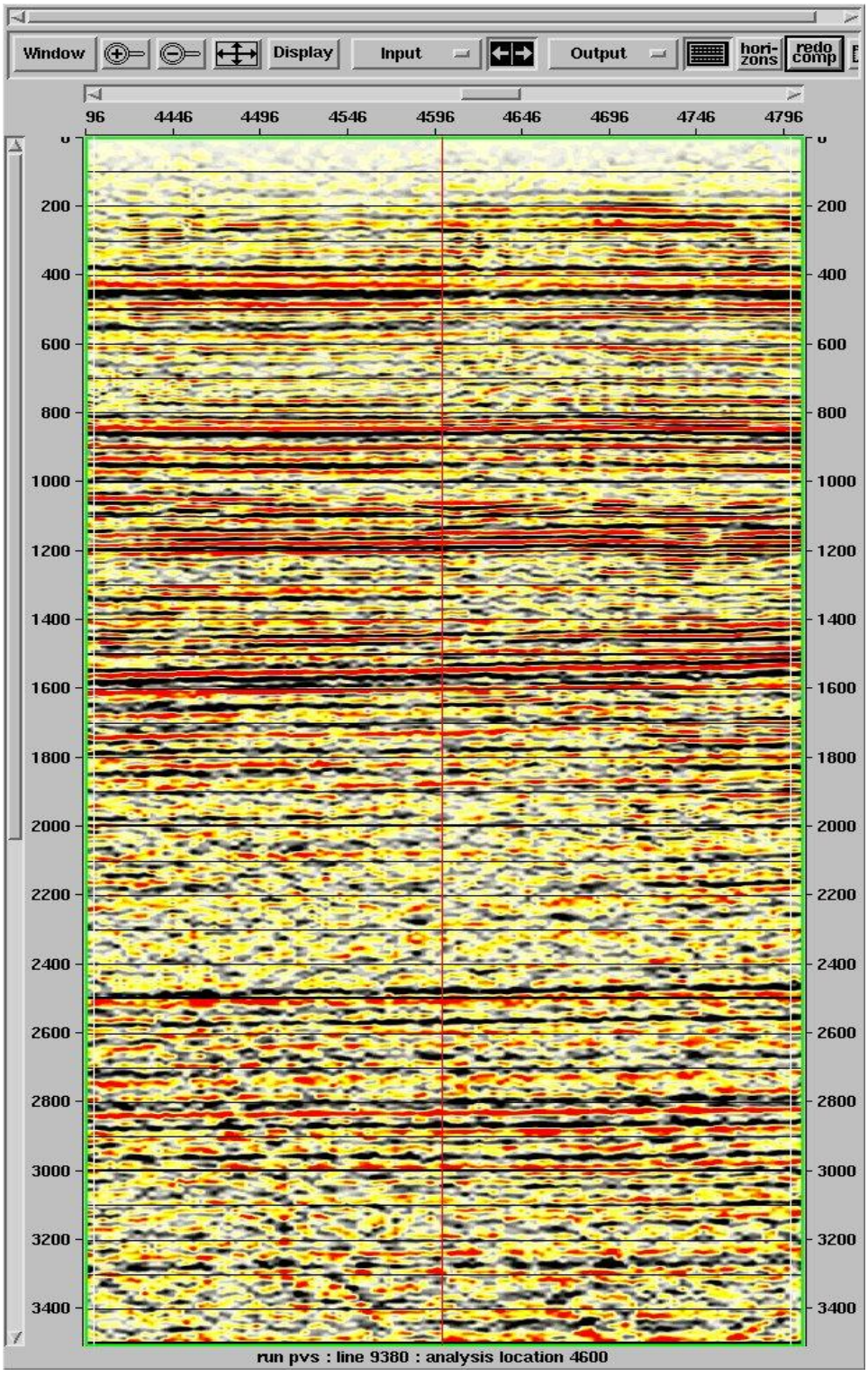

Figure 4.8. The stack response after applying the velocities

4.3 CASE THREE: Poor signal to noise ratio

This case presents seismic data that has very poor signal to noise ratio and subsequently the semblance method and other methods based on continuity or coherency totally fails. This case usually leaves the seismic data analyst puzzled about how to pick velocities in that seismic section. The semblances in such seismic data can show minimal coherency instead of maximum coherency (Figure 4. 9).

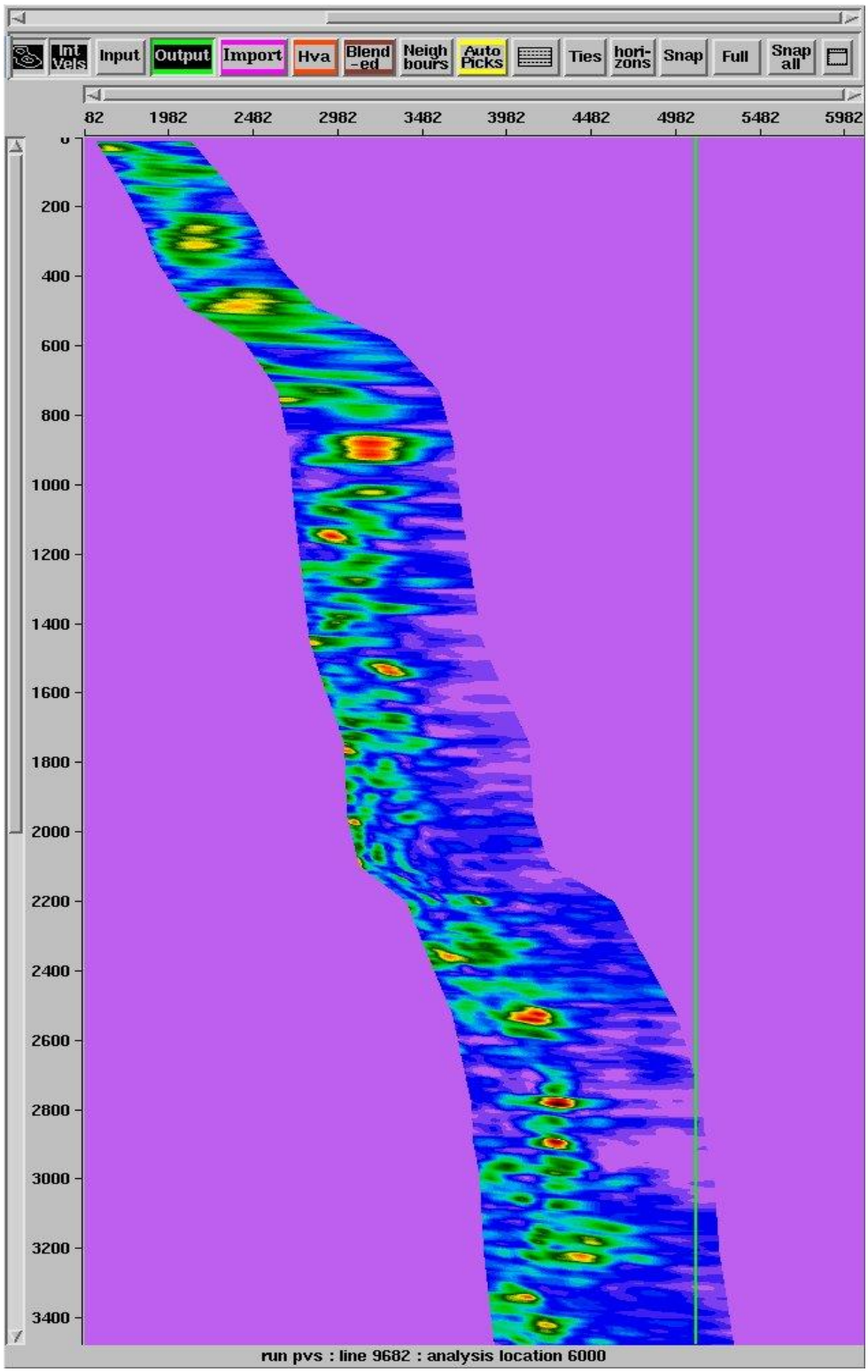

Figure 4.9. The semblance shows poor coherency as a result of poor signal to noise ratio in the actual data.

The study can provide time and velocity values for the seven key horizons that were compiled, interpolated, and integrated. The time values and velocity values were posted on the semblances as indicated in the Figure 4.10

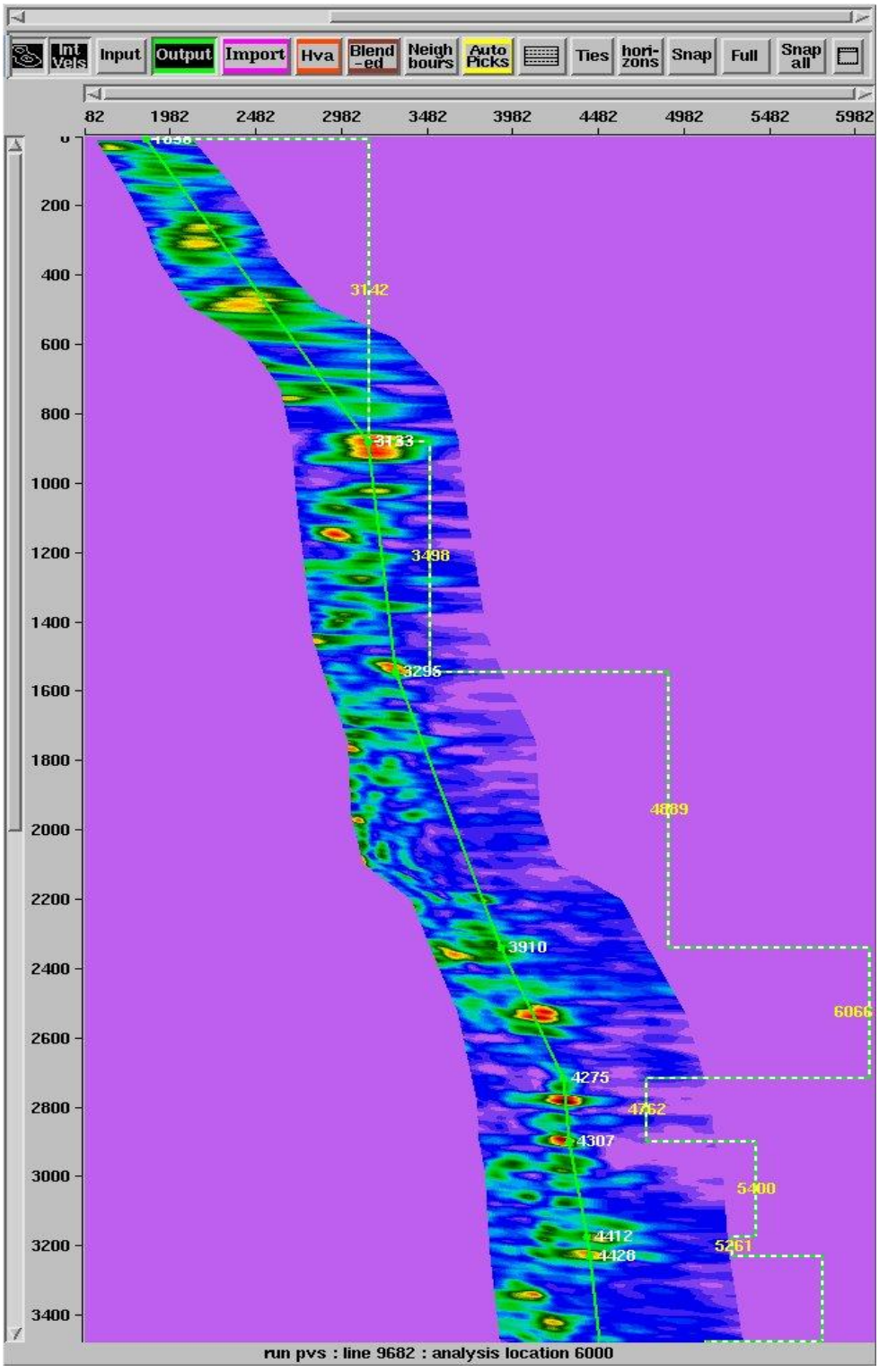

Figure 4.10. The same semblance as in Figure 4.9 with the time picks and velocity values applied for the 7 Horizons.

The stack response is quite indicative of the effectiveness of the method, major improvements are obvious in the signal to noise ratio throughout the time scale on the location of the seismic line on the location of the seismic line where the red line passes. (Figure 4.11 versus Figure 4.12).

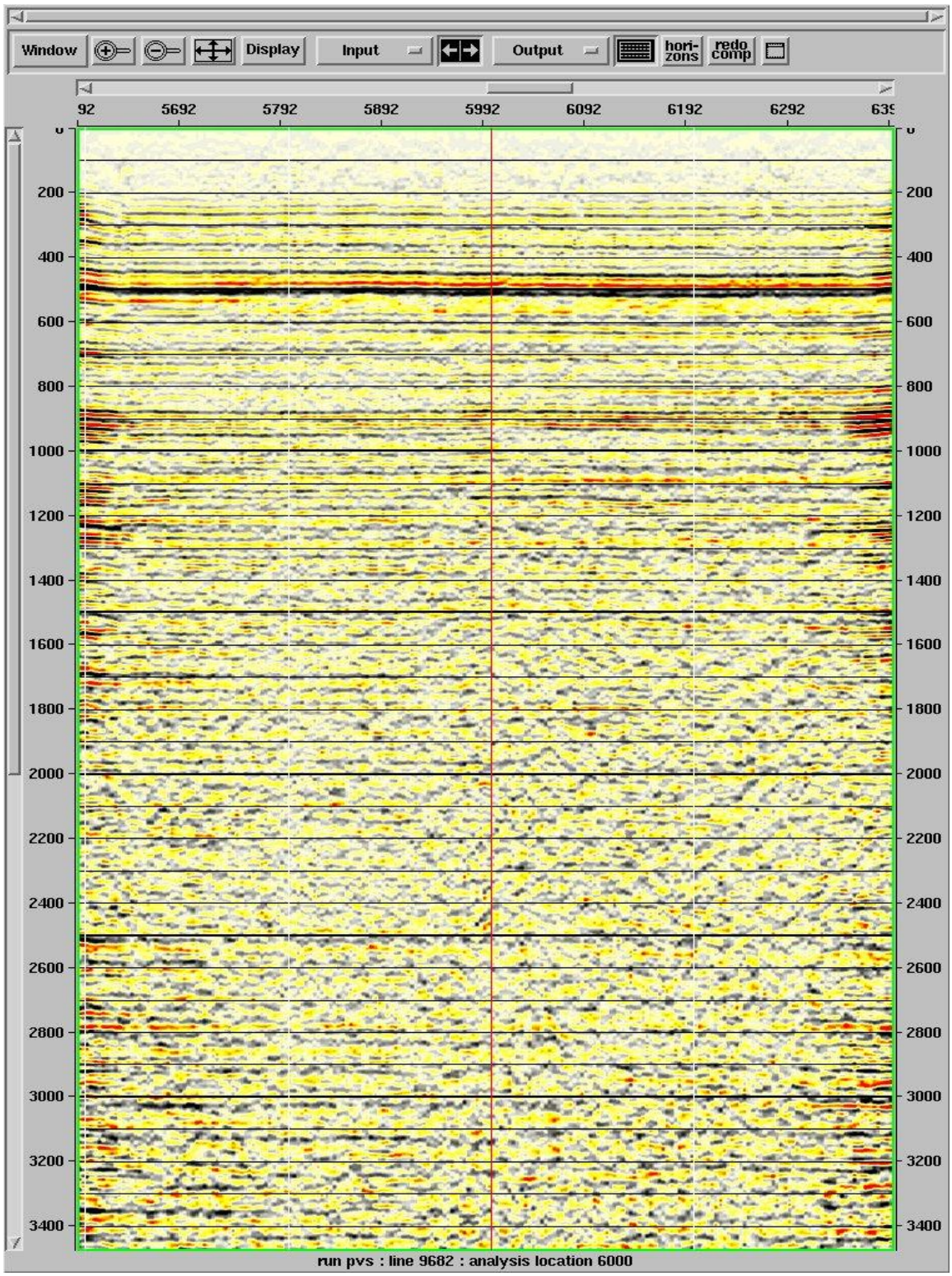

Figure 4.11. The stack response before applying the velocities

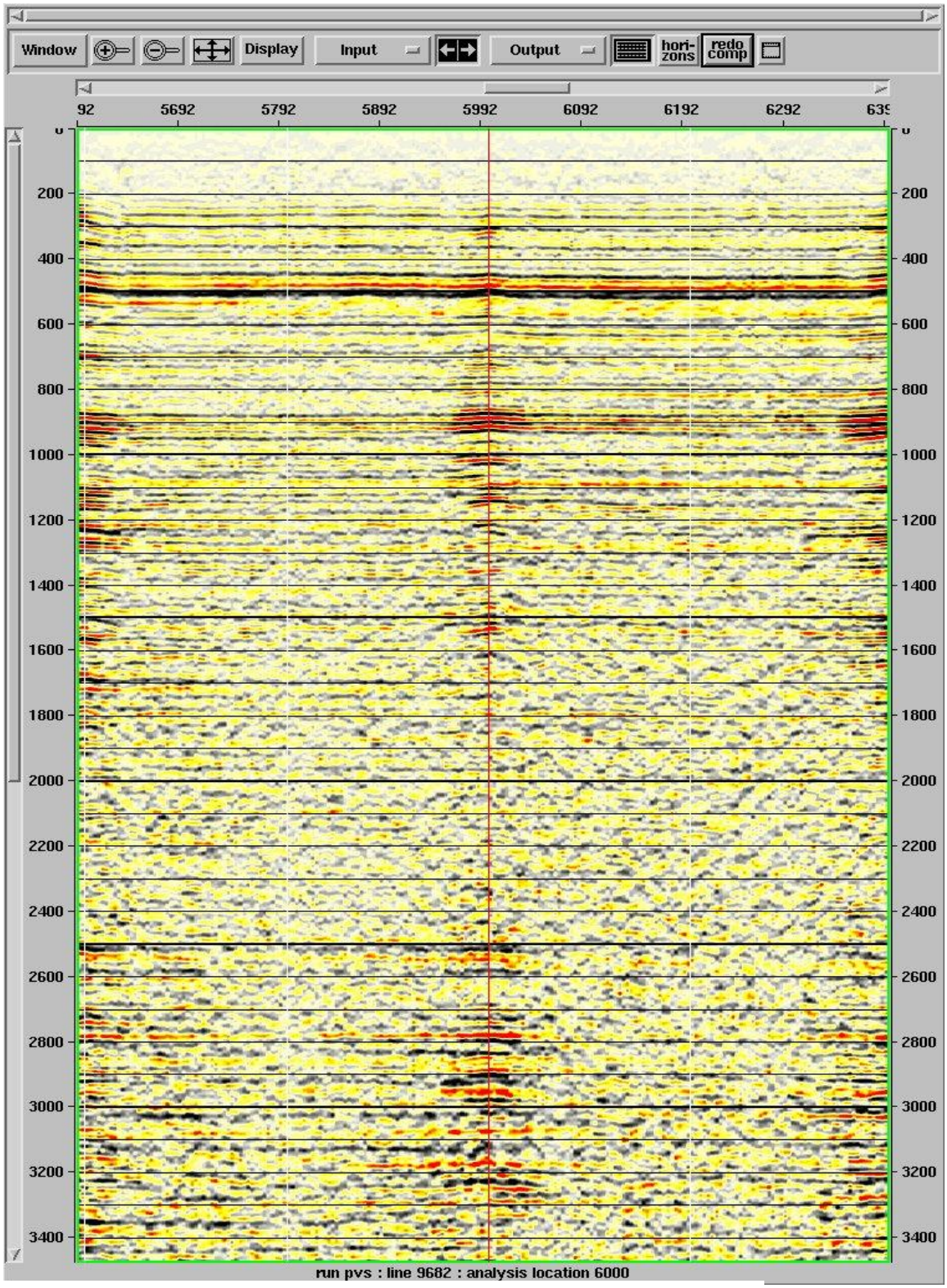

Figure 4.12. The stack response after applying the velocities

4.4 CASE FOUR: Poor stack response

This case presents seismic data that has very poor signal to noise ratio and subsequently the semblance method and other methods based on continuity or coherency totally fail. In addition to the problem that was in CASE THREE, this stack has very poor response. This case usually leaves the seismic data analyst puzzled about how to pick velocities in that seismic section. The semblances in such seismic data can show minimal coherency instead of maximum coherency. The stack shows poor response in this case (Figure 4.13).

The semblance throughout the stack would provide minimal assistance (Figure 4.14). However, when the time and velocity values from the study is applied on the semblances (Figure 4.14), the improvements become obvious on the stack (Figure 4.15).

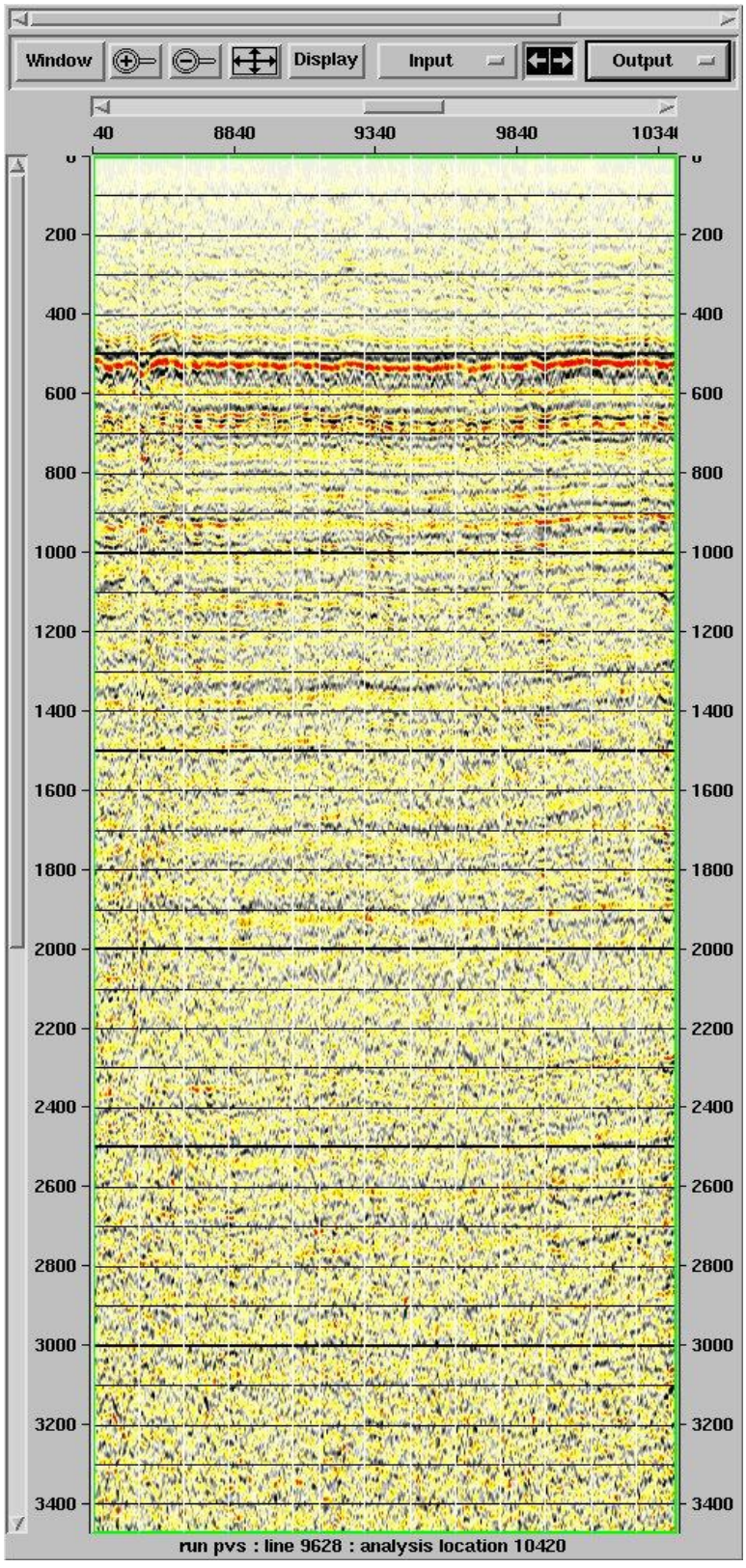

Figure 4.13. The stack shows poor response.

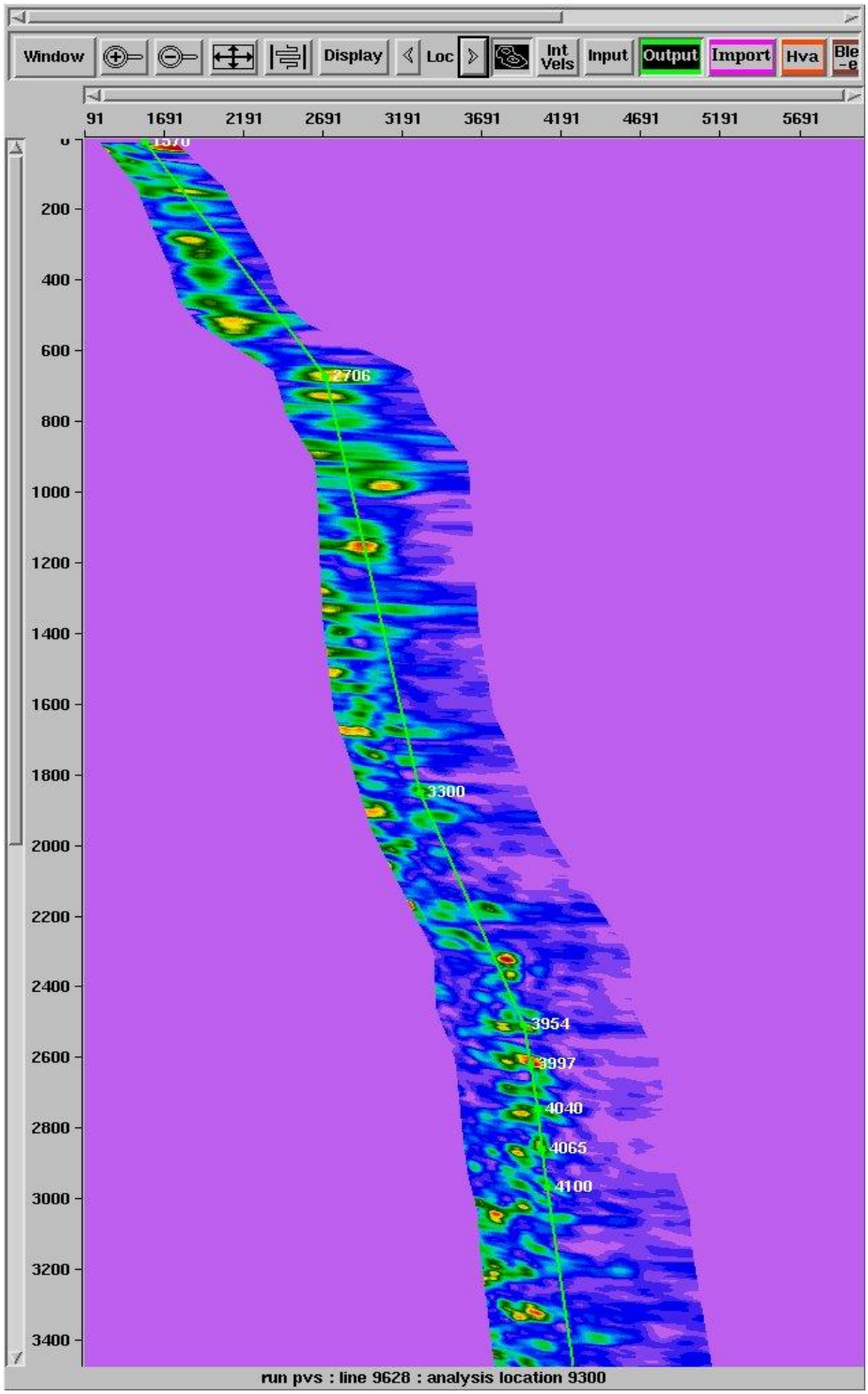

Figure 4.14. The semblance provides minimum assistance in picking the velocities but with the help of the results we know better where the horizon picks should be and at what velocity values.

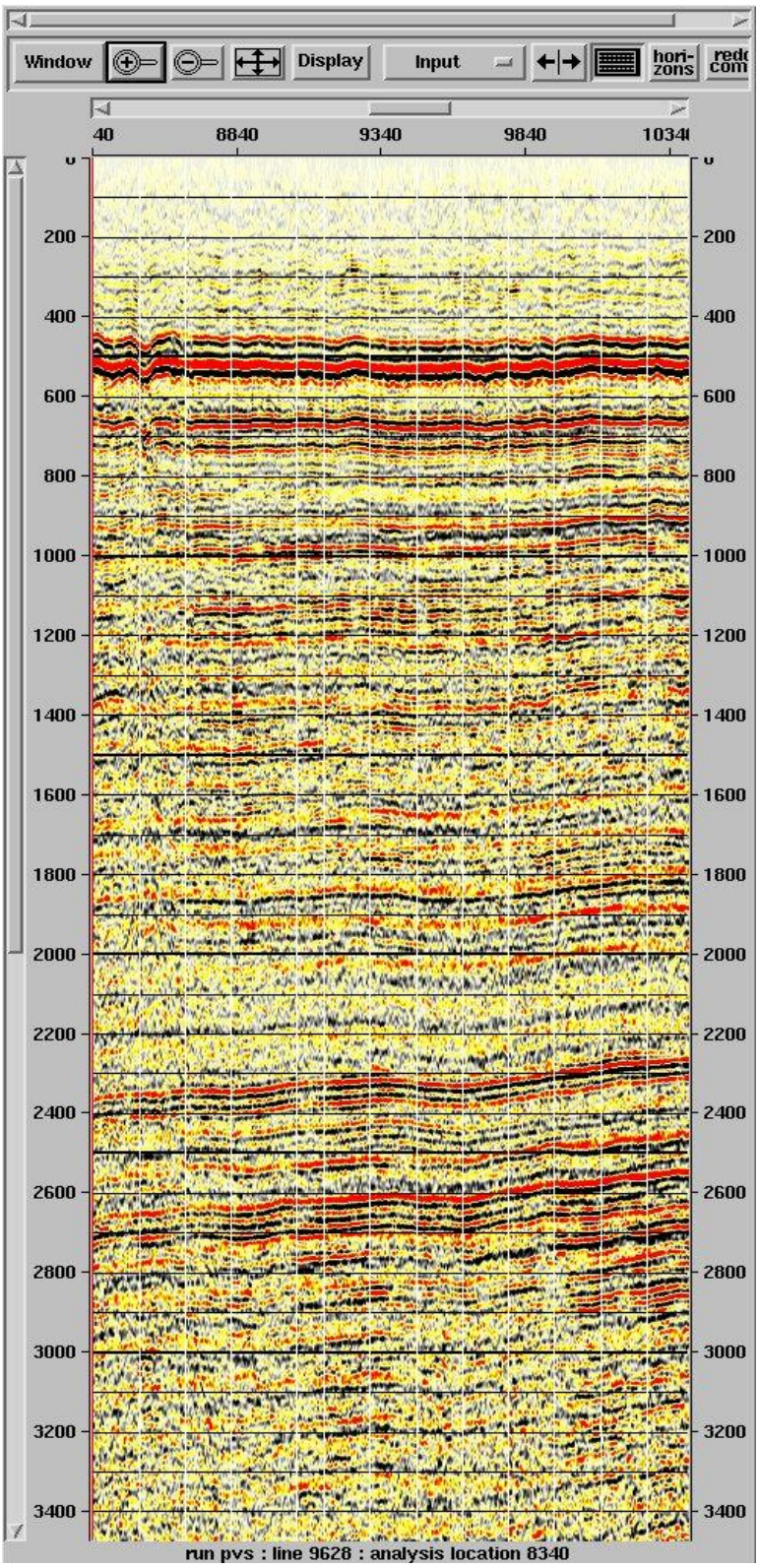

Figure 4.15. The stack response after applying the velocities

4.5 CASE FIVE: Subsurface collapses/Wadis/karsting

This case presents seismic data around subsurface collapses, wadis and/or karsting. It is known ahead of time that karstingwill have no continuity and that coherency will not exist and thus the conventional methods will not provide the proper solution for the velocities. The stacks will indicate the karsting clearly (Figure 4. 16). Even though it is common among seismic data processors not to pick inside the karsting (Figure 4.17) because any pick would not be based on signal to noise values, they still need to pick seismic velocities at least on each side of the karsting.

Relying on the study, time and velocity values were posted on the stack to provide a more reasonable way of getting what the velocity value should be throughout the stack (Figure 4.18).

To prove the uniform case of velocity picks outside the karsting, the results show how the semblance shows the confidence in the results (Figure 4.19). The result on the stack provides confidence in the method (Figure 4.20).

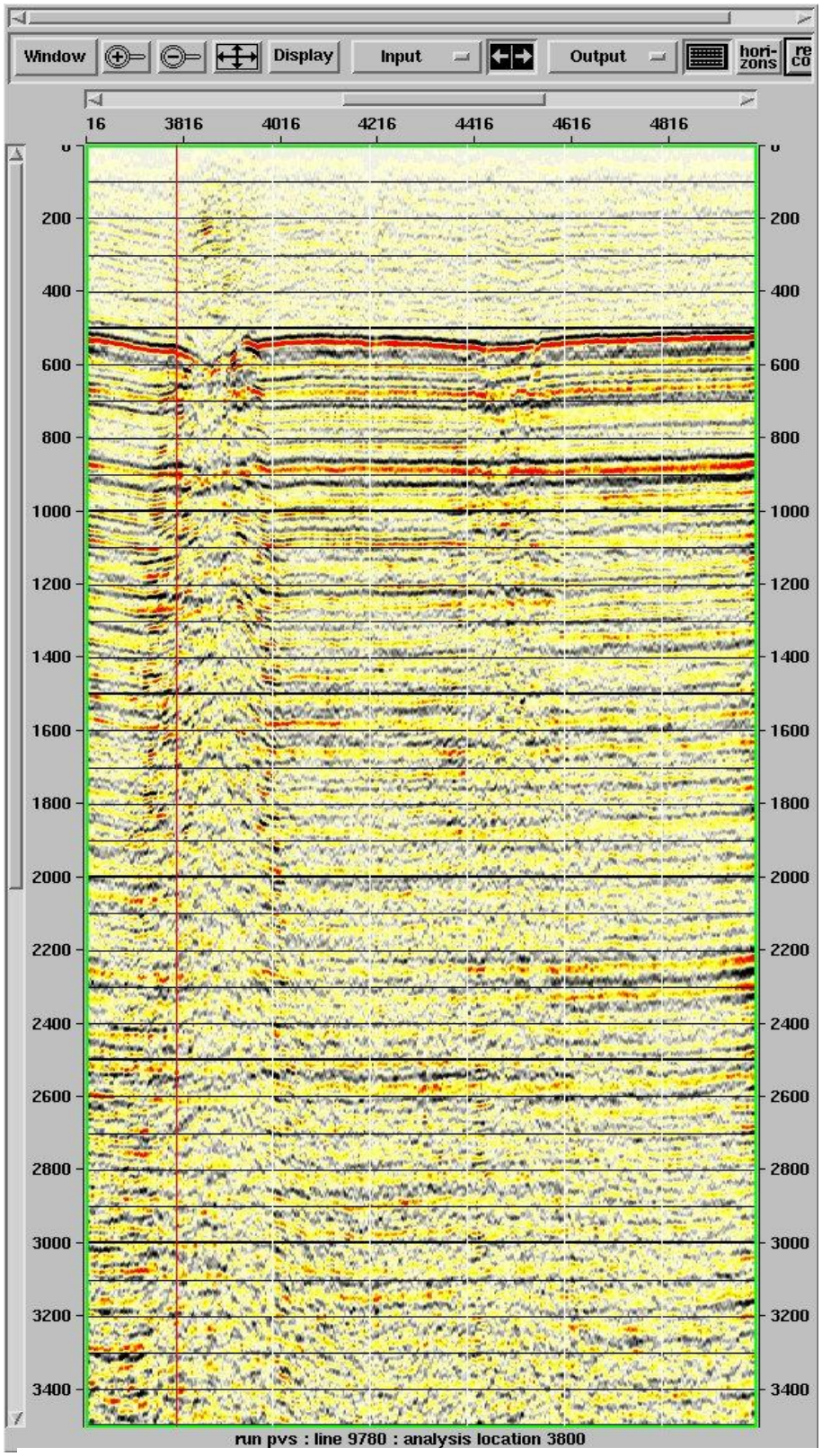

Figure 4.16. The stack indicates the karsting between CMPs 3816 and 4816.

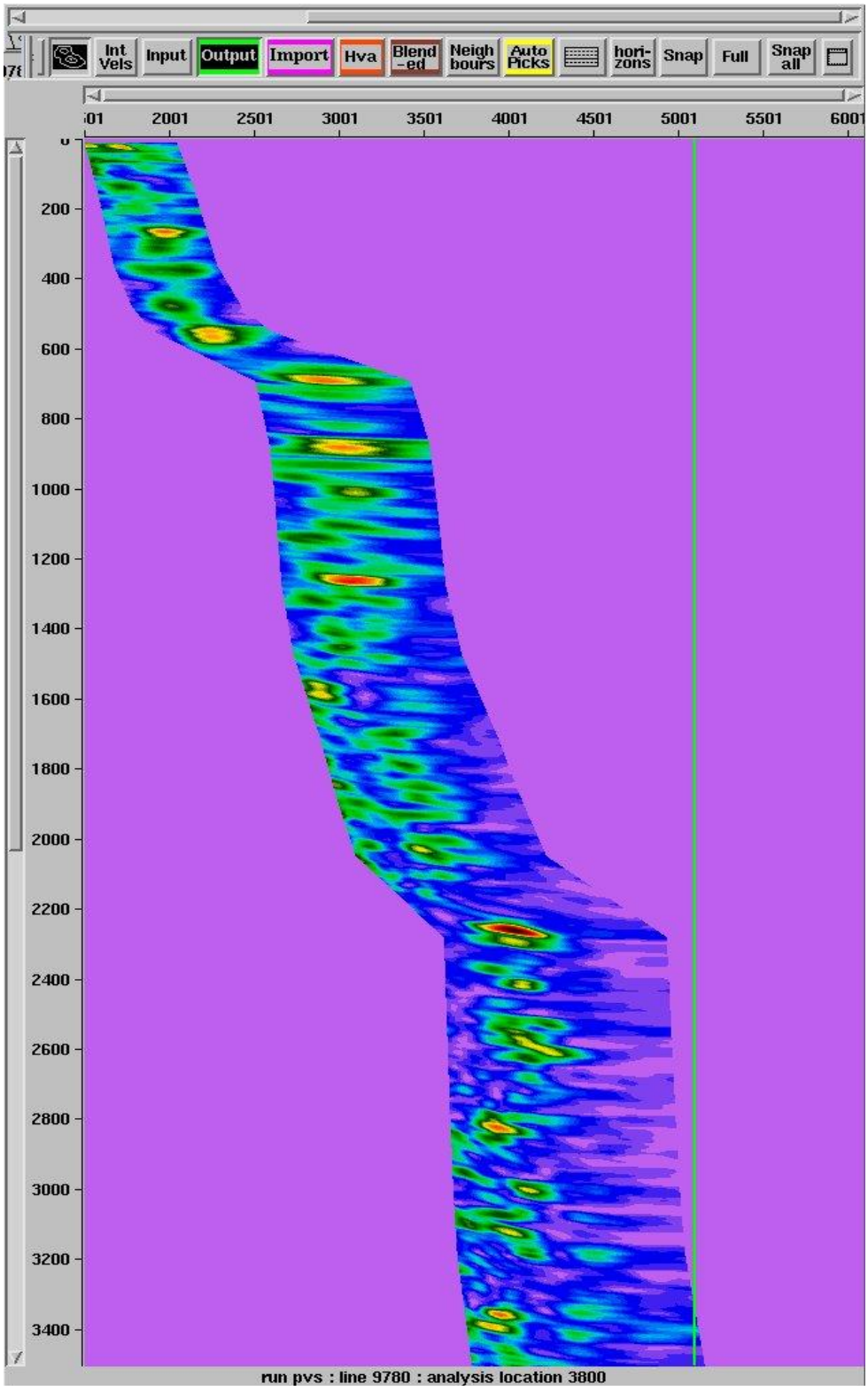

Figure 4.17. Semblance from inside the karstingat CMP 3800. Making any pick inside the karstingcan cause erroneous time and/or velocity values.

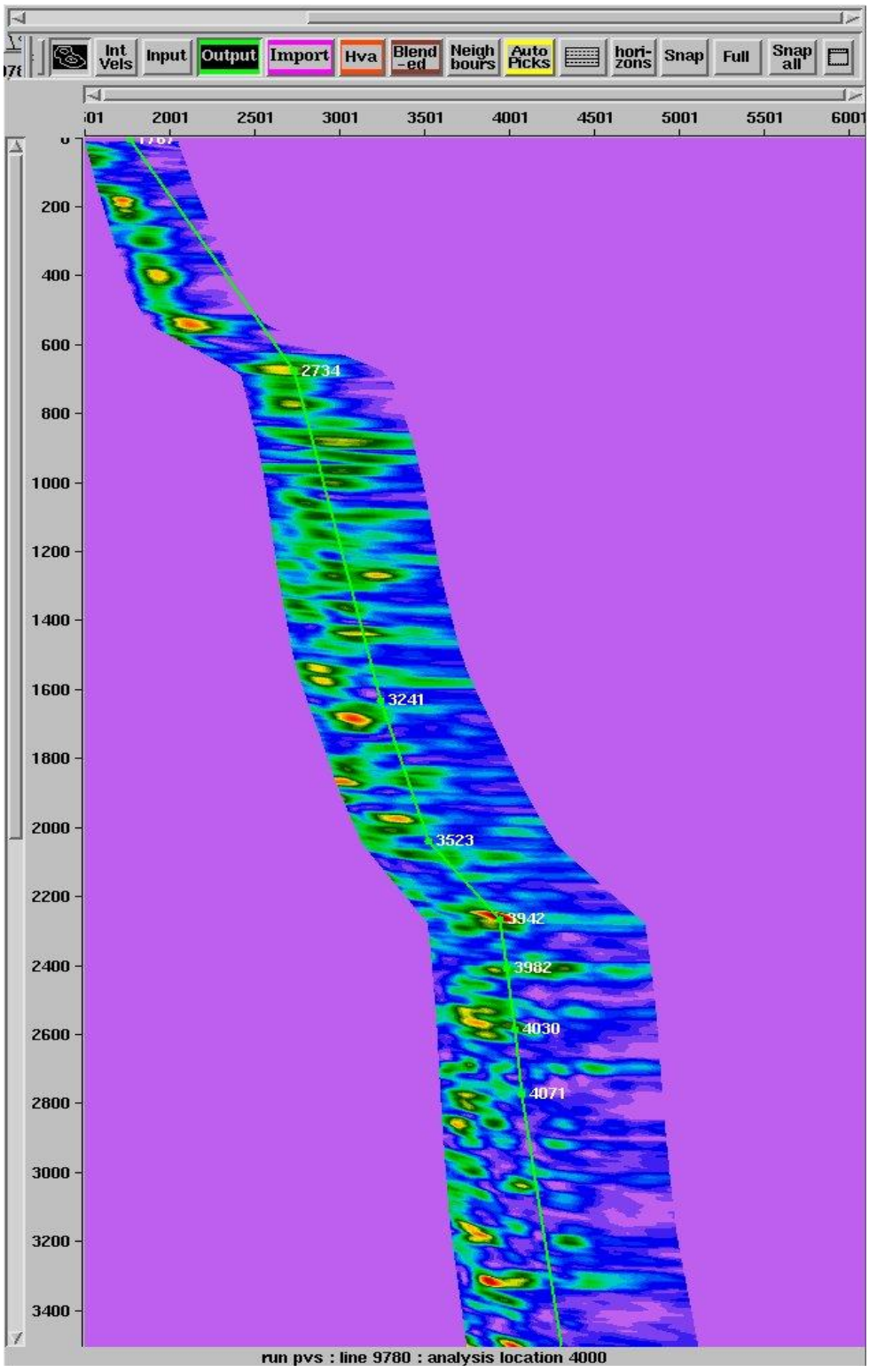

Figure 4.18. The semblance inside the karsting, as given from the results of this study at CMP 4000.

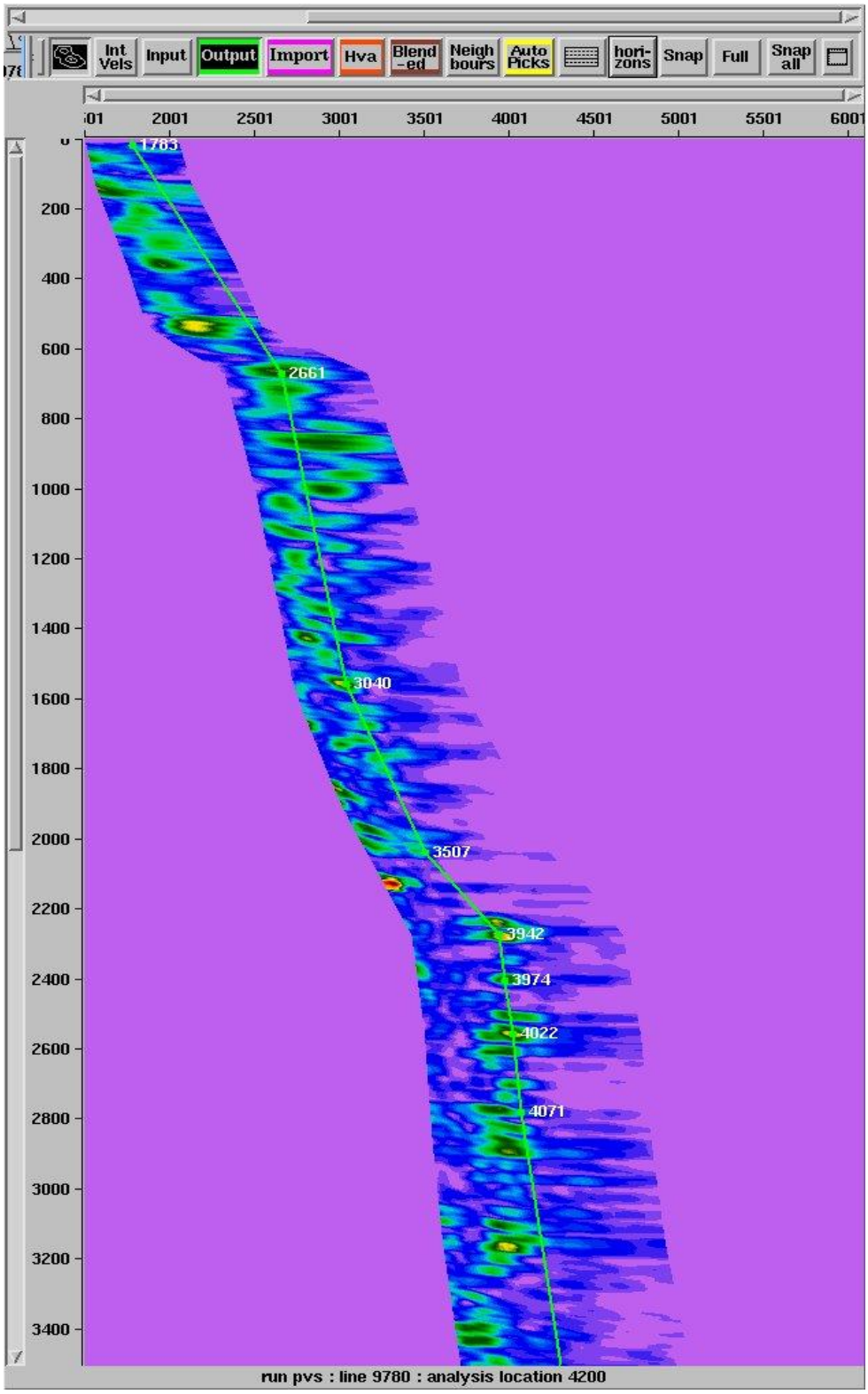

Figure 4.19. The semblance outside the karsting, as given from the results of this study at CMP 4200. It gives us a more confident reading of time picks and velocity.

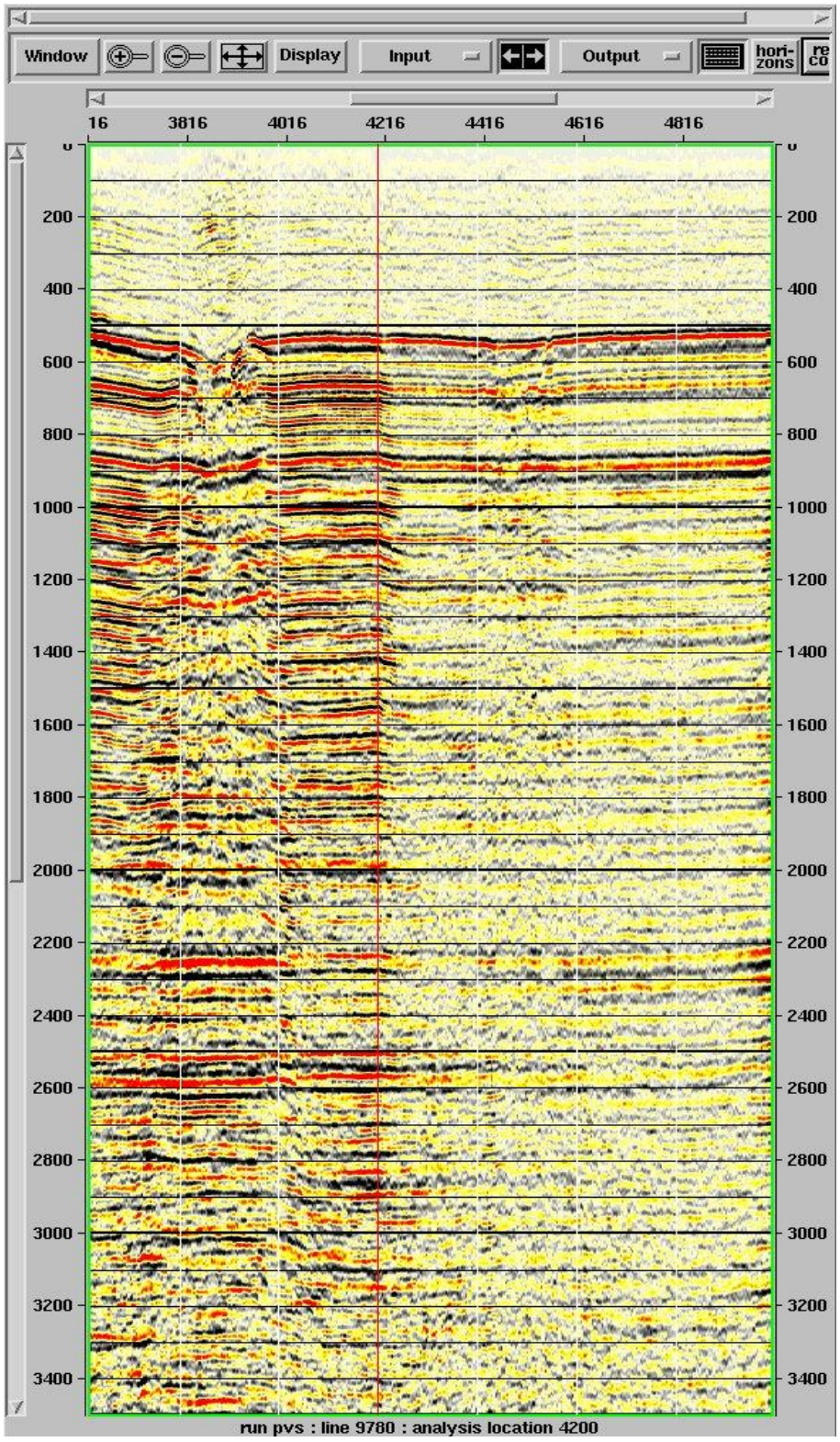

Figure 4.20. The stack response in the karsting case with the improvements provided by the method.

CHAPTER 5

CONCLUSIONS AND RECOMMENDATIONS

5.1 CONCLUSIONS

The precision of the current available methods of estimating stacking velocity is limited in vertical and horizontal velocity resolution, especially in cases involving multiples and limited-offset data sets. There has been numerous cases where it is difficult to discriminate stacking velocities in areas with stretched or poor semblance peaks.

This study provides an innovative model-based velocity integration procedure that has the capability to fulfill some of the shortcomings in the current available methods of determining stack velocities.

This study has conclusively demonstrated that previous works on seismic data processing provide valuable velocity analysis data that can be advanced into meaningful models. This model can provide resourceful platforms for all types of geologic and geophysical data for integration. Some of the controversial issues with stacking velocity picking were ruled out during this study, Seismic stacking velocities that have been picked using auto pickers, don't affect the accuracy of the velocities when interpolated on surfaces.

When the role of seismic data processing is complete by delivering the best stackable data to interpretation, the gap between seismic data processing and interpretation can be

closed through this proposed study with higher accuracy for both processing and interpretation.

The confidence of seismic stacking velocities is much higher when the velocity data is tied to solid interpretation data. The current available techniques for seismic stacking velocity picking have some shortcomings that are clear in many cases. These shortcomings can be resolved by the proposed study. Since coherency and continuity do not provide complete tools to subsurface analysis of seismic data, a more comprehensive integration approach has resolved the shortcomings of coherency and continuity tools. Starting the processor velocity picking with such confidence makes the process of fine tuning the velocities more intuitive and gives a better advantage as to what seismic picks should be selected. It also makes the process of identifying multiples much easier than the conventional methods.

5.2 RECOMMENDATIONS

This study has open new frontiers of picking stacking velocities with more confidence and higher accuracy. To further advance this concept and improve upon it, there can be substantial expansion on the data elements of this study to accommodate sonic data and other borehole data for more solid geological correlation between the seismic method and subsurface geology. Furthermore, the velocity data that were included can be updated with picks that were made after 2001.

An obvious recommendation is to populate the seismic time picks with more key horizons. This can even secure more confidence for the processor to cover the whole time scale with as many verified horizon picks as possible.

As for the imprints on the time and velocity grids, it is recommended to use geostatistical methods such as factorial co-krigging for enhancing irregular imprints of erroneous seismic lines inputs (Geostatistics for seismic data integration in earth models, 2003)

REFERENCES

Bergler, S., and Hubral, P. 2002, 3D common-reflection surface stack and kinematic wavefield attributes : *The Leading Edge*, 21:1010-1015.

Biondi, B. 1992, Velocity estimation by beam stack*: Geophysics*, 57:1034-1047.

Chira, P. and Hubral, P. 2003, Traveltime formulas of near-zero-offset primary reflections for a curbed 2-D measurement surface: *Geophysics*, 68: 255-261.

Dubrule, O. 2003, *Geostatistics for seismic data integration in earth models*: EAGE Distinguished Instructor Series, No. 6

Hubral, P. 1980, Computation of the normal movement velocity in 3D laterally inhomogeneous media with curved interface: *Geophysical Prospecting*, 28:221-239.

Kabir, M.N. and Verschuur, D. J. 1994, Integrated velocity estimation and stacking using parabolic Radon transform: *SEG 64th annual meeting, SEG expanded abstracts with Biographies*, pp. 1473-1476.

Mallet, J. 2002, *Geomodeling*: Oxford University Press, 2002.

Mann, J., Mueller, T., Jaeger, R., Hoecht, G., and Hubral, P. 1999, Application of the common reflection surface stack*: SEG 69th annual meeting, SEG Expanded abstracts and Biographies*, 69:1829-1832.

Matsushima, J., Rokugawa, S., and Yokota, T. 2001, Diffraction stacking with stacking velocity analysis in surface seismic survey: *Geophysical Exploration*, 54:73-89.

Schmidt, J. 1994, Stacking velocity determination using neural networks: *Boletin de Geociencias da PETROBRAS*, 8:335-345.

Tieman, H. J. 1993, Description of scanless method of stacking velocity analysis: *Geophysics*, 58:1596-1606.

Weizhong, W., Zhaoqi, B., and Tong, C. 1988, Automatic stacking velocity analysis: *Geophysical Prospecting*, 23:188-198.

Yilmaz, O. 1987, *Seismic Data Processing* : SEG.

VITA

Name: Abdulaziz Mohammed Al-Moqbel
Nationality: Saudi Arab
Specialty Geophysicist

Education

- High school graduate of Sciences 1991
- Saudi Aramco College Preparation Qualification program 1991-1992
- B.S. Geophysics (University of the Pacific, Stockton CA) 1992-1995
- M.S. Geophysics (King Fahad University of Petroleum and Minerals) 2010

Working Experiences

- 1995- 1998 Seismic Data Processor
- 1998- 2001 Seismic Data Acquisition Specialist (Seismic Crew Supervisor)
- 2001- 2004 Seismic Data Modeling
- 2004- 2007 Seismic Data Interpreter
- 2007- 2010 Seismic Data Management specialist

Contact Information

Dhahran, Saudi Arabia
Tel : 00966-505925857
e-mail : Abdulaziz.moqbel@gmail.com